HYPERSPECTRAL REMOTE SENSING FOR ECOLOGICAL ANALYSES OF GRASSLAND ECOSYSTEMS

SPECTRAL SEPARABILITY AND DERIVATION OF NPP RELATED BIOPHYSICAL AND BIOCHEMICAL PARAMETERS

Dissertation

zur

Erlangung der naturwissenschaftlichen Doktorwürde

(Dr. sc. nat.)

vorgelegt der

Mathematischen-naturwissenschaftlichen Fakultät

der

Universität Zürich

von

Achilleas Psomas

aus Griechenland

Promotionskomitee
Prof. Dr. Klaus I. Itten (Vorsitz)
Dr. Niklaus E. Zimmermann
Dr. Mathias Kneubühler

Zürich, 2008

Abstract

Grasslands, both man made and natural, cover nearly 20% of the Earth's land surface representing a unique variety of colours, structure and biodiversity. These natural and semi-natural habitats are of great ecological importance for biodiversity conservation, since they provide a wide range of habitats for plants and animals, many of which are classified as endangered or threatened. Furthermore, grasslands play a significant role in the global carbon cycle, accounting for at least 10% of the global carbon pools. Additionally, it is estimated that they are responsible for as much as 20% of the total terrestrial net primary production (NPP). In the face of global climate change and the growing demand for agricultural productivity, pressure on grassland ecosystems is expected to increase. Therefore, the development of management strategies that ensure the protection of biodiversity and an improved knowledge of the grasslands carbon cycle and its spatial representation are of critical importance, specifically also under current and future climatic conditions.

This dissertation evaluates the synergistic use of hyperspectral remote sensing and ecosystem process modelling for biodiversity conservation of grassland habitats and for improved understanding of their biogeochemical cycles at local to regional scales. The major goals of the presented work are to explore the potential of hyperspectral remote sensing for mapping species-rich grassland habitats and for deriving vegetation properties relevant to ecosystem productivity. The dissertation consists of three main research parts. The first part addresses the use of intra and inter-annual spectral measurements of different grassland habitats collected with a field spectroradiometer for exploring their seasonal spectral separability. In the second part, the dissertation focuses on the development of statistical models for predicting above-ground biomass of grasslands from spectral measurements recorded with a field spectroradiometer and evaluates the potential of up-scaling these models to spaceborne hyperspectral data (Hyperion). Finally, the third part explores the extraction of quantitative information on grassland foliar biochemical concentrations (nitrogen) from airborne hyperspectral remote sensing (HyMap) using novel statistics. Subsequently, the HyMap extracted foliar biochemical information is used to initialise and drive an ecosystem process model (Biome-BGC) in a spatially-distributed manner to estimate NPP of the grassland ecosystems.

Results from the first part of this dissertation demonstrated that species-rich grassland habitats could be discriminated successfully by using hyperspectral remote sensing. Specific parts of the spectrum that contributed best to the separability of the grasslands types during the growing seasons were identified. More importantly, it was shown that the beginning of the growing season was the best period for discriminating grassland habitats from hyperspectral remote sensing measurements. Results from the second part of the dissertation showed that

construction of robust statistical models for grassland biomass estimation from hyperspectral remote sensing is feasible, provided that multiple samples during the growing season were collected. Seasonal sampling, especially early in the growing season, was shown to be very important in order to cover normally occurring variability, due to variations in phenology stage, spatial patterns and management. Furthermore, it was concluded that up-scaling of field developed statistical models for biomass estimation could best be achieved when narrow band NDVI type indices were used. Finally, results from the third part of this dissertation revealed that accurate predictions of foliar biochemical information could be achieved, provided that continuum-removal transformation was applied to the HyMap reflectance spectra prior to calibrating the statistical models. It was also shown that it was possible to run the Biome-BGC model in a spatially distributed mode, thus deriving detailed NPP estimates of the study area. More important findings, however, were that NPP of the study area using spatial predictions of C:N was significantly higher than NPP estimated using C:N values widely applied in literature or even from using regionally measured mean C:N values. These findings suggested that carbon sequestration dynamics of certain ecosystems − in our case of managed grassland habitats − might be underestimated regionally if standard methods are used that do not feed spatially distributed C:N values into model runs.

Overall, the work presented in this dissertation has demonstrated the high potential of hyperspectral remote sensing for the spectral separability and the retrieval of biomass and foliar nitrogen concentration of species-rich grassland ecosystems. Furthermore, it emphasised the importance of using high accuracy products derived from hyperspectral remote sensing as input to ecosystem process models. Coupling these two synergistic technologies is expected to enhance our understanding on terrestrial carbon cycle dynamics at local to regional scales.

Zusammenfassung

Natürliche und vom Menschen geschaffene Grassländer bedecken fast 20% der Erdoberfläche und stellen eine einzigartige Vielfalt an Farben, Strukturen und Biodiversität dar. Gerade für die Biodiversitätserhaltung sind diese natürlichen und halbnatürlichen Habitate von grosser ökologischer Bedeutung. Denn Grassländer beinhalten eine Vielzahl von Habitaten für Pflanzen und Tiere, von welchen viele als gefährdet oder bedroht klassiert sind. Zudem spielen Grassländer eine entscheidende Rolle im globalen Kohlenstoffkreislauf. Mindestens 10% des globalen Kohlenstoffvorrats werden nämlich Grassländern zugeschrieben. Zusätzlich schätzt man, dass bis zu 20% der gesamten terrestrischen Nettoprimärproduktion (NPP) von Grassländern geleistet wird. Angesichts des globalen Klimawandels und der zunehmenden Forderung nach einer produktiveren Landwirtschaft wird sich der Druck auf Grasslandökosysteme wohl erhöhen. Darum ist die Entwicklung von Bewirtschaftungsstrategien zum Schutz der Biodiversität besonders wichtig. Speziell in Bezug auf gegenwärtige und zukünftige Klimabedingungen ist dabei ein vertieftes Wissen über den Kohlenstoffkreislauf und seine räumliche Verteilung in Grassländern entscheidend.

Diese Dissertation untersucht die synergistische Verwendung von hyperspektraler Fernerkundung und ökosystemarer Prozessmodellierung zur Erhaltung der Biodiversität von Grasslandhabitaten und einem verbesserten Verständnis des biogeochemischen Kreislaufes auf lokaler bis regionaler Skala. Die Hauptziele der Untersuchung sind die Abklärung der Möglichkeiten von hyperspektraler Fernerkundung zur Kartierung von artenreichen Grasslandhabitaten und für Ökosystemproduktivität relevante Vegetationseigenschaften. Die Dissertation gliedert sich darum in drei Forschungsteile. Der erste Teil untersucht die Verwendung von intra- und inter-annuellen Spektralmessungen mit einem Feldspektroradiometer zur saisonalen und spektralen Unterscheidung verschiedener Grasslandhabitate. Der zweite Dissertationsteil konzentriert sich auf die Entwicklung von statistischen Modellen zur Schätzung von oberirdischer Biomasse von Grassländern auf Grund von spektralen Messungen mit einem Feldspektroradiometer. Gleichzeitig wird damit das Potential abgeschätzt diese Modelle auch für satellitengestützte Hyperspektraldaten (Hyperion) zu verwenden. Schliesslich wird im dritten Dissertationsteil die Erfassung von quantitativen Informationen zu biochemischen Blattkonzentrationen (Stickstoff) mittels flugzeuggestützter hyperspektraler Fernerkundung (HyMap) und neuartiger Statistik untersucht. Anschliessend wird die aus HyMap-Daten erfasste biochemische Blattkonzentration weiterverwendet um ein ökosystemares Prozessmodell (Biome-BGC) zur Schätzung der NPP von Grasslandökosystemen zu initialisieren und räumlich-explizit umzusetzen.

Resultate des ersten Teils der Dissertation zeigten, dass artenreiche Grasslandhabitate mittels hyperspektraler Fernerkundung erfolgreich unterschieden werden konnten. Dabei wurden spezifische Bereiche des Spektrums identifiziert, welche am meisten zur Unterscheidung von Grasslandtypen innerhalb der Wachstumsperioden beitrugen. Wichtig war dabei die Erkenntnis, dass der Beginn der Wachstumsperiode der beste Zeitraum war, um Grasslandhabitate auf Grund von hyperspektralen Fernerkundungsmessungen zu unterscheiden. Resultate des zweiten Teils der Dissertation zeigten, dass robuste statistische Modelle für die Schätzung von Grasslandbiomasse auf Grund von hyperspektralen Fernerkundungsdaten möglich sind, jedoch nur unter der Voraussetzung dass mehrere Stichproben während einer Wachstumsperiode erfasst wurden. Gerade diese saisonale Stichprobenerhebung, speziell am Anfang der Wachstumsperiode, zeigte sich als sehr wichtig, um die vorhandene Variabilität auf Grund des phänologischen Zustandes, räumlichen Musters und Bewirtschaftung einzubeziehen. Zusätzlich zeigten die Resultate, dass statistische Modelle zur Biomassenschätzung basierend auf Felddaten auch auf höhere Skalen übertragen werden konnten wenn engbandige, NDVI-ähnliche Indizes verwendet wurden. Schlussendlich zeigte der dritten Teil der Dissertation, dass korrekte Schätzungen der biochemischen Blattzusammensetzung möglich sind, jedoch nur unter der Voraussetzung dass vor der Kalibrierung der statistischen Modelle eine ‚continuum-removal' Transformation auf die Reflektanzspektren von HyMap angewendet wurde. Es konnte auch gezeigt werden, dass Biome-BGC räumlich-explizit umgesetzt werden konnte, das heisst auch detaillierte NPP Schätzungen für das Untersuchungsgebiet möglich sind. Noch viel wichtiger war aber die Erkenntnis, dass NPP signifikant höher geschätzt wurde auf Grund von räumlich-expliziten C:N Verhältnissen als geschätzt aus weit verbreiteten Literaturwerten oder sogar regional gemittelten C:N Messwerten. Diese Resultate legen nahe, dass die Dynamik der Kohlenstofffixierung in bestimmten Ökosystemen – in unserem Fall bewirtschaftete Grasslandhabitate – möglicherweise regional unterschätzt werden mit Standardmethoden, die nicht räumlich-explizite C:N-Werte in die Modellbildung einbeziehen.

Die Untersuchungen dieser Dissertation haben das grosse Potential der hyperspektralen Fernerkundung aufgezeigt, indem artenreiche Grasslandökosysteme spektral unterschieden, sowie spezifisch Biomasse und Blattstickstoffkonzentration erfasst werden konnte. Zudem zeigte sich die Wichtigkeit von sehr genauen Produkten aus hyperspektraler Fernerkundung als Eingangsgrössen in ökosystemare Prozessmodelle. Eine Verbindung dieser beiden synergistischen Technologien hat grosse Chancen unser Verständnis des terrestrischen Kohlenstoffkreislaufes auf lokaler wie auch regionaler Skala zu verbessern.

Table of Contents

List of Figures

List of Tables

List of Acronyms

Adj.-R^2	Adjusted coefficient of determination
AOV	Analysis of Variance
APAR	Absorbed Photosynthetically Active Radiation
APEX	Airborne Prism Experiment
ARES	Airborne Reflective Emissive Spectrometer
ASD	Analytical Spectral Devices
ATCOR	Atmospheric and Topographic CORrection software
AVHRR	Advanced Very High Resolution Radiometer
BOREAS	Boreal Ecosystem Atmosphere Study
CAI	Cellulose Absorption Index
CART	Classification and Regression Trees
CASI	Compact Airborne Spectrographic Imager
CI	Carter Index
C:N	Carbon to Nitrogen Ratio
CHRIS	Compact High Resolution Imaging Spectrometer
CV	Cross Validation
CV-RMSE	Cross Validation Root Mean Square Error
CWL	Center WaveLength
DN	Digital Number
DTM	Digital Terrain Model
EnMap	Environmental Mapping and Analysis Program
EO-1	Earth Observation
ESA	European Space Agency
FOV	Field of View
FWHM	Full Width Half Maximum
GCP	Ground Control Points
GM2	Gitelson and Merzlyak Index 2
GMI	Gitelson and Merzlyak Index
GPP	Gross Primary Production
HDF	Hierarchical Data Format
HR	Heterotrophic Respiration
HyMap	Hyperspectral Mapping imaging spectrometer
IFOV	Instantaneous Field of View
IPCC	Intergovernmental Panel on Climate Change
LAD	Leaf Angle Distribution
LAI	Leaf Area Index
LIDAR	Light Detecting & Ranging
MCARI	Modified Chlorophyll Absorption Ratio Index
MLR	Multiple Linear Regression
MNF	Minimum Noise Fraction
MR	Maintenance Respiration
MSMI	Multi Sensor Microsatellite Imager
NDVI	Normalized Difference Vegetation Index
nb_NDVI_{type}	narrow band Normalized Difference Vegetation Index type
NDWI	Normalised Difference Water Index
NEP	Net Ecosystem Production
NIR	Near Infra-Red
NPP	Net Primary Production
NTSG	Numerical Terradynamic Simulation Group
OSAVI	Optimized Soil Adjusted Vegetation Index
PARGE	Parametric Geocoding
PLS	Partial Least Squares

PRI	Photochemical Reflectance Index
PSN	Photosynthesis
PWI	Plant Water Index
RDVI	Renormalized Difference Vegetation Index
RESP	Red Edge Spectral Parameter
RMSE	Root Mean Square Error
RT	Radiative Transfer
SAR	Synthetic Aperture Radars
SAVI	Soil Adjusted Vegetation Index
SNR	Signal-to-Noise Ratio
SR	Simple Ratio
SRWI	Simple Ratio Water Index
SWIR	Short Wave Infra-Red
TM	Thematic Mapper
TOPS	Terrestrial Observation and Prediction System
TRVI	Triangular Vegetation Index
TSAVI	Transformed Soil Adjusted Vegetation Index
TVI	Transformed Vegetation Index
UNFCCC	United Nations Framework Convention on Climate Change
VI	Vegetation Indices
VIS	VISible
VOGa	Vogelmann Index a
VOGb	Vogelmann Index b
VOGc	Vogelmann Index c
WDVI	Weighted Difference Vegetation Index

1. Introduction

Earth has undergone major changes during its history. Even though change is a natural property of the Earth System, mounting evidence reveals that those imposed during the last 150 years cannot be compared with any in the past (European Space Agency 2006). In fact, human activities have driven greenhouse-gas concentrations beyond the maxima reached during the last one million years, thus increasingly affecting the climate of Earth (IPCC 2007). On terrestrial ecosystems, major anthropogenic disturbances like clearing of tropical forests, transforming vast areas into agriculture and intensifying farmland production to supply resources for the society (Foley et al. 2005), have significantly affected the carbon cycle and sequestration dynamics (Sellers et al. 1997), the biological diversity (Araújo and Rahbek 2006), and the overall ecosystems services and structure (Brown and Funk 2008; Defries and Bounoua 2004). To ensure the sustainable future management of the Earth, both natural system variability and the consequences of human activities have to be fully understood and quantified.

A major challenge for predicting the consequences of global climate change is the quantification of above/belowground carbon stocks and better understanding of carbon sequestration dynamics. Monitoring land use changes and vegetation dynamics represent key components of the carbon cycle in terms of biomass production and of their role regarding the interaction between land surface and the atmosphere (National Research Council 1999). The importance of monitoring land use changes such as afforestration, reforestration and deforestration, is stressed within the context of the Kyoto Protocol to the United Nations Framework Convention on Climate Change (UNFCCC). Additionally, the linkage between the carbon and the nitrogen cycle is crucial for a better understanding of the carbon cycle (Vitousek et al. 1997). Fertilization of agricultural crops and nitrogen depositions affect carbon storage by increasing nitrogen losses as gases and solute from soil and by generating vegetation degrading with prolonged nitrogen additions (Schulze et al. 1989). Proper linkage between the carbon, water and nitrogen cycles is therefore important for understanding feedbacks of the terrestrial ecosystem to the atmosphere (Ustin et al. 2004a).

Monitoring the state of biological diversity is another key challenge for the sustainable management of the Earth System. Over the last 50 years biodiversity has been lost more rapidly than any time during the course of the human history (Seabloom et al. 2002) while predictions and scenarios show that these rates will not decrease in the future (DIVERSITAS 2002; Gaston 2000). Since ecosystems collectively determine the biogeochemical processes that regulate the Earth System, loss of biodiversity and its ecological consequences significantly affect functional properties like productivity, decomposition rates and nutrient cycling (Loreau et al. 2001). In Switzerland, efforts to map, monitor and preserve biodiversity

are driven by Federal Laws on the protection of nature and landscape in fulfillment of the Convention on the Conservation of Biological Diversity of Rio de Janeiro (UNCED 1992). Since 1994 major efforts to identify, map and monitor species-rich habitats like dry grassland sites across the country are ongoing (Eggenberg et al. 2001). These ecologically valuable natural or semi-natural habitats represent a very promising opportunity to restore and conserve biodiversity in agricultural landscapes (Duelli and Obrist 2003) since more than 350 species (13.1%) of the red list of higher plants and pteridophytes depend on these habitats (Delarze et al. 1999).

Equally important to monitoring the current status of terrestrial ecosystems, is our ability to anticipate and prepare for their response to anthropogenic disturbances in the future. Forecasting the state of ecosystems and ecosystem goods and services under different scenarios of climate, land use change and human population growth provides an advanced decision-making tool to be used in the mitigation of natural hazards (Clark et al. 2001). Climate forecasting capabilities of ocean-atmosphere circulation models have significantly improved over the years (Zebiak 2003) driving successful ecological forecasting in other fields such as agriculture (Cane et al. 1994), health (Thomson et al. 2006) and water resources (Wood et al. 2001). Overall, reliable ecological forecasting depends on experimental and observational data of parameters like CO_2, temperature, moisture and nutrients that extend to landscapes and whole ecosystems. The provisioning of data at these scales are needed since landscape processes are most of the times very difficult to infer from fine-grained studies (Carpenter 1996; Reich et al. 2001).

It is becoming evident that timely, high-quality and long-term global information on ecosystem properties is required to improve our understanding of the effects of human activities on the terrestrial ecosystems and forecast their future development. Ideally, extensive in-situ experimental data would be collected over a wide range of conditions. Even though this approach has the benefit of acquiring highly accurate measurements, time and human resources constrain the data collection only to local-scale studies. The only available data source that may provide us with systematic observations at scales ranging from local to global and with information extending over several decades is remote sensing (Kumar et al. 2001; Wulder et al. 2004). The role of remote sensing is therefore central in our efforts to improve our understanding of the effects of human activities on the terrestrial environment and to ensure sustainable management of the Earth's natural resources.

1.1 Remote sensing for ecological applications

The main ecological contribution of remote sensing is its provision of macroscopic and temporal information on key environmental variables required to monitor and asses the

evolution of an ecosystem (Aplin 2005; Cohen and Goward 2004; European Space Agency 2006). Turner et al. (2003b) outline two types of ecological remote sensing: (1) direct, which involves direct observation of vegetation or animal populations and (2) indirect, where environmental variables derived from remotely sensed data are used as proxies for underlying ecological phenomena. Derived environmental variables can be either categorical/discrete (eg. land cover) or continuous (eg. biomass, LAI). Historically, one of the primary uses of ecological remote sensing has been land cover classification. During the last decades several land cover maps at regional to global scales have been produced (Bartalev et al. 2003; DeFries et al. 1994; Loveland et al. 2000; Mücher 2000; Vogelmann et al. 2001). Additionally, various continuous variables that provide information on ecosystem state and functions over large areas have been derived from remote sensing. These include fractional vegetation cover that is critical for the parameterization of biogeochemical models (Turner et al. 2004b) and has been derived from sensors like MODIS, MERIS and others at regional to global scales (DeFries et al. 1999; Hansen et al. 2002; Schwarz and Zimmermann 2005), LAI that characterises the vegetation canopy functioning and its energy absorption capacity (Cohen et al. 2006; Deng et al. 2006; Shimabukuro et al. 2005; White et al. 1997a) and the fraction of absorbed PAR by green vegetation that is a key indicator of productivity (Bacour et al. 2006; Gower et al. 1999; Myneni et al. 2002; Roujean and Breon 1995). Other continuous environmental variables derived from remote sensing include above ground biomass (Dengsheng 2006; Foody et al. 2003; Todd et al. 1998; Wylie et al. 2002), vegetation canopy moisture content (Chen et al. 2005a; Chuvieco et al. 2002; Jackson et al. 2004; Zarco-Tejada et al. 2003) or surface albedo (Schaaf et al. 2002).

Numerous ecological applications of remote sensing exist. Since land cover characteristics influence mass and energy exchanges between biosphere and atmosphere (Cihlar et al. 1997), global land cover maps derived from coarse AVHRR data have been used to reduce the uncertainties in the estimates of CO_2 fluxes (DeFries et al. 1994; DeFries et al. 1999; Los et al. 2000). Remote sensing data collected with high spatial resolution sensors have been used to create detailed land cover maps (Bartalev et al. 2003) and maps of vegetation communities or individual plant species (Clark et al. 2005; Pengra et al. 2007; Schmidt et al. 2004). Using these derived products, ecologists have been able to predict the distribution of species across large areas that otherwise could not be surveyed (Kerr and Ostrovsky 2003). Another major ecological contribution of remote sensing is change detection (Zhan et al. 2002). The ability of remote sensing to provide continuous temporal information has been utilised to monitor ecosystem changes (Andréfouët et al. 2001; Coppin and Bauer 1994; Rogan et al. 2003; Symeonakis and Drake 2004) and to build up essential knowledge to predict ecosystem response under future environmental changes (Filella et al. 2004). In particular, increased focus has been put towards the detection of deforestation

(Achard et al. 2002; Batistella et al. 2003) due to the impact it has on biodiversity and global warming (Feddema et al. 2005; UNEP 2007). Other ecological applications of remote sensing include biodiversity monitoring (Gould 2000; Nagendra 2001; Oindo and Skidmore 2002; Oindo et al. 2003; Turner et al. 2003b), ecosystem NPP estimation (Kimball et al. 2000; Ollinger and Smith 2005; Turner et al. 2006), vegetation phenology (Ahl et al. 2006; Piao et al. 2006; White and Nemani 2006), detection of disease infection (Leckie et al. 2004) or fire risk assessment and damage (Chuvieco et al. 2002; Justice et al. 2002).

1.1.1 Hyperspectral remote sensing for ecological applications

Hyperspectral remote sensing is a relatively new technology of environmental observation. Contrary to multispectral satellites like TM or SPOT that record few rather broad spectral channels, hyperspectral sensors acquire images in a large number of channels (over 40) which have a width of typically 10 to 20 nm and are contiguous (Goetz et al. 1985). Therefore, the resulting reflectance spectra, at a pixel scale, can be directly compared to the same target measured in the field or the laboratory (Van de Meer et al. 2002). Hyperspectral sensors are passive and can be either spaceborne or airborne. At altitudes of 700 km, spaceborne sensors receive approximately 10,000 times less radiation than airborne sensors at 5 km (Kumar et al. 2001). Therefore, the satellite sensor signal-to-noise ratio is much lower compared to an aircraft sensor. However, satellite data are better suited for environmental applications that require repetitive coverage and they are considerably cheaper. The main advantages of airborne hyperspectral sensors are their flexible use, their high spectral and spatial resolution and the high signal-to-noise ratio of the recorded signal. Nevertheless, the cost of airborne data is high and due to the small spatial coverage of the data, such data are mainly used for local to regional studies (Van de Meer et al. 2002). Several airborne hyperspectral sensors currently exist like the AVIRIS (Airborne Visible/Infrared Imaging Spectrometer), the Compact Airborne Spectrographic Imager (CASI), the Airborne Visible near Infrared Imaging Spectrometer (AVIS) and the Hyperspectral Mapping Imaging Spectrometer (HyMap). On the contrary, there are only two spaceborne hyperspectral sensors, the Hyperion from NASA and the Compact High Resolution Imaging Spectrometer (CHRIS) from ESA. Currently, initiatives towards development of new state-of-the art hyperspectral sensors include the Airborne Prism Experiment (APEX) (Nieke et al. 2004), the Environmental Mapping and Analysis Program (EnMap) (Kaufmann et al. 2005), the Airborne Reflective Emissive Spectrometer (ARES) (Müller et al. 2005) and the South African Multi Sensor Microsatellite Imager (MSMI) (http://www.sunspace.co.za).

Absorption, reflectance and scattering properties of natural surfaces are defined by their chemical bonds and their three dimensional structure (Ustin et al. 2004b). For leaves in

particular, these properties are determined by the concentration of pigments, water, and by the internal leaf cell structure (Kumar et al. 2001). The wavelength range of optical sensors measuring the reflected part of the optical spectrum extends from 400 nm to 2500 nm and can be divided in to three spectral regions, namely the visible (400 – 700 nm), the near-infrared (700 – 1300 nm) and the shortwave-infrared region (1300 – 2500 nm). The visible region of the spectrum is dominated by strong absorption of foliar pigments, mainly chlorophyll, carotenoids and xanthophylls (Gitelson and Merzlyak 1994; Knipling 1970). Spectral characteristics of the near-infrared region are determined by multiple scattering of photons by internal leaf structure resulting in high reflectance and transmittance (Gausman 1985). Minor water absorption features are located at 975 and 1175 nm (Peñuelas et al. 1994; Thenkabail et al. 2000), while absorption features due to cellulose, lignin and other carbohydrates can also be observed but primarily on dry leaves (Elvidge 1990). The mid-infrared region is characterised by strong leaf water absorption. Cellulose, starch, proteins and nitrogen have additional absorption features in this region, but they are not very strong and thus are generally masked by water absorptions in fresh leaves (Knipling 1970; Kumar et al. 2001). Curran (1989) and Fourty et al. (1996) provide detailed summaries of known absorption features of biochemical components, their wavelength position and their absorption mechanism. Leaf biochemical properties, however, are not enough to characterise the remotely sensed reflectance of a vegetation canopy (Kupiec and Curran 1995). Considerable research has taken place to investigate the effects on leaf optical properties during the transition from leaf to canopy level. These studies have identified a number of parameters that build up the overall canopy reflectance. In particular, parameters like solar and sensor view angles, LAI, Leaf Angle Distribution (LAD), fractional cover (fcover), litter and stem optical properties together with background and understory reflectance are significant factors defining the canopy reflectance signal that is eventually recorded by the sensor (Asner 1998; Asner et al. 2000; Baret et al. 1994; Dawson et al. 1999; Jacquemoud et al. 1995a).

Improved understanding of leaf absorption characteristics and of the factors contributing to vegetation canopy reflectance, coupled with the ability of hyperspectral remote sensing to acquire multiple narrow bands across the electromagnetic spectrum, have led to a number of ecological studies ranging from leaf to canopy level and from local to regional spatial scales. Hyperspectral remote sensing has been used to identify key biochemicals like chlorophyll and nitrogen on dry (Elvidge 1990) and fresh leaves (Elvidge 1990; Gitelson et al. 2003; Gitelson and Merzlyak 1996) but also across forest (Dawson et al. 1999; Huang et al. 2004; Schaepman et al. 2004; Townsend et al. 2003; Zarco-Tejada et al. 2004; Zarco-Tejada et al. 2001) and grassland canopies (Beeri et al. 2007; Mutanga and Skidmore 2004b; Vohland and Jarmer 2008). Several biophysical parameters giving insight on the ecosystem status have been estimated with high accuracies, namely biomass (Cho et al.

2007; Mirik et al. 2005; Rahman and Gamon 2004; Tarr et al. 2005), LAI (Gong et al. 2003; Meroni et al. 2004), canopy water content (Riaño et al. 2005; Serrano et al. 2000; Ustin et al. 1998) and forest structural variables (Schlerf and Atzberger 2006; Schlerf et al. 2005). Hyperspectral remote sensing has also been used for land cover classification, producing much higher accuracies when compared to traditional remote sensing sources like Landsat TM (Goodenough et al. 2003) and for discriminating individual plants (Clark et al. 2005; Cochrane 2001; Schmidt and Skidmore 2001) or plant functional types (Galvão et al. 2005; Schmidt and Skidmore 2003). Other significant contributions of hyperspectral remote sensing to ecology include the mapping of biodiversity and plant species richness (Carlson et al. 2007; Carter et al. 2005), the monitoring of seasonal changes and phenology of plants and vegetation communities (Gitelson and Merzlyak 1994; Miller et al. 1991), the discrimination of crops and weed species (Peña-Barragan et al. 2006; Smith and Blackshaw 2003), the fire risk assessment (Koetz et al. 2004; Riaño et al. 2002; Roberts et al. 2006) or the identification of invasive plant species (Laba et al. 2005; Lawrence et al. 2006; Pengra et al. 2007; Underwood et al. 2003). Finally, foliar biochemical concentrations derived from hyperspectral remote sensing have been used for carbon and productivity estimates of forest habitats (Ollinger and Smith 2005; Smith et al. 2002; Turner et al. 2004b) and for deriving essential information required by the Kyoto protocol (Kurz and Apps 2006) thus supporting a better understanding of small scale interactions of the biogeochemical cycles.

1.2 Ecosystem simulation modelling and the role of remote sensing

Carbon, nitrogen, sulfur and water are transported and transformed into different substances between the atmosphere, biosphere and geosphere linking these domains at time scales ranging from seconds to centuries (Ustin et al. 2004a). Increased anthropogenic disturbances, however, have affected the distribution and timing of these local to global processes, changing their feedback relationships and thus affecting the Earth's climate. The capability to predict the response of ecosystems to these environmental and climate changes relies on the ability to understand and model the functioning of these biotic processes, in particular of the terrestrial carbon cycle at regional to global scales. The magnitude of carbon pools varies in space and time and the monitoring of carbon cycle processes like net primary production (NPP) and net ecosystem production (NEP) is critical for understanding the role of biosphere in regulating atmospheric CO_2 concentrations (Turner et al. 2004b). NPP is the rate at which plants in an ecosystem fix CO_2 from the atmosphere (gross productivity) minus the rate at which it returns CO_2 to the atmosphere through plant respiration (Field et al. 1995). NPP represents the net carbon input from the atmosphere into vegetation and thus is widely used as an indicator for sequestration of atmospheric CO_2 by terrestrial ecosystems (Field et

al. 1995). When additional releases of CO_2 by heterogenic respiration of decomposing dead organic matter are taken into account, carbon retention of an ecosystem is significantly less than NPP and is defined as NEP (Jiang et al. 1999).

To improve our understanding and capability to estimate NPP accurately at regional to global scales there is a need to integrate multiple, complementary and independent environmental data sources that drive its spatial and temporal variability. The only feasible way is to use ecosystem simulation models, which synthesize environmental data that regulate NPP into single coherent analysis of terrestrial carbon fluxes (Curran 1994). Ecosystem simulation models are simplified versions of reality and according to Ruimy et al. (1994) they can be classified into three categories: (a) statistical models (Lieth 1975), (b) parametric models (Law and Waring 1994; Potter et al. 1993) and (c) process models (Foley 1994; Melillo et al. 1993; Running et al. 1989). Statistical models attempt to link NPP with meteorological parameters or evapotranspiration through regression analysis, putting considerable efforts in developing a quantitative understanding of short term ecosystem processes at the plant and population scale (Lieth and Whitaker 1975). Parametric models use the efficiency concept from incident radiation and its absorption coefficient by vegetation canopies to drive spatial estimates of NPP. Finally, ecosystem process models operate by simulating biological processes that drive NPP, namely photosynthesis, respiration and transpiration (Running and Hunt 1993).

Ecosystem process models should be considered more reliable since they are based on the processes that regulate the ecosystem and its functioning (Liu et al. 1997). Consequently, process models are more suitable to investigate the response of ecosystems to increasing temperature and atmospheric CO_2 concentrations since they provide an insight on the mechanisms of biomass production and plant-environment interactions (White et al. 1997b). Considerable research in developing ecosystem process models of varying complexity has taken place in the last decades. Cramer et al. (1999) provide a detailed description and an intercomparison of some of them. While different in complexity, early ecosystem process models were typically non-spatial (Running and Hunt 1993), thus making it difficult to up-scale from point processes to large regions. To overcome this problem a number of scale-independent deterministic models have been developed that require spatial estimates of climate, soil and vegetation variables to parameterise, drive and validate them (Curran 1994). Remote sensing is a major source that provides temporal and spatial information on a number of these parameters, thus offering the potential to explicitly link ecosystem functions to the structure of the landscape in space and time (Wessman 1994b) and extrapolate the non-spatial ecosystem process models to regional and global scales (Aber et al. 1993; Curran 1994).

Linking remote sensing and ecosystem process modelling is a rapidly growing field with a number of approaches at different spatial and temporal scales (Cohen and Goward

2004; Turner et al. 2004b). In a review paper, Plummer (2000) outlines four major strategies that are used to link ecosystem process models and remote sensing:

a) Use of remotely sensed data for driving ecological process models (Green et al. 1996; Lucas et al. 2000; Running et al. 1989). This is the most common strategy where remotely sensed data are used to generate model initialisation products that correspond to forcing functions or state variables in ecological modelling.
b) Use of remotely sensed data to test, validate or verify predictions of ecological process models (Running and Nemani 1988). Here either the outputs of the ecological process model are compared against estimated variables from remote sensing like LAI and albedo or if the ecological model is coupled with a radiative transfer model, the predicted canopy reflectance is compared to the one recorded from remote sensing.
c) Use of remotely sensed data to constrain ecological process models (Hazarika et al. 2005; Knorr and Heimann 2001). This is the data-assimilation strategy, where new remotely sensed variables are constantly used to update the model state variables provided there are enough and regular observations.
d) Use ecological process models to aid the interpretation of remotely sensed data (Turner et al. 2003a). Here ecosystem models are used to constrain reflectance model inversion or to assess the predictive and diagnostic capacity of remotely sensed data and algorithms.

From the above discussed strategies, the most demanding use of remote sensing is providing variables for the parameterisation and driving of ecosystem process models (Curran 1994; Turner et al. 2004b). Some of these key variables are presented in detail below. Remote sensing can provide accurate maps of cover types that are essential in order to simulate the processes corresponding to each land cover class (Nemani and Running 1996). Vegetation cover types show very different morphological and ecophysiological parameters as a result of adaptations to the environmental conditions (Reich et al. 1997). Especially for forest habitats, the ability to map forest structure and successional stages with remote sensing greatly improves the accuracy of ecosystem process models (Goward and Williams 1997) since changes in NPP with stand age is a proven fact (Turner et al. 2004b). Significant contributions of remote sensing have been the development of global land cover maps (DeFries et al. 1994; Field et al. 1995; Los et al. 2000; Loveland et al. 2000; Zhan et al. 2002) or of fine-scale maps of landscape structure using only Landsat TM (Cohen et al. 2002) or combined with canopy reflectance models over areas of ecological importance like the boreal ecosystems (Sellers et al. 1995). LAI is another key parameter that determines the rate at which energy and matter

are exchanged in ecosystems (Curran 1994). Thus, estimation of LAI by remote sensing can be used in ecosystem process models to infer the rate of canopy photosynthesis and evapotranspiration over large areas (Running and Coughlan 1988). Remotely sensed estimates of LAI are usually derived through its significant correlation to NDVI, even though this relationship becomes problematic at high but also at low vegetation densities (Fassnacht et al. 1997; Gower et al. 1999; Myneni et al. 2002; White et al. 1997a). LAI has also been estimated through the inversion of MODIS (Fang and Liang 2005) or hyperspectral data (Meroni et al. 2004; Schlerf et al. 2005) and from the fusion of lidar and hyperspectral data (Koetz et al. 2007; Morsdorf et al. 2006). Accurate estimates of above-ground vegetation biomass are very important for improving the assessment of global carbon budgets (Curran 1994). Ecosystem process models use vegetation biomass in order to initialise carbon pools, simulate local carbon budgets and more importantly, to estimate autotrophic respiration (Turner et al. 2004b). Remote sensing data from optical sensors have been widely used to estimate the spatial and temporal variability of biomass (De Jong et al. 2003; Filella and Peñuelas 1994; Moreau et al. 2003; Todd et al. 1998; Van Tuyl et al. 2005). Nevertheless, since information on standing woody biomass parameters, like the tree stem size are also required, data from Synthetic Aperture Radars (SAR) (Ranson et al. 1997; Rauste 2005) and lidar (Lefsky et al. 1999; Riaño et al. 2003) which can penetrate the canopy and therefore interact with the woody components of vegetation have been used. Fusion of SAR and lidar to map the spatial distribution of biomass has also been applied (Hyde et al. 2007; Treuhaft et al. 2004). Dengsheng (2006) provides a thorough review on the existing techniques and future challenges for remote sensing-based biomass estimation.

Measuring foliar biochemical content is another crucial parameter for accurate modelling of spatial patterns of biochemical processes. The canopy concentration of chlorophyll, nitrogen and lignin drives key processes in ecological models since chlorophyll is directly related to the rate of photosynthetic production (Curran 2001), nitrogen to the availability of nutrients and to carbon allocation (Schimel 1995) and lignin to the rate of nutrient cycling via its influence on decomposition rates (White et al. 2000). Remote sensing estimates of canopy foliar concentrations like chlorophyll (Gitelson and Merzlyak 1994; Jago et al. 1999; Yoder and Pettigrew-Crosby 1995; Zarco-Tejada et al. 2004), nitrogen (Boegh et al. 2002; Mutanga et al. 2003; Serrano et al. 2002; Thulin et al. 2004; Townsend et al. 2003) and lignin (Serrano et al. 2002) have been derived from hyperspectral sensors and some broadband sensors (Jacquemoud et al. 1995a; Lucas and Curran 1999; Phillips et al. 2006).

Several studies exist where the remotely sensed parameters mentioned above were used to parameterise and drive ecosystem process models. These parameters were: land cover maps (DeFries et al. 1999; He et al. 1998; Kimball et al. 2000; Liu et al. 1997; Matsushita and Tamura 2002; Ollinger et al. 1998; Running et al. 1999; Turner et al. 2004a), LAI (Hazarika

et al. 2005; Liu et al. 1997; Lucas and Curran 1999; Running et al. 1989), aboveground biomass (Green et al. 1996; Kimball et al. 2000) and foliar biochemical concentrations (Lucas and Curran 1999; Ollinger and Smith 2005).

1.3 Ecological challenges of grassland habitats

Grasslands, both human made and natural, cover nearly 20% of the land surface world-wide (Scurlock and Hall 1998). They interweave with croplands and patches of forest or stretch across vast natural plains, they are part of seasonally flooded lowlands or they cover high mountain areas and plateaus. Overall, grasslands represent a unique variety of colours, structure and biodiversity of the Earth surface. Grassland habitats can either be natural or managed. Managed grasslands are those habitats where humans actively intervene with management practices in order to change the feed availability and quality for livestock production (Tueller 1998). Hill (2004) distinguishes two types of managed grasslands: (a) human made pastures and meadows, which are the result of removal of forest and woodlands; pastures are sown grass and/or legume-based agricultural fields, irrigated or dryland, used for intensive animal production; meadows are long established areas of diverse grasses, forbs and herbs that have reached an ecological equilibrium and are used for hay, grazing, game, or as wildlife preserves, (b) highly managed natural grasslands, which are vast natural areas which have been modified by humans and are used for intensive grazing by domesticated livestock.

Natural and semi-natural grasslands are species-rich habitats being of major ecological importance for biodiversity conservation in agricultural landscapes (Alrababah et al. 2007; Duelli and Obrist 2003; Stenseke 2006). Their unique biological and structural characteristics are the result of centuries of traditional management practices like mowing, grazing and partly artificial fertilisation (Garcia 1992). These semi-natural grasslands provide a wide range of habitats supporting a high biological diversity of plants, insects and animals, many of which are classified as endangered or threatened (Delarze et al. 1999; Pärtel et al. 1999). However, growing evidence shows that the diversity of grasslands has significantly decreased within the last decades, threatening biodiversity and posing a serious conservation problem (Klimek et al. 2007). In particular, pressure for agricultural production has led to intensification of grasslands sites when they are easily accessible, and at the same time increasing abandonment of the remote sites (Tasser and Tappeiner 2002). When traditionally managed grasslands are abandoned, their plant composition changes and their agricultural quality decreases, eventually leading to reforestation associated with a loss of biodiversity (Fischer and Wipf 2002). In addition, when grassland sites are managed more intensely, application of fertilisers has shown to decrease the species richness as well (Theodose and Bowman 1997). Apart from human induced disturbances, additional threats regarding the balance between biodiversity,

ecosystem stability and ecosystem processes of grassland habitats arise from climate change and its impacts. Climate change is expected to enhance opportunities for invasions (Buckland et al. 2001), namely: (a) invasion of grasslands by woody species, which would lead to loss of the grassland system; or (b) the invasion of grasslands by alien and relatively unpalatable species (Watkinson and Ormerod 2001). Overall, at such unique ecosystems, where productivity, conservation and climate impacts are three very closely related aspects, increased attention is required to preserve the habitats and its biodiversity.

Grassland habitats play a significant but poorly recognised role in the global carbon cycle as well (Hall et al. 1995). Grasslands are major carbon pools accounting for at least 10% of the global total (Eswaran et al. 1993). It is also estimated, that grasslands are responsible for as much as 20% of the total terrestrial net primary production (Scurlock and Hall 1998). Interactions between climate change and grassland biogeochemical cycles have received considerably less attention compared to forests (Hall and Scurlock 1991). Research has shown that future environmental changes like increasing atmospheric CO_2 and climate change will have an important impact on carbon exchanges between vegetation, soil and the atmosphere (Cao and Woodward 1998) and on the grassland soil carbon stocks worldwide (Parton et al. 1995). In particular, Owensby (1997) has shown that elevated CO_2 concentrations in the atmosphere may lead to increased sequestration of carbon in grasslands due to (a) a raise in photosynthesis rates in C_3 species, (b) increases in water and nitrogen use efficiency in C_4 species and (c) reduced rates of plant decomposition due to higher C/N ratios. Under these circumstances the role of managed grasslands is becoming ever more significant for the global carbon balance (Riedo et al. 1999). Managed pastures and grasslands have higher net primary production rates than natural grasslands and savannas. Additionally, they are often located adjacent to the highest sources of greenhouse gas emissions, namely industrial and urban areas (Hill 2004).

In the face of global climate change and the growing demand for agricultural productivity, the pressure on grassland ecosystems is expected to increase in the future. Sustainable management strategies that ensure the protection and conservation of biodiversity are therefore required. Also a better understanding of the grassland carbon cycle and its spatial representation are mandatory in order to judge the role of grasslands upon the global carbon cycle, currently and under possible futures. As described above, hyperspectral remote sensing and ecosystem process modelling are two synergistic technologies that have the potential to offer scientists and decision-makers accurate, reliable and timely information on the current and future available resources of any ecosystem. This dissertation aims at evaluating the potential of hyperspectral remote sensing and ecosystem process modelling for conserving biodiversity by mapping species-rich grassland habitats and for providing an improved understanding of their biogeochemical cycles at the local to regional scales.

1.4 Objectives and structure of the dissertation

The major objectives of this dissertation are to explore the potential of hyperspectral remote sensing for (a) biodiversity conservation by mapping species-rich grassland habitats and for (b) deriving vegetation properties relevant to ecosystem productivity that will eventually be used to initialise an ecosystem process model. The dissertation consists of three main research parts. In the *first part* we use intra and interannual spectral measurements of different grasslands habitats collected with a field spectroradiometer to explore their spectral seperarability. In the *second part* we focus on the development of statistical models for predicting above-ground biomass of grasslands from spectral measurements recorded with a field spectroradiometer and evaluate the potential of up-scaling these models to spaceborne hyperspectral data (Hyperion). Finally, the *third part* focuses on initialising and driving an ecosystem process model using quantitative information of foliar biochemical concentrations estimated from airborne hyperspectral remote sensing (HyMap).

The following research questions have been developed and will be investigated in this dissertation:

Part 1: Spectral separability of grassland habitats (chapter 4)

- Can we identify spectral regions that allow significant discrimination between grassland types during a season?
- Which are the best wavebands and what is the best season for discriminating between the grassland types using classification trees (CART)?
- How does the number and the variance of significantly discriminating wavebands and the classification accuracy differ between two years?
- Is continuum removal transformation suitable for enhancing differences and thus discrimination between grassland types during the growing season?

Part 2: Biomass estimation of grassland habitats (chapter 5)

- Can we develop a method using field spectrometer data for estimating above ground biomass in grasslands that is independent of specific habitats or phenological period?
- Is it possible to scale models calibrated from plot based measurements to larger landscapes as seen from spaceborne sensors?
- To what extent can estimated biomass distribution maps be used to explore the relationship between species richness and biomass on grassland habitats?

Part 3: Remote sensing and ecosystem process modelling (chapter 6)

- Can statistical models be calibrated from airborne HyMap hyperspectral data to predict foliar C:N concentration of grassland habitats at the regional scale?
- Can we use these spatial predictions of foliage C:N to initialise and drive an ecosystem process model in order to estimate NPP of grassland habitats?
- Do NPP estimates using spatial foliar C:N predictions derived from HyMap hyperspectral data differ from those where values from "global" or "regional" C:N field measurements are used instead?
- What is the sensitivity of the ecosystem process model to errors of predicted foliar C:N, induced during the statistical modelling process?

The structure of the dissertation is as follows: chapter one gives a general background, introduction, problem description and it presents the research questions of the dissertation. Chapter two describes the study area, and the materials used, such as field and laboratory measurements together with the acquisition and preprocessing of airborne HyMap and spaceborne Hyperion data. Chapter three presents the statistical methodologies used to explore the spectral separability of grasslands and to retrieve biomass and biochemical estimates. Details on the Biome-BGC ecosystem process model are also discussed here. Chapter four presents the results of the spectral separability of the grassland habitats, chapter five of the biomass estimations from the field and Hyperion spectral data while results from the biochemistry assessment from the Hymap data together with the NPP estimates derived from the ecosystem process model are presented in chapter six. Finally, chapter seven summarises the main conclusions of this dissertation and provides an outlook for future research potential.

2. Materials

The variety of material used to investigate the potential of hyperspectral remote sensing for spectral discrimination of grasslands types and for deriving biophysical and biochemical characteristics of these habitats are discussed here. In particular, the study site, the field sampling strategies, the laboratory analyses and the hyperspectral imagery acquired and processed are described in this chapter.

2.1 Study area

The study area selected for this dissertation is located at the Central part of the Swiss Plateau (8°02' E, 47°25'N) near the city of Aarau (Figure 2.1) with an elevation ranging from 350 to 500 m. Grassland samples were collected in 2004 and 2005 from four characteristic low elevation grassland types (Table 2.1) previously mapped in a national mapping campaign (Eggenberg et al. 2001). These grassland types belonged to a classification scheme developed by Eggenberg et al. (2001) that was based on the phytosociological composition of the vegetation species with an additional effort to create a vegetation key that was valid for the whole of Switzerland up to the tree-line. The four semi-natural grassland types sampled (AE, AEMB, MBAE, MB) were purposely selected due to their differences in species composition and nutrient availability.

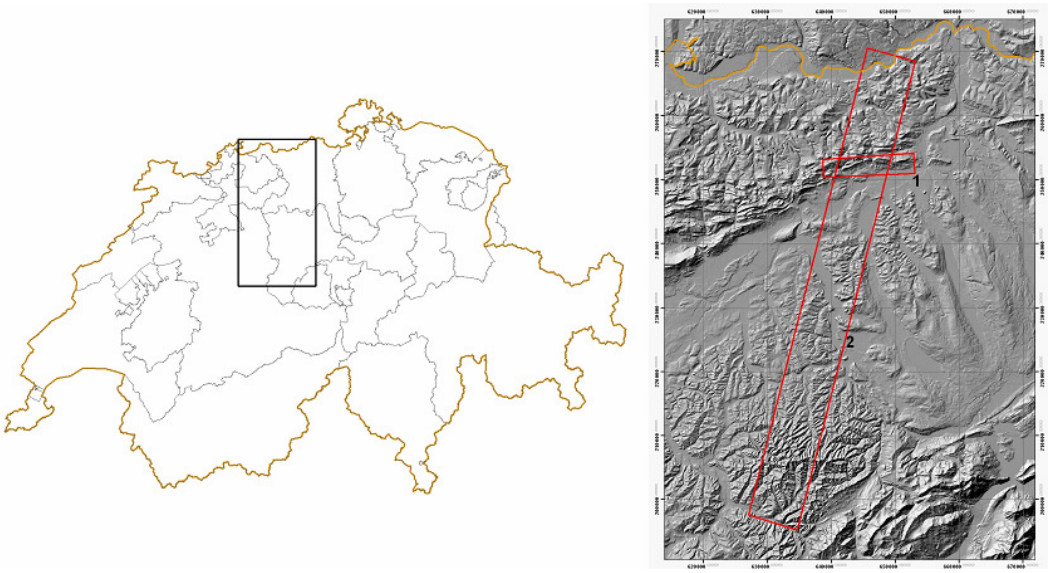

Figure 2.1 Overview of the study area location in Switzerland (left) and of the coverage of the acquired hyperspectral data (right) from the HyMap (1) and Hyperion (2) sensors.

These differences enabled the collection of a wider range of biomass and foliar chemistry samples. In particular, AE is a species-rich *Arrhenatherion* type managed grassland, that is

mesic and nutrient rich. The mesic and species-rich type AEMB includes tall, dense and multi-layered stands composed of many grasses, several herb species, and is still comparably nutrient-rich (Eggenberg et al. 2001). The type MBAE stands in-between AEMB and MB with respect of species richness, nutrients and canopy height. Finally, true semi-dry MB grasslands are comparably nutrient-poor and are generally dominated by *Bromus erectus* or *Brachypodium pinnatum* with stems standing well above the surrounding shorter herb vegetation. These stands are generally colourful and rich in herbs. The main management practice on the grasslands in the study area is production of hay and very few are used as pastures. The research described in chapter 4 involves data from three grassland types, namely AE, AEMB an MB whereas research described in chapter 5 and chapter 6 involves data from all four grassland types.

Table 2.1 Description of the four grassland types sampled.

Type code	Phytosociology	Description
AE	species-rich Arrhenatherion type	Mesic, species rich, nutrient–rich, managed
AEMB	Transition Arrhenatherion to Mesobromion	Moderately-mesic, species-rich
MBAE	Transition Mesobromion to Arrhenatherion	Moderately-dry, species-rich
MB	Mesobromion type	Species-rich, semi-dry grassland

2.2 Field sampling of biophysical and biochemical grassland parameters

2.2.1 Biomass - Species Richness sampling

For the research described in chapter 5, a total of 11 fields belonging to the four grassland types were selected from the existing national campaign map. The fields were chosen to have a total area larger than five Hyperion pixels and were checked for purity: we only kept grasslands where the major vegetation type covered at least 75% of the mapped polygon. Sampling was performed at four times during the growing season of 2005 (10th June, 23rd June, 28th July, 10th August). We did so to ensure that normally occurring variation due to canopy growth stage and management factors was recorded. Biomass samples were clipped at ground level using a 32 cm radius metal frame. Within each field, three randomly selected plots were sampled to account for the spatial variability of biomass.

A total of 155 biomass samples were collected from the 11 grassland fields during the growing season of 2005.

Grassland species richness data were extracted from a dataset that was collected during a previous mapping project (Eggenberg et al. 2001) and covered scattered patterns throughout Switzerland. For every grassland field that was mapped in the national campaign, a circular sampling plot with a radius of 3 m was established and each individual plant species and its abundance were recorded. The total number of plant species recorded at the sampling plot was therefore assigned to the whole mapped grassland. A total of 106 grassland fields with a maximum distance of 14 km from our sampling sites were available within the Hyperion scene. These fields were finally selected and used for further analyses.

2.2.2 Foliar biochemical sampling

To determine foliar C and N concentrations, for the research described in chapter 6, grassland samples were collected from 27 plots on 30th July 2004, one day after the HyMap image acquisition. The sampling plots were located on fields belonging to the 4 grassland types (AE, AEMB, MBAE, MB). The sampling plots had an area of 5 x 5 meters and were homogenous in species composition and cover. Coordinates of the centre of each plot were recorded with a Trimble GeoXT GPS receiver, which corrects for multipath biases. To improve the positional accuracy of the centre of the plot, 20 to 30 GPS measurements were recorded and a post processing differential correction to the recorded data was applied using the Pathfinder Office software (Trimble 2005). The mean GPS precision for the centre of the 27 sampling plots was 3.2 m. Representative samples from each plot were collected by randomly clipping grass from several spots in the 5 x 5 m plot. Eventually, the samples from several spots in each plot were mixed and collected in paper bags for laboratory analysis.

2.3 Laboratory analyses

2.3.1 Biomass analyses

As mentioned above, a total of 155 biomass samples were collected for the research described in chapter 5. The collected material was stored in pre-weighted air-sealed plastic bags and brought to the laboratory where the total fresh biomass was measured. Samples were then dried in the oven at 65 ºC for 72h and weighted again to measure the total dry biomass. The plant water content was calculated as the difference between fresh and dry weight. Finally, the mean value of the three fresh biomass samples collected at each field was assigned as the measured biomass at that field.

2.3.2 Foliar biochemical analyses

In order to extract foliar C and N concentrations for the research described in chapter 6, the grassland samples from within each plot were collected in paper bags and then taken to the laboratory for further analysis. Initially, grassland samples were dried in the oven at 65 ºC for 48h and afterwards were ground to powder. Finally, they were injected into an elemental analyser (NA 2500; CE Instruments, Milan, Italy) to measure C and N foliar concentrations. Two sub-samples were analyzed from each sample to check for within-sample variation. None of the samples exceeded a threshold of 3 % variation between the two sub-sample measurements and its mean. All the analyses were performed at the ISO certified laboratories of the Swiss Federal Research Institute WSL.

2.4 Field spectral sampling of grasslands

2.4.1 Field spectral sampling for evaluating the spectral separability of grasslands

The research described in chapter 4 concentrated on exploring the seasonal and annual spectral separability of different grassland types. Therefore, only spectral sampling was performed on these grassland habitats. A total of nine fields belonging to the three previously introduced grassland types (AE, AEMB, MB) were selected from the national campaign map. The fields were chosen to have an area larger than five Landsat TM pixels. Spectral profiles of the grassland types were collected using the Analytical Spectral Devices (ASD) FieldSpec Pro FR spectroradiometer. This spectroradiometer has a 350-2500 nm spectral range and 1 nm spectral resolution with a 25° field-of-view (ASD 2000). Collected spectra were converted to absolute reflectance by reference measurements over a Spectralon reflectance panel (Labsphere, Inc., North Sutton, N.H.) with known spectral properties. Reflection panel measurements were made every 20 spectra to minimize errors due to changes in atmospheric condition. Spectral samples were collected during the growing seasons of 2004 and 2005 at six time steps from May to September, respectively (Table 2.2). Reflectance spectra were taken under sunny and cloud free conditions between 10:00 and 16:00 h local time while walking along two diagonal transects across the length of every field to ensure that the sampling would capture the in-field spectral variability. Each field was sampled using the same transect lines throughout the growing season for both years. Reflectance spectra were taken from nadir at a height of ~1.5 m above vegetation canopy and approximately 60-100 spectra were collected per field. Additionally, a detailed field protocol was maintained. Data in the spectral range of 1350 -1415 nm and 1800 -1950 nm were seriously affected by atmospheric water vapour absorption. Hence, they were removed from any subsequent analyses. We additionally applied a 95% confidence interval threshold around the mean

spectral signature of every field in order to identify and remove potentially erroneous recordings.

Table 2.2 Spectral sampling dates and number of spectral signatures collected for the grassland separability study (chapter 4) during the growing seasons of 2004 and 2005.

Year	Date	Julian Day	Spectral signatures collected
2004	25-May	146	611
	10-June	162	595
	25-June	177	480
	28-July	210	1030
	15-August	228	497
	18-September	262	711
2005	20-May	140	776
	10-June	161	694
	23-June	174	712
	28-July	209	761
	10-August	222	772
	23-September	266	600

2.4.2 Field spectral sampling for estimating aboveground biomass patterns in grassland habitats

For the research described in chapter 5 a total of 11 fields belonging to the four grassland types were selected and biomass sampling was performed at four times during the growing season of 2005 (10th June, 23rd June, 28th July, 10th August). Parallel to the biomass sampling, canopy spectral profiles of these grassland fields were collected using the Analytical Spectral Devices (ASD) FieldSpec Pro FR spectroradiometer. Spectral measurements for three grassland types (AE, AEMB, MB) were the same for this study as they were for the grassland spectral separability study (chapter 4), while a similar spectral sampling procedure was followed for the grassland sites belonging to the MBAE type. Overall, spectral measurements were collected while walking along 2 diagonal transects across the length of every field. This resulted in 60-100 spectral measurements covering the whole extent of the grassland fields and not specifically the plots where biomass samples were collected from. The ASD field spectra were then resampled to simulate Hyperion spectral bands using the spectral center wavelength (CWL) and full-width half-maximum

(FWHM) information for each individual Hyperion band (Barry 2001). After investigation for erroneous spectral measurements, the mean spectral reflectance of each grassland field was calculated as the mean of the 60-100 spectral measurements collected over the whole extent of this field.

2.5 Hyperspectral image acquisition and processing

2.5.1 Airborne HyMap data

Imaging spectrometer data were recorded over the study area on the 29th July 2004 using HyVista's Hyperspectral Mapping Imaging Spectrometer (HyMap). The HyMap sensor was flown on a Dornier Do 228 aircraft at an altitude of 3000 m and acquired data in 126 wavebands from 450 to 2480 nm, with a spectral resolution of 15–20 nm (Cocks et al. 1998). The instantaneous field of view (IFOV) of the sensor is 2.5 mrad along-track and 2.0 mrad across-track and the field of view (FOV) 60 degrees or 512 pixels. For this study the spatial resolution of the data was 5 m. One 2.5 x 12 km scene was acquired covering the study area under cloud free conditions. Subsequent analyses steps were to transform the HyMap at-sensor radiance to apparent surface reflectance using the ATCOR4 software (Richter and Schlaepfer 2002) that performs a combined atmospheric/topographic correction. Thus, effects of terrain such as slope, aspect and elevation of the observed surface are accounted for. As a second step of the correction process, the HyMap data were orthorectified based on the parametric geocoding procedure PARGE. PARGE is a procedure which considers the terrain geometry and allows attitude and flightpath dependent distortions to be corrected (Schläpfer and Richter 2002). The Swisstopo-DHM25 was used to geo-register the HyMap data. The resolution of the DHM25 was 25 m. In order to be used for geo-registration it had to have the same resolution like the Hymap data. Therefore, the DHM25 was resampled to 5 m using the method of bilinear interpolation (Richter 2003).

Once the atmospheric correction was applied, HyMap surface reflectance data were compared to field spectroradiometer measurements collected simultaneously with the image acquisition. The Analytical Spectral Devices (ASD) FieldSpec Pro FR was used to record reflectance values over a number of different surfaces like asphalt, grasslands and water. A comparison of a grassland surface recorded with an ASD and with HyMap is presented in Figure 2.2. The absolute reflectance differences for grassland surfaces between the HyMap and the ASD measurements were 3.2 % at 740 nm and 3.6 % at 1500 nm.

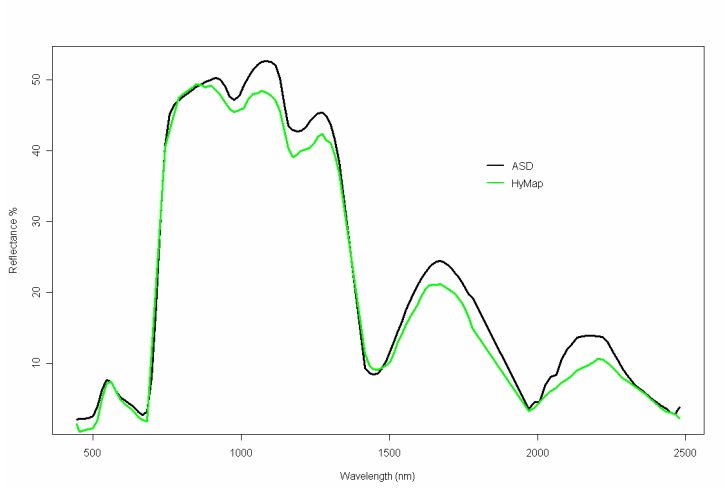

Figure 2.2 Comparison of a grassland spectral reflectance measured with an ASD field spectroradiometer on the ground (black) and from the atmospherically corrected HyMap scene (green).

2.5.2 Spaceborne Hyperion data

Hyperion data were acquired over the study area at nadir (overhead) pass on 10th August 2005 at 10:06:49 GMT. The EO-1 satellite has a sun-synchronous orbit at 705 km altitude. The Hyperion sensor collects 256 pixels with a spatial resolution of 30 m over a 7.65 km swath with a maximum acquisition length of 180 km. Data is acquired in pushbroom mode with two spectrometers. One operates in the VNIR range (70 bands between 356-1058 nm with an average FWHM of 10.90 nm) and the other in the SWIR range (172 bands between 852-2577 nm, with an average FWHM of 10.14 nm) (Pearlman et al. 2003). From the 242 Level 1R bands, 44 are set to zero by software (bands 1-7, 58-76, 225-242). Hyperion radiometrically corrected Level 1R data acquired over the study area were delivered by the USGS in Hierarchical Data Format (HDF). The length of the Hyperion stripe for the particular study was 75 km.

Before any further analyses could take place, corrections for a number of issues concerning the Hyperion data were applied. In particular, post-Level 1R data processing scene included correction for striping pixels, smoothing using forward and inverse Minimum Noise Fraction transformation (MNF), atmospheric correction and image orthorectification. Dark vertical striping is visually apparent in several of the Hyperion bands especially those of the VNIR and some of the SWIR. These stripes are caused by miscalibrated, dead and stuck detectors in the pushbroom sensor of the Hyperion (Datt et al. 2003). Striping anomalies can appear as (a) columns that are consistently darker than the columns on either side but follow the changes in digital number (DN) of those two adjacent columns or (b) columns that are

darker than their two adjacent columns but do not track with their changes in digital number. A correction algorithm to correct for this problem was used (Eckert and Kneubühler 2004). This algorithm was applied at each band horizontally to compare the DN value of each pixel with the value of its immediate left and right neighbouring pixels. A pixel was labelled as a potential erroneous pixel if its DN value was smaller than the DN's of neighbouring pixels. Once this procedure was finished, each band was scanned vertically to measure the number of potentially erroneous pixels in each column. Given that the number of consecutive potentially erroneous pixels and the percentage of erroneous pixels in a column were larger than a certain threshold, this column was marked as a stripe. Then, the erroneous DN values of the pixels were replaced with the average DN values of the immediate left and right neighbouring pixels. After removal of Hyperion bands that (a) were set to zero, (b) were in the spectral range of 1350 -1415 nm and 1800 -1950 nm and were seriously affected by atmospheric water vapour absorption and (c) bands that overlapped between the two spectrometers, a total of 167 bands were available for further analysis (426 – 2355 nm).

Atmospheric correction of the Hyperion data was then performed using the ATCOR-4 software (Richter 2003), an atmospheric correction program that is based on look-up tables generated with the radiative transfer code of MODTRAN-4. Atmospheric correction was first applied using vaying parameters for atmospheric water vapour content and visibility. Each time the Hyperion surface reflectance was compared to field spectroradiometer measurements collected simultaneously with the image acquisition over grassland areas (Figure 2.3). Eventually, the parameters selected for applying the atmospheric correction were: rural aerosol model, water vapour column of 1.0 gm^{-2} and visibility of 40 km. The resulting atmospheric correction yielded absolute reflectance differences for grassland surfaces between the Hyperion and the ASD measurements of 7 % at 740 nm and 5 % at 1500 nm.

Additionally, smoothing of the Hyperion data was applied using first a forward and then an inverse Minimum Noise Fraction transformation (MNF) as described by Datt et al. (2003). The MNF transformation was used since it did not degrade the spatial resolution of the Hyperion data. The initial MNF transformation extracted information dimensions relative to an assumed noise structure in the data. Then, the components corresponding to low SNR and unstructured spatial statistics could be eliminated from the data by applying an inverse MNF transformation to the MNF components not affected by noise. For better application of the dimensional noise reduction Datt et al. (2003) suggest that the VNIR and SWIR data of the Hyperion should be handled separately due to the different structure of the two arrays. Therefore, for this study forward MNF transformation was applied to the VNIR and SWIR separately and after inspection of the MNF components, the first ten from the VNIR and the first six from the SWIR were chosen to apply the inverse-MNF to finally acquire the corrected Hyperion data.

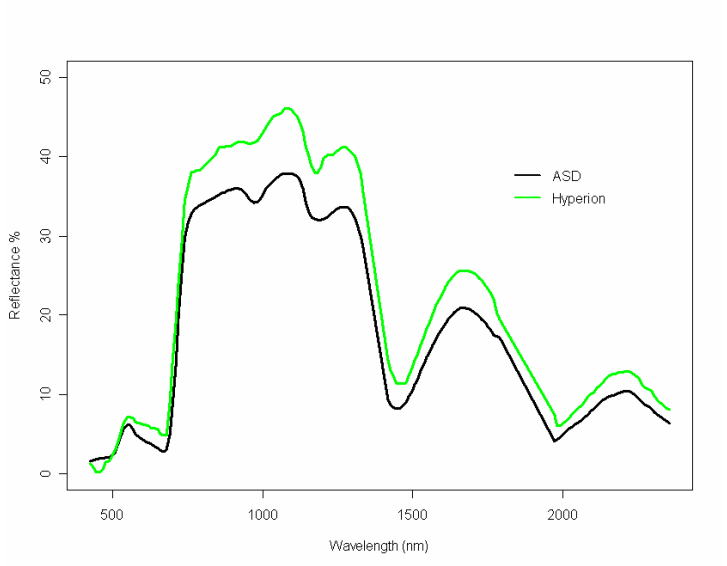

Figure 2.3 Comparison of a grassland spectral reflectance measured with an ASD field spectroradiometer on the ground (black) and from the atmospherically corrected Hyperion scene (green).

Finally, orthorectification of the Hyperion scene was performed with the software package PCI Geomatica Orthoengine that uses the parametric sensor model (Eckert and Kneubühler 2004; PCI Geomatics 2006). Hyperion orbit and scene parameters were selected and a total of 25 ground control points (GCP's) were collected. Using these 25 points, the model root mean square error was 7.03 m in X direction and 7.63 m in Y direction, whereas the overall geo-registration error was 10.38 m. The digital terrain model (DTM) of Switzerland with a resolution of 25 m (Swisstopo 2007) was used for the orthorectification.

3. Methods

In this chapter a short introduction on the existing methodologies for retrieving biophysical and biochemical parameters from remote sensing data is given, followed by a more detailed discussion of the approaches followed in this dissertation. In particular, we present the statistical methodologies followed to (a) explore the seasonal and annual spectral separability of grassland habitats, (b) estimate above-ground biomass and (c) retrieve foliar biochemical information of grassland habitats using different hyperspectral remote sensing sources. Additionally, the method for up-scaling field developed statistical models to Hyperion data (chapter 5) is discussed and finally a detailed description of the Biome-BGC ecosystem process model and its parameterisation, used in chapter 6, is given.

3.1 Introduction

In the lasts decades, several algorithms have been developed to retrieve biophysical and biochemical variables from reflective remote sensing data. Based on Liang (2004) these algorithms can be classified into three groups: (a) statistical methods, (b) physical methods and (c) hybrid methods. Statistical methods search for a consistent relationship between the spectral signature of the leaf or canopy reflectance and the variable of interest. In order to establish such relationships, several measurements under varying field conditions and for different plant species and phenological development stages have to be collected. This is especially important, since the portability of the developed relationships heavily depends on the accuracy of the measurements and the range of conditions considered (Sims and Gamon 2002). The physical approach for the retrieval of biophysical and biochemical variables is based on the inversion of canopy radiative transfer (RT) models. Canopy RT models simulate interactions between solar radiation and the elements constituting the canopy following physical laws. Modelling reflectance of canopies is done by combining a leaf optical model, a canopy reflectance model and a soil reflectance model to estimate top-of-canopy reflectance. Canopy top-of-atmosphere radiance can also be simulated by including a further model that calculates the radiance propagation through the atmosphere (e.g., MODTRAN-4). Eventually, retrieval of vegetation variables is achieved by inverting a canopy RT model against remote sensing data using one of the many inversion methods available (Kimes et al. 2000). Finally, a hybrid method is a combination of extensive simulations using a canopy RT model and a nonparametric inversion model. The canopy RT model is used to generate a database by changing the values of key variables and the nonparametric model is used to map the relationship between spectral directional reflectance and various land surface variables (Liang 2004).

Table 3.1 Comparison of statistical and physical techniques for retrieving biophysical and biochemical parameters of vegetation (Dorigo et al. 2007).

Statistical	**Physical**
- Many field or laboratory measurements required for establishment of statistical relationship	- Field or laboratory measurements only used for validation
- Spectral data usually transformed	- Original spectra used for inversion
- Function usually based on a limited number of spectral bands	- Inversion usually based on complete spectral information
- Statistical function accounts for one variable at the time	- Various parameters estimated at the same time
- Not possible to incorporate information of other variables	- Possibility to incorporate prior information on distribution of different variables
- Computationally not very demanding	- Computationally very intensive
- Atmosphere, view, and sun geometry are not d directly accounted for	- Influences of atmosphere, view and sun geometry are directly incorporated
- Statistical approaches normally based on nadir measurements	- Possibility to use multiangular information
- Little knowledge of user required	- Knowledge of user required for the choice of appropriate canopy reflectance model, inversion technique, and distribution of variables

Each of the statistical and physical approaches outlined above has a number of advantages and disadvantages reported in detail in Table 3.1. In this dissertation, the statistical approach was chosen for estimating biophysical and biochemical variables of grassland habitats. In particular, a number of statistical approaches, ranging from single regressions to multiple linear regression using the novel branch-and-bound algorithm (Miller 2002) were used for estimating grassland biomass (chapter 5), while promising alternatives to regression techniques, like Partial Least Squares (PLS) that cope better with the non-linear character of the canopy reflectance (Dorigo et al. 2007), were utilised for retrieving biochemical concentrations of grasslands (chapter 6). These statistical approaches, together with the Classification and Regression Trees (CART) that were used for selecting the optimal wavebands for classifying the grassland types throughout the growing season (chapter 4), are described in detail below.

3.2 Spectral data transformation

Processing the spectral information recorded by remote sensing sensors is a common practice in order to enhance subtle spectral features and to reduce effects due to soil background reflectance, sun and view geometry, atmospheric composition and other canopy properties. Standard methods include calculation of the first and second derivatives (Laba et

al. 2005), logarithmic (Jacquemoud et al. 1995b) and continuum removal transformation (Kokaly and Clark 1999) but mainly creation of vegetation indices. In this dissertation, continuum removal transformation and several existing and new vegetation indices were used as spectral transformation methods. Since continuum removal transformation was used both in chapter 4 and chapter 6 it will be presented in detail here. Vegetation indices (VI's) were used only in chapter 5 for the retrieval of above-ground grassland biomass, thus they will be presented in detail in the section where all the methodological details of the corresponding chapter are discussed.

3.2.1 Continuum removal transformation

Continuum removal is a normalisation technique, resulting in a curve with values from 0 to 1, that enhances the location and depth of individual absorption features (Clark and Roush 1984) By putting the collected spectra on the same level it facilitates a better inter-comparison (Clark 1999). Several studies exist that exhibit the potential of continuum removal analysis for estimating biochemical concentrations from hyperspectral remote sensing data (Curran et al. 2001; Huang et al. 2004; Kokaly and Clark 1999; Mutanga and Skidmore 2004b; Mutanga et al. 2003) and for vegetation differentiation (Galvão et al. 2005; Schmidt and Skidmore 2003). The continuum is formed by fitting a convex hull over the top of a spectral curve and using the straight line segments between the local maxima. The continuum-removed reflectance $R_{cr(\lambda)}$ is calculated by dividing the reflectance value at a specific waveband $R_{(\lambda)}$ by the corresponding value of the convex hull at the same waveband $R_{ch(\lambda)}$ (Eq. 1) (Kokaly and Clark 1999) :

$$R_{cr(\lambda)} = \frac{R_{(\lambda)}}{R_{ch(\lambda)}} \quad (1)$$

Most studies have focused on subsets of wavelengths that correspond to certain absorption features of vegetation (Curran et al. 2001; Kokaly and Clark 1999; Kokaly et al. 2003; Mutanga and Skidmore 2004b) for the extraction of the continuum removed reflectance spectra. In this dissertation the continuum removal analysis was applied across the whole wavelength range, since we did not attempt to isolate specific absorption features (Huang et al. 2004; Schmidt and Skidmore 2003). Nevertheless, in order to normalise the absorption features of the chlorophyll in the visible and of the water absorption in the NIR and SWIR part of the spectrum the convex hull was forced to go through wavelengths where grassland reflectance spectra had their maxima, namely 555, 920, 1095, 1275, 1673 and 2209 nm for

ASD bands and through 554, 922, 1093, 1281, 1679 and 2213 nm for HyMap spectral bands. Once the continuum lines were formed between the defined bands the continuum removed reflectance spectra were calculated by dividing the reflectance values by the corresponding values of the continuum line (Kokaly and Clark 1999).

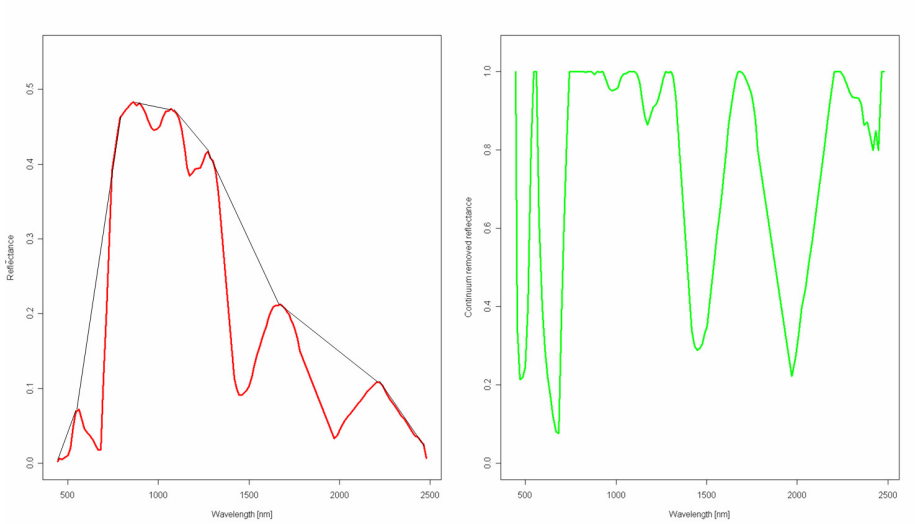

Figure 3.1 Example of a grassland reflectance spectrum extracted from the HyMap atmospherically corrected data before (left) and after the continuum removal transformation was applied (right). The black lines on the left graph indicate the continuum convex hull.

In this dissertation we used continuum removal to examine its usefulness for discriminating grassland types on a seasonal and inter-annual basis (chapter 4) and for assisting with the retrieval of foliar biochemistry of grasslands (chapter 6). For the research described in chapter 4, the continuum removal transformation was applied to all spectra collected with the ASD field spectroradiometer throughout the growing seasons of 2004 and 2005. For the research described in chapter 6, the continuum removal transformation was applied to the HyMap surface reflectance as shown in Figure 3.1. For comparison purposes, both the reflectance and the continuum removed reflectance spectra were used in all subsequent statistical analyses of chapters 4 and 6.

3.3 Methodology for evaluating the spectral separability of grasslands using multi-temporal spectroradiometer data

3.3.1 Statistical approaches for determining significantly different wavebands between grassland types

For each waveband, all single spectra collected per grassland type per date were used to test the hypothesis that reflectance values would discriminate between grassland types. To do so, we conducted a two-sided one-way analysis of variance (AOV) for each individual recording date. Results from the one-way AOV showed whether there was a significant difference between reflectance values of grassland types at a specific waveband, but they did not show which grassland types in particular were different to each other. We therefore performed the Tukey's Honestly significance post-hoc test (Crawley 2005) to establish differences between each of the grassland types. The significance level was set to $p<0.01$ and significant differences between pairs of grassland types were calculated per waveband for every sampling date during the two growing seasons. This analysis provided a basis for identifying the most important wavebands for discriminating grassland types and their change over time. The AOV and the Tukey's tests were applied to the reflectance and to the continuum removed reflectance spectra of each individual sampling date. We did not perform analyses between spectra of different dates of the same season nor between the two years.

3.3.2 Statistical approaches for determining optimal wavebands for seasonal and year-to-year grassland classification

Although the value of hyperspectral imagery lies in the wealth of spectral information, neighboring wavebands are often highly correlated and thus do not always provide independent additional information (Broge and Leblanc 2001; Thenkabail et al. 2004; Thenkabail et al. 2002). To optimize the classification of grassland types throughout the growing season of each year we determined the optimal waveband combinations using Classification and Regression Trees (CART) (Breiman et al. 1984). Only few studies exist that used CART for optimal hyperspectral band selection (Bajcsy and Groves 2004; Bittencourt and Clarke 2004). CART models result in a statistically optimised dichotomous tree explaining the presence or absence of the nominal (classification tree) or continuous (regression tree) response of a dependent variable (here grassland types) as a function of decision rules for independent variables (here reflectance at different wavelengths) (Crawley 2005). Some of the main advantages of CART models is that they represent a nonparametric and nonlinear method, thus no assumption regarding the shape of the dependent and the

independent variables distribution needs to be made, and interpretation of the results summarised by a tree are clear and give a highly intuitive insight into the interactions between variables (Hill and Lewicki 2006)

We built CART models for each sampling date using all single spectra collected per field. Models selected only the wavebands where measured reflectance best discriminated grassland types for each date and thus resulted in the greatest amount of deviance (=variability) explained (Crawley 2005). To prevent overfitting of CART models and to ascertain their generality, a 10-fold cross-validation procedure (Diaconis and Efron 1983) was applied to each fully trained classification tree. This allowed us to "prune off" those terminal nodes that represented overfitting and a reduction in precision, when applied to iteratively left-out data portions during cross-validation. This process reduced each classification tree to its optimal size to balance between precision regarding training data and generality regarding independent test data (Crawley 2005). We performed CART analyses to both the reflectance and to the continuum removed reflectance spectra for every sampling date during the seasons 2004 and 2005. All analyses were implemented in the statistical software platform R (R Development Core Team 2004) and the extension package *rpart* (Ripley 2005).

3.4 Methodology for estimating aboveground biomass patterns in grassland habitats at the landscape scale

3.4.1 Statistical approaches for estimating aboveground grassland biomass

The mean spectral reflectance of the 60-100 spectral measurements (collected with the ASD and then resampled to simulate Hyperion bands) and the mean biomass of the three samples collected at each grassland field were used in the statistical analysis. Biomass samples and spectral reflectance recorded at 11 grassland fields, repeated for four time steps during the 2005 growing season, were used to calibrate the statistical models. This was done to ensure that normally occurring variation in biomass and spectral reflectance due to vegetative growth stage or management practices on the different grassland types was included in the models. As a result, models could account for a larger temporal and across-grassland type variability than those calibrated using samples collected from only one date. Initial data screening revealed a heavily skewed distribution of the biomass data. Therefore, to improve the regression modelling we log-transformed the biomass data to approach a normal distribution.

The relationship between biomass and several hyperspectral and broadband VI's was investigated (Table 3.2). These were VI's related to vegetation structure (NDVI, RDVI, SR, SAVI, TSAVI, OSAVI, and MTVI1), to vegetation water status (NDWI, SRWI, PWI, and

WDVI), to chlorophyll and the red edge (RESP, GMI, CI_1, CI_2, VOGa, VOGb, VOGc, MCARI and TRVI) and other features (CAI, CAI_ATSAVI, TVI and PRI). A detailed description about properties and advantages of these VI's can be found in Broge and Leblanc (2001), Haboudane et al. (2004) and Zarco-Tejada et al. (2005). All the above mentioned indices were used to calibrate linear regression models with the biomass samples collected in the field.

Table 3.2 Vegetation indices for estimating above-ground biomass investigated in this study.

Vegetation Index	Equation	Reference
	Structural Indices	
Normalized Difference Vegetation Index (NDVI)	$NDVI = (R_{NIR} - R_{red})/(R_{NIR} + R_{red})$	(Rouse et al. 1974)
Renormalized Difference Vegetation Index (RDVI)	$RDVI = (R_{800} - R_{670}) / \sqrt{(R_{800} + R_{670})}$	(Rougean and Breon 1995)
Simple Ratio Index (SR)	$SR = R_{NIR}/R_{red}$	(Rouse et al. 1974)
Soil Adjusted Vegetation Index (SAVI)	$SAVI = (1+L)*(R_{800} - R_{670})/(R_{800} + R_{670} + L)$ (L = 0.5)	(Huete 1988)
Transformed Soil Adjusted Vegetation Index (TSAVI)	$TSAVI = \alpha*(R_{NIR} - \alpha*R_{red} - b) / (\alpha*R_{NIR} + R_{red} - \alpha*b + X*(1 + \alpha^2))$ α = slope of the soil line b = soil line intercept X = adjustment factor to minimize soil noise	(Baret and Guyot 1991)
Optimized Soil-Adjusted Vegetation Index (OSAVI)	$OSAVI = (1 + 0.16) * (R_{800} - R_{670}) / (R_{800} + R_{670} + 0.16)$	(Rondeaux et al. 1996)
Modified Triangular Vegetation Index (MTVI1)	$MTVI1 = 1.2 * [1.2 * (R_{800} - R_{550}) - 2.5 * (R_{670} - R_{550})]$	(Haboudane et al. 2004)
	Water indices	
Normalised Difference Water Index (NDWI)	$NDWI = (R_{860} - R_{1240})/(R_{860} + R_{1240})$	(Gao 1996)
Simple Ratio Water Index (SRWI)	SRWI = R850/R1240	(Zarco-Tejada et al. 2003)
Plant Water Index (PWI)	PWI = R970/R900	(Peñuelas et al. 1997)
Weighted Difference Vegetation Index (WDVI)	WDVI = Rred – α*RNIR ; α = slope of the soil line	(Clevers 1991)
	Chlorophyll and red edge indices	
Red-edge spectral parameter (RESP)	RESP = R750/R710	(Vogelmann et al. 1993)
Gitelson and Merzlyak Index	GMI=R750/R550 GM2=R750/R700	(Gitelson et al. 2003)
Carter Indices	CI_1 = (R695)/(R420); CI_2 = (R695)/(R760)	(Carter 1994)

(continued on next page)

Vogelmann indices	VOGa = (R740)/(R720) VOGb = (R734 – R747)/(R715 + R726) VOGc = (R734 – R747)/(R715 + R720)	(Vogelmann et al. 1993)
Modified Chlorophyll Absorption Ratio Index (MCARI)	MCARI = ((R700 – R670) – 0.2* (R700 – R550))* (R700 / R670)	(Daughtry et al. 2000)
Triangular Vegetation Index (TRVI)	$TVI = 0.5 * [120 * (R_{750} - R_{550}) - 200 * (R_{670} - R_{550})]$	(Broge and Leblanc 2001)
Photochemical Reflectance Index (PRI)	PRI = (R528 - R567)/(R528 + R567)	(Gamon et al. 1992)
	Other indices	
Cellulose Absorption Index (CAI)	CAI = 0.5* (R2000 + R 2200) – R 2100	(Nagler et al. 2003)
Litter Corrected-Adjusted Transformed Soil Adjusted Vegetation Index (CAI_ATSAVI)	$CAI\_ATSAVI = \frac{\alpha * (R_{800} - \alpha * R_{670} - b)}{\alpha * R_{800} + R_{670} - \alpha * b + X * (1 + a^2) + L * CAI}$ α = slope of the soil line b = soil line intercept X = adjustment factor to minimize soil noise CAI = Cellulose Absorption Index	(He et al. 2006)
Transformed Vegetation Index (TVI)	$TVI = \sqrt{(R_{NIR} - R_{RED})/(R_{NIR} + R_{RED}) + 0.5}$	(Deering et al. 1975)

Most of the above mentioned VI's consider only certain parts of the spectrum, primarily the chlorophyll absorption region (680 nm), the near-infrared (NIR) reflectance (800 nm) and/or the green reflectance peak (550 nm). Given this limitation and in an attempt to use the depth of information included in the large number of bands of hyperspectral data we built narrow band NDVI-type indices (nb_NDVI_{type}) (Thenkabail et al. 2000) as shown in Eq. (1).

$$nb\_NDVI_{type}[\lambda_1, \lambda_2] = \frac{\lambda_1 - \lambda_2}{\lambda_1 + \lambda_2} \qquad (1)$$

All possible two-pair combinations were used in Eq. (1) where λ_1 and λ_2 were the Hyperion simulated bands from the field reflectance measurements. A total of 27,889 narrow band indices were calculated. These indices were used in linear regression models to determine their predictive power to explain measured biomass.

The disadvantage of existing VI's and of the nb_NDVI_{type} indices is that they only consider very few of the available hyperspectral bands. Although much of the information provided by neighbouring bands is often redundant (Thenkabail et al. 2004) it is still possible that the spectral information is not optimally used by these indices. Therefore, multiple linear regression (MLR) that selected the best combination of linear predictors from the Hyperion simulated bands was used for biomass estimation. Branch-and-bound (Miller 2002) variable search algorithms were chosen to identify spectral bands that best explained biomass

variability. A branch-and-bound algorithm searches the complete space of solutions for a given problem for the best solution. Since explicit enumeration is normally impossible due to the exponentially increasing number of potential solutions, the use of bounds for the function to be optimized combined with division of sets of solutions into subsets enables the algorithm to search parts of the solution space only implicitly (Clausen 1999). We only built models using one to four spectral bands in an attempt to avoid multi-collinearity (Curran 1989; De Jong et al. 2003), overfitting of the models (Crawley 2005) and because preliminary results showed that accuracies improved only marginally when using more than four bands.

The overall capability of each model to explain the variability in the biomass samples was evaluated by the adjusted coefficient of determination (adj.R^2) (Hill and Lewicki 2006). We used the adj.R^2 since it will only increase if the new variable added will improve the model more than would be expected by chance (Crawley 2005). The model prediction error for estimating biomass was assessed by using a 4-fold cross-validation (CV) (Diaconis and Efron 1983). A 4-fold cross-validation randomly split all mean biomass measurements per grassland fields (n=50) into four bins, then it iteratively determined regression parameters using a sample of three bins and tested the resulting model on the left out bin. This procedure was repeated until each bin was left out once. Since predicted samples were not used to build the model, the calculated cross-validation root mean square error (CV-RMSE) is a good indicator of the model accuracy and predictive power. In addition, to investigate the effect of seasonal variability on the predictive power of the models we used a 4-fold "Date" CV procedure. By this, we calibrated models using data collected from three dates and then validated their predictions with data collected on the fourth. This process was repeated 4 times until each date was used for validation of model predictions once.

3.4.2 Up-scaling of field calibrated models

Statistical models with the highest accuracy and predictive power were up-scaled to the geometrically and atmospherically corrected Hyperion scene to predict the spatial distribution of biomass over the study area. Due to the differences between the two instruments (ASD-Hyperion) certain measures had to be taken to ensure accurate spectral and spatial scaling of these models. Spectral up-scaling was achieved by (a) resampling the ASD spectral bands to simulate those of the Hyperion sensor before any regression modelling was performed, and (b) by applying atmospheric correction to the acquired Hyperion scene. Thus, the at-sensor radiance recorded by the Hyperion sensor was transformed to top-of-canopy reflectance after accounting for solar and sensor geometries, atmospheric optical properties and sensor band specifications (Richter 2003). To account for the 30 m spatial resolution of the spectral signal recorded by the Hyperion sensor, each grassland was assigned the aggregated mean signal of

60-100 spectral signatures collected with the ASD spectroradiometer along transects over the whole extent of the field. In addition, to ensure the "purity" of the Hyperion pixels extracted from the scene, an algorithm was developed that only selected pixels from the centre of the grassland field for further analyses. Pixels adjacent to the edge of the fields were excluded since chances were high that the spectral signal recorded was mixed with the contribution of other land-use types. Finally, to deal with the spatial scaling difference between the 30 m Hyperion pixel size and the relatively small size of the biomass sampling plots we averaged multiple biomass samples within each of the relative homogeneous grasslands and assigned this value to the whole grassland field (White et al. 1997a).

On the date of the Hyperion data acquisition, two sources of canopy reflectance measurements existed for the sampled grassland fields, i.e., reflectance measurements from the ASD field spectroradiometer (that were resampled to simulate Hyperion spectral bands) and reflectance measurements from the Hyperion sensor. Therefore, VI's and nb_NDVI$_{type}$ indices were calculated for the sampled grasslands using both the ASD and the Hyperion sensor reflectance measurements. Then, differences (measured in RMSE) between absolute reflectance, VI's and nb_NDVI$_{type}$ derived from these two sources were calculated. Only models whose predictors (VI's, nb_NDVI$_{type}$ indices, absolute reflectance) had the smallest differences between the ASD and the Hyperion sensor estimates were selected. These models were subsequently used to up-scale biomass predictions to the Hyperion scene and to create the biomass distribution maps across the landscape. Finally, biomass estimates for 106 grassland fields, where species richness data were available were extracted.

While we recognise that empirical regressions between biophysical parameters and reflectance or VI's are limited to the place and time over which the ground data are collected (Verstraete et al. 1996) we believe that this did not pose a problem with up-scaling our biomass prediction models following the above mentioned methodology. The reason was because extracted biomass estimations were restricted only to comparable low-elevation grassland types growing under the same environmental and management conditions as the grasslands from where we collected our samples.

3.5 Methodology for retrieving foliar biochemistry of grasslands and for parameterisation of the Biome-BGC ecosystem process model

3.5.1 Statistical approaches for grassland biochemistry estimation

After atmospheric and geometric correction and the continuum removal transformation were applied to the HyMap data, the point map with the centre coordinates of the sampling plots was overlaid on the HyMap image. The reflectance spectra and the continuum-removed

reflectance spectra extracted for the 27 sampling plots, together with the foliar C and N samples collected over these plots were used for the subsequent statistical analyses. In this study partial least squares (PLS) regression was used to calibrate statistical models for estimating foliar N concentration from hyperspectral reflectance. PLS is a bilinear calibration method that works in a similar way to principal component analysis. The multidimensional feature space is linearly transformed so that the large number of collinear variables are combined into a few non-correlated factor variables where background effects and noise are explained by the less important factors (Geladi and Kowalski 1986). PLS requires few statistical assumptions compared to the other multivariate extensions of the multiple linear regression model and can be used in situations were datasets have many highly correlated bands and fewer observations than predictor variables (Hill and Lewicki 2006).

For the particular case of hyperspectral remote sensing, the main advantage of PLS regression over multiple linear regression is to avoid multi-collinearity (Curran 1989; De Jong et al. 2003). PLS regression has been used for estimating vegetation parameters from hyperspectral data, like biomass (Cho et al. 2007) and foliar biochemical concentrations (Hansen and Schjoerring 2003; Huang et al. 2004; Smith et al. 2002; Zagolski et al. 1996) with high accuracies. In this dissertation, PLS regression analysis was performed between the foliar N concentrations measurements and (a) the HyMap reflectance and (b) the HyMap continuum-removed reflectance spectra extracted for the 27 sampling plots. A 10-fold cross-validation procedure (Diaconis and Efron 1983) was used to select the optimal number of PLS factor variables to be used in the regression models (Geladi and Kowalski 1986). This process was applied to prevent overfitting of the model, thus ensuring a balance between precision regarding training data and generality regarding independent test data (Crawley 2005).

Once the optimal number of PLS factor variables were selected, the model was applied on a 4.8 x 2.3 km subset of the HyMap scene where the sampling plots were located to derive spatial predictions of grassland foliar N concentrations. Since the PLS model was calibrated for grassland habitats, all forest, impervious and other non-grassland areas were masked-out prior to the application of the PLS model on the HyMap scene. Approximately 150.000 HyMap pixels were used in the subsequent analyses.

3.5.2 Parameterization of the Biome-BGC model

NPP estimates for the study area were simulated using the Biome–BGC ecosystem process model. Biome-BGC (Running and Hunt 1993; Thornton et al. 2002) is a deterministic process-based ecosystem model that simulates above- and belowground daily storage and fluxes of carbon, nitrogen, and water of various terrestrial biomes. The Biome-BGC modelling approach integrates biological and geochemical considerations to describe

processes of the carbon (i.e., assimilation, respiration), nitrogen (i.e., mineralization, denitrification), and water (i.e., evaporation, transpiration) cycles in a mechanistic manner (Figure 3.2). Model requirements are detailed information on soil properties, atmospheric conditions (i.e., climate data, CO_2 concentration, nitrogen deposition), and ecophysiological parameters of the vegetation types under investigation. Biome-BGC simulates growth, regeneration and mortality of an ecosystem. However, the approach for modelling vegetation

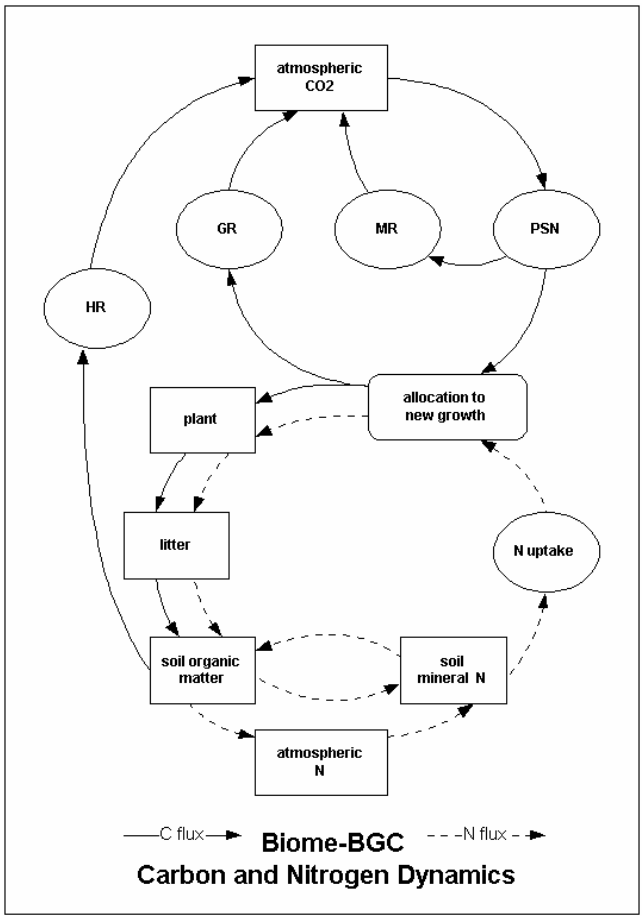

Figure 3.2 Simple summary of the fluxes (arrows) and state variables (square boxes) for the carbon and nitrogen components of the Biome-BGC model. Processes are shown as rounded boxes while solid lines indicate C fluxes and dashed lines indicate N fluxes. The plant, litter and soil organic matter boxes shown here consist of multiple model state variables (PSN: photosynthesis, MR: maintenance respiration, GR: growth respiration, HR: heterotrophic respiration). Graph taken from the internet site of the Numerical Terradynamic Simulation Group (NTSG), University of Montana (http://www.ntsg.umt.edu/ecosystem_modeling/BiomeBGC/bgc_basic_flowchart.htm).

dynamics is based on some simplifying assumptions to facilitate its application at scales ranging from a single stand to the globe. Most ecosystem processes within Biome-BGC are calculated on a daily basis (e.g., soil water balance, photosynthesis) while others, like the allocation of carbon and nitrogen for the growth of new tissue, are simulated with an annual time step (Thornton 1998).

In this study, Biome-BGC was applied in a spatially distributed mode (i.e., cell-by-cell) at the 5 m resolution of the HyMap pixel. For each 5 x 5 m pixel, Biome-BGC input parameters like daily meteorological data, ecophysiological (except for mass ratio of carbon:nitrogen in live foliage) and allometric variables were held constant for the whole study area.Daily meteorological data for the study area were generated by the weather generator MTCLIM 4.3 (Thornton and Running 1999) using measurements of a close-by meteorological station of MeteoSwiss for the years 1931-2001. Input ecophysiological parameters were based on the literature review by White et. al (2000) and expert knowledge (Table 3.3). Soil properties required for model initialisation (i.e., sand, silt and clay percentage by volume of rock-free soil) were estimated from a combination of field soil measurements and existing regional soil maps and thus were also in a spatially explicit form. Therefore, Biome-BGC soil input parameters for each 5 x 5 m pixel were assigned based on the underlying soil map value.

Table 3.3 Parameterisation of the Biome-BGC ecophysiological parameters for the grassland sites of the study area.

Value	Type	Description
0	(flag)	1 = WOODY 0 = NON-WOODY
0	(flag)	1 = EVERGREEN 0 = DECIDUOUS
1	(flag)	1 = C3 PSN 0 = C4 PSN
0	(flag)	1 = MODEL PHENOLOGY 0 = USER-SPECIFIED PHENOLOGY
0	*(yday)	yearday to start new growth (when phenology flag = 0)
364	*(yday)	yearday to end litterfall (when phenology flag = 0)
1	*(prop.)	transfer growth period as fraction of growing
1	*(prop.)	litterfall as fraction of growing season
1	(1/yr)	annual leaf and fine root turnover fraction
0	(1/yr)	annual live wood turnover fraction
0.1	(1/yr)	annual whole-plant mortality fraction
0	(1/yr)	annual fire mortality fraction
2	(ratio)	(ALLOCATION) new fine root C : new leaf C
0	(ratio)	(ALLOCATION) new stem C : new leaf C
0	(ratio)	(ALLOCATION) new live wood C : new total wood C
0	(ratio)	(ALLOCATION) new croot C : new stem C

(continued on next page)

0.5	(prop.)	(ALLOCATION) current growth proportion
Scenario-based	(kgC/kgN)	C:N of leaves
49	(kgC/kgN)	C:N of leaf litter, after retranslocation
42	(kgC/kgN)	C:N of fine roots
0	(kgC/kgN)	C:N of live wood
0	(kgC/kgN)	C:N of dead wood
0.39	(DIM)	leaf litter labile proportion
0.44	(DIM)	leaf litter cellulose proportion
0.17	(DIM)	leaf litter lignin proportion
0.3	(DIM)	fine root labile proportion
0.44	(DIM)	fine root cellulose proportion
0.17	(DIM)	fine root lignin proportion
0	(DIM)	dead wood cellulose proportion
0	(DIM)	dead wood lignin proportion
0.021	(1/LAI/d)	canopy water interception coefficient
0.6	(DIM)	canopy light extinction coefficient
2	(DIM)	all-sided to projected leaf area ratio
45	(m2/kgC)	canopy average specific leaf area (projected area basis)
2	(DIM)	ratio of shaded SLA:sunlit SLA
0.15	(DIM)	fraction of leaf N in Rubisco
0.005	(m/s)	maximum stomatal conductance (projected area basis)
0.00001	(m/s)	cuticular conductance (projected area basis)
0.04	(m/s)	boundary layer conductance (projected area basis
-0.6	(MPa)	leaf water potential: start of conductance reduction
-2.3	(MPa)	leaf water potential: complete conductance reduction
930	(Pa)	vapor pressure deficit: start of conductance reduction
4100	(Pa)	vapor pressure deficit: complete conductance reduction

One of the most important parameters, exerting significant control on NPP of all biomes is foliar C:N ratio (White et al. 2000). While foliar C:N ratio within Biome-BGC is usually assumed constant for a given biome, we varied this value in a spatially explicit manner to assess its effect over constant values. In this study, four foliar C:N ratio scenarios were applied (Table 3.4). First, the *"Global C:N"* scenario where the C:N value (i.e., $C:N_{GLO}$ = 25) was based on the literature review by White et. al (2000). This scenario is the most frequently used in ecosystem process modelling studies, since availability of regional data is often limited. Second, the *"Regional C:N"* scenario where the C:N value (i.e., $C:N_{REG}$ = 22.24) was the mean of the C:N values measured at the 27 sampling plots. This scenario is likely to be applied in studies that have specific C:N data for the ecosystem under investigation at a given study area. Third, the *"HyMap C:N"* scenario, where the C:N values were the result of a constant C_{CNT} value (i.e., mean C value measured at the 27 sampling plots, C_{CNT} = 44.05) and the N predictions of the HyMap PLS regression model for the study area. Fourth, the *"HyMap C:N + ε"* scenario where N prediction errors of the HyMap PLS

model, were randomly added to the predicted N values before C:N was calculated. C:N values for the *"Global C:N"* and *"Regional C:N"* scenarios were kept constant for every 5 x 5 m pixel within the study area. On the contrary, C:N values for the *"HyMap C:N"* and the *"HyMap C:N+ ε"* scenarios were spatially explicit and differed for every 5 x 5 m pixel within the study area. As mentioned above, the C fraction for these two scenarios was held constant (C_{CNT}) since grassland samples varied very little. Thus, we could apply the mean of the regional measurements in order to obtain accurate estimates of the spatial C:N ratio patterns.

Table 3.4 Description of the four C:N ratio scenarios employed in this study.

Scenario	Description	C:N Value
Global C:N	C:N selected from the literature review of White et. al (2000) C:N value was kept constant for the whole study area	25
Regional C:N	C:N estimated as the mean of the foliar C:N measurements at 27 grassland plots at the study area. C:N value was kept constant for the whole study area	22.24
Hymap C:N	C:N estimated from the mean foliar C concentration at 27 grassland plots at the study area and the foliar N concentration predictions of the PLS regression model. C value was kept constant (C_{CNT} = 44.05) for the whole study area	Spatially explicit range: 5.83 – 44.98
Hymap C:N + ε	Similar to the above except that PLS model errors were added to the foliar N predictions before C:N was estimated	Spatially explicit range: 5.83 – 44.98 + ε (ε range: -1.94 – 2.84)

.

Once all the input parameters for every 5 x 5 m pixel were established, a spin-up run of the Biome-BGC model was performed until equilibrium between levels of net ecosystem carbon exchange were reached. From that equilibrium state, another run was performed to simulate daily carbon exchange processes for the period 1931-2001. Finally, estimates of yearly NPP of our study area for the same time period were derived.

For the *"HyMap C:N + ε"* scenario, N prediction errors (i.e., residuals) of the PLS model were estimated by splitting the 27 measurements of foliar N and HyMap reflectance into two datasets, 20 for training and 7 for testing. We calibrated the PLS model using the training data and extracted the residuals from the independent test data. We iterated the procedure of randomly splitting the data and extracting PLS model residuals 140.000 times, thus establishing the residual distribution. Then, we randomly selected values from that distribution equal to the number of the 5 x 5 m pixels within our study area and added these values on the initial PLS model foliar N predictions.

Finally, to compare the different C:N ratio scenarios, we randomly selected 100 pixels and extracted the Biome-BGC NPP estimations for each scenario. We then performed a

paired t-test between the NPP values of each scenario to check for statistically significant differences

4. Spectral Separability of Grasslands Along a Dry-mesic Gradient Using Multi-temporal Spectroradiometer data

4.1 Introduction

Grasslands are one of the Earth's largest biomes. They represent the most important source of livestock feeding and contribute highly to the diversity and cultural history of rural and agricultural landscapes. More important, however, is their contribution to ecological goods and services. They are one of the major sources of biodiversity in Europe, where they cover 50% of the total cultivated area (Tueller 1998). These natural or seminatural grassland habitats represent a promising opportunity to restore or conserve biodiversity in agricultural landscapes (Duelli and Obrist 2003). In Switzerland, more than 350 species (13.1%) of the red list of higher plants and pteridophytes depend on these habitats (Delarze et al. 1999). Yet, dry and nutrient-poor grassland sites of Switzerland are endangered. Since 1945 their area has decreased by 90% mainly due to intensification of agricultural use (Eggenberg et al. 2001). Designing effective management schemes that optimize the sustainability of such ecosystems requires an understanding and monitoring of the vegetation dynamics and characteristics during the growing season.

One of the major sources of information for the study of landscape and vegetation is remote sensing (Kumar et al. 2001). Price and co-workers (Price et al. 2001) emphasized the importance of remote sensing for monitoring and better management of grasslands to ensure their productivity and sustainability. Contrary to traditional methods of mapping vegetation that involve time consuming and extensive field work (Küchler and Zonneveld 1988), remote sensing can provide spatially distributed information giving an overview of the landscape elements and their connectivity (De Jong et al. 2005). Aerial photographs at the scale of 1:10.000 or larger have been used extensively for identification and mapping of vegetation (Colwell 1983). Additionally multispectral sensors like Landsat TM were used to discriminate grassland types under different management practices (Guo et al. 2003; Price et al. 2002) or in arid environments (Langley et al. 2001).

Recently, new remote sensing instruments, such as hyperspectral sensors (Van der Meer et al. 2001), have been developed that make use of the unique spectral characteristics of vegetation (Curran 1989; Elvidge 1990; Kumar et al. 2001). Such sensors are well suited to record finer scale and continuous differences in vegetation (Ustin et al. 2004b). For instance, Mutanga and Skidmore (2003) analysed the spectral characteristics of tropical grasses under different nitrogen treatments, whereas Schmidt and Skidmore (2001) analysed the spectral discrimination between eight African rangeland grasses. Spectral reflectance measurements for both studies were carried out under controlled laboratory conditions. Thenkabail and co-

workers collected spectral reflectance measurements in the field to assess the optimal wavelengths for discriminating and mapping shrubs, grasses, weeds, and crop species (Thenkabail et al. 2004; Thenkabail et al. 2000; Thenkabail et al. 2002). Data collected from field spectrometers were also used for mapping coastal dune vegetation (Schmidt and Skidmore 2003), and for estimating canopy chlorophyll concentration in grasslands of differing soil contamination levels (Jago et al. 1999). Apart from field spectrometers, data collected from airborne hyperspectral sensors were used for applications such as mapping grassland quality (Mutanga and Skidmore 2004b), grassland species richness (Carter et al. 2005), invasive plants (Lawrence et al. 2006; Underwood et al. 2003) or saltmarsh coastal vegetation (De Lange et al. 2004).

Seasonal changes in the phenology of plants and vegetation communities affect their spectral properties (Gitelson and Merzlyak 1994; Miller et al. 1991) by changing LAI, pigment concentration and canopy structure (Asner 1998). Time series of hyperspectral recordings taken in the lab were used to examine the discrimination of tropical grasses (Mutanga et al. 2003) and cannabis leaves (Daughtry and Walthall 1998) under different nitrogen treatments, for estimating foliar biochemicals of pine needles (Curran et al. 2001) and photosynthetic pigments of tree leaves on various stages of senescence (Blackburn 1998b). With regard to canopy level analyses, scientists have used multitemporal hyperspectral recordings to investigate the seasonal spectral differences between invasive weed plant and sunflower crop (Peña-Barragan et al. 2006) and to determine the optimal date for discriminating invasive wetland plant species (Laba et al. 2005). Strachan and co-workers (Strachan et al. 2002) used reflectance recordings from corn fields at nine time steps during a growing season to investigate whether nitrogen and environmental stress could be detected from hyperspectral data, and Peñuelas and co-workers (Peñuelas et al. 1994) studied the seasonal changes in spectral reflectance of sunflower crops growing under water and nitrogen stress. Seasonal hyperspectral recordings were also used to monitor physiological parameters of wheat (Oppelt and Mauser 2004), to detect biophysical parameters of grasslands under burned and unburned treatments in an arid environment (Rahman and Gamon 2004) and to investigate the seasonal variability in spectral reflectance of fallow land from six arable crops (Piekarczyk 2005).

While a number of studies exist that use imaging spectroscopy for a range of applications, only very few investigate the spectral differences and discrimination power of semi-natural dry grassland habitats throughout a growing season and none, to our knowledge, that has explored the consistency of identified differences at an inter-annual basis. In order to fill this knowledge gap, the objectives of our study were fourfold: First, we wanted to identify spectral regions that allow significant discrimination between grassland types along a dry-mesic gradient during a season. Second, we aimed at identifying the best wavebands for

discriminating between the grassland types using classification trees (CART). Third, we aimed at comparing how a) the number and the variance of significantly discriminating wavebands and b) the classification accuracy differed between two years. Finally, we wanted to evaluate, whether continuum removal that is used to primarily assist in the detection of foliar chemistry, is also a suitable spectral transformation technique for enhancing differences and thus discrimination between grassland types during the growing season.

4.2 Results

The averaged spectral reflectance curves of the three grassland types from our field sampling are given in Figure 4.1 for the 2004 and in Figure 4.2 for the 2005 season. Even though curves are rather similar following the typical vegetation reflectance pattern, differences of varying magnitude exist during the growing season. First, we analyse these reflectance differences for statistical significance and present their annual frequency per waveband. Next, we demonstrate the seasonal variability of these differences in four spectral regions. Finally, we present the selection of optimal wavebands for discriminating the grassland types using CART models and seasonal classification accuracies thereof. Due to the high number of wavebands we separate some results by spectral regions: visible (VIS from 350 - 700 nm), near-infrared (NIR from 700 - 1300 nm), shortwave-infrared1 (SWIR1 from 1300 - 1900 nm) and shortwave- infrared2 (SWIR2 from 1900 – 2500 nm). For clarity, we specify that by waveband we refer to the reflectance recorded at a specific wavelength.

4.2.1 Annual frequency of significantly different wavebands between grassland types

For the 2004 and 2005 seasons, twelve sampling dates were available, six per year. The annual frequency of a waveband allowing significant discrimination between the three grassland types is summarised in Figure 4.3. Results from the analysis of the 2004 season reflectance spectra (Figure 4.3a) revealed that no single waveband was statistically significant in differentiating the grassland types for the whole season. Apart from the 2460-2500 nm region all remaining wavebands were significant in differentiating grasslands for at least two sampling dates. Several spectral domains were identified that allowed to discriminate the grassland types for five out of the six sampling dates, namely: at ~415 nm the blue absorption region, at ~720 nm the red-edge region, at the first reflectance peak in the shortwave-infrared (1610-1750 nm) and at the right side of the second shortwave-infrared reflectance peak (between 2270-2339 nm and at ~2415 nm and ~2455 nm). Results from the use of continuum removal for the 2004 season (Figure 4.3b) revealed several spectral domains that significantly discriminated the grassland types for all six sampling dates, namely: at the red-edge region (703-721 nm), near the first shortwave-infrared reflectance peak (1708-1712 nm, 1746-1756

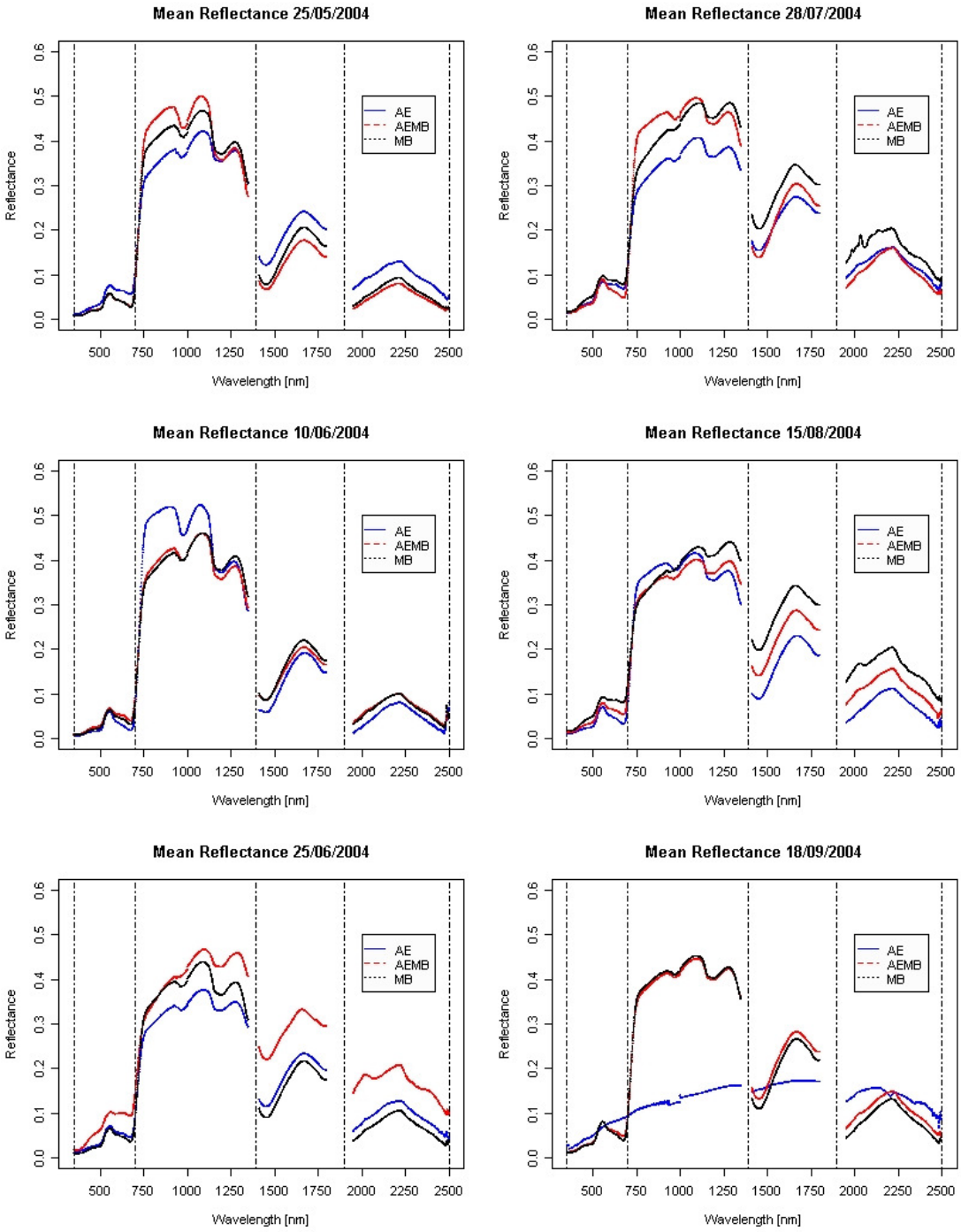

Figure 4.1 Spectral reflectance curves of the three grassland types averaged for all transects and fields for the sampling dates of the growing season 2004. Vertical dotted lines indicate the boundaries of the VIS, NIR, SWIR1 and SWIR2 spectral regions.

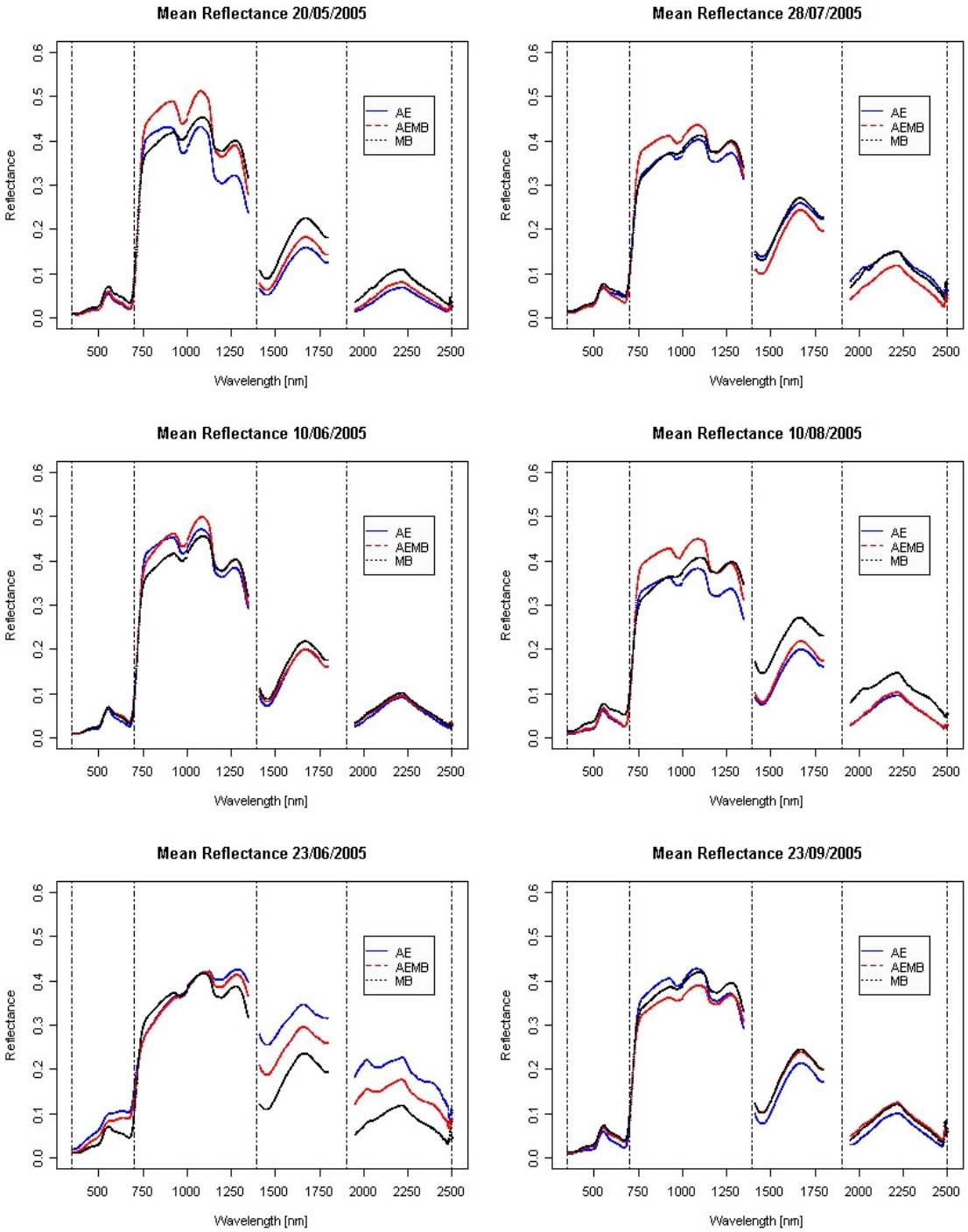

Figure 4.2 Spectral reflectance curves of the three grassland types averaged for all transects and fields for the sampling dates of the growing season 2005.Vertical dotted lines indicate the boundaries of the VIS, NIR, SWIR1 and SWIR2 spectral regions.

nm), and at the left side of the second shortwave-infrared reflectance peak (~2100 nm). Overall, the annual frequencies of wavebands that significantly discriminate grassland types increased in the visible and decreased in the near-infrared domain when continuum removal was used. In particular, wavebands between 756-836 nm and 850-910 nm were not significantly different between the grassland types, for any sampling date.

Results from the analysis of the 2005 season reflectance spectra revealed that wavebands from three spectral domains allowed a significant discrimination of the three grassland types for all six dates (Figure 4.3c), namely: at the red absorption region (591-609 nm), the red-edge region (708-713 nm) and at the downward slope of the near-infrared plateau (1318-1345 nm). Additionally, wavebands at several spectral domains allowed discrimination of the grassland types for five out of the six sampling dates, namely: around 450 nm and at the green peak (535-560 nm). Surprisingly, the chlorophyll absorption maxima (669-682 nm) was found to significantly differentiate between grassland types for only two sampling dates. Overall, the vast majority of wavebands from the visible region significantly differentiated at least for four sampling dates, while wavebands from the near-infrared reflectance peak (902-948 nm) only allowed significant differentiation for one sampling date. Results from the use of continuum removal for the 2005 season (Figure 4.3d) revealed only one spectral domain that significantly discriminated the grassland types for all six sampling dates, which is at the red-edge region (724-736 nm). Significant differences between grassland types for five sampling dates were found for the following wavebands: the blue absorption region (407-418 nm), the first shortwave-infrared reflectance peak (1584-1603 nm and 1718-1727 nm) and the 2058 nm region. Wavebands from the red absorption region (650-664 nm) were only significantly differentiating the grassland types for one single date, while the near-infrared shoulder-peak (760-947 nm) and the second shortwave-infrared reflectance peak (2196-2300 nm) did not allow for any significant differentiation of the three grassland types.

4.2.2 Seasonal variability by spectral region of significantly different wavebands between grassland types

The percentages of the total number of wavebands per spectral region where reflectance of the three grasslands types allowed for a significant differentiation are shown in Figure 4.4. Analyses of the 2004 reflectance spectra (Figure 4.4a), showed that for the two dates in the middle of the season (June 25th and July 28th) only the NIR part of the spectrum had more than 60% of wavebands significantly differentiating grasslands, while the other regions remained below 35%. From the first four sampling dates, only June 10th had a high fraction of differentiating wavebands in the VIS region. For the last two dates in 2004 the VIS region

became important again with 95% and 65% percent of the wavebands differentiating significantly between grassland types. The SWIR1 and SWIR2 spectral regions exhibited very similar behaviours during the growing season, yet the first two dates were both very significant (100%,78% for SWIR1; 95%,57% for SWIR2). The NIR spectral region behaved almost opposite to the three other regions with the middle two dates being best in significantly discriminating grasslands during the whole season.

Use of continuum removal for the 2004 season (Figure 4.4b) gave similar results to the above regarding VIS, SWIR1 and SWIR2, but overall the second date (10th June) had a higher fraction of significantly discriminating wavebands in all three spectral domains. Additionally, the NIR region was overall less powerful in discriminating grasslands from continuum removed reflectance spectra (except on 10th June). Both the VIS and SWIR1 region had >70% of the wavebands significantly differentiating in all sampling dates except for 28th July. In summary, we observed an overall increase of the percentage of significantly different wavebands in the VIS and SWIR1 and a decrease in the NIR and SWIR2 regions when analysing continuum removed reflectance spectra.

Analyses of the 2005 reflectance spectra (Figure 4.4c) showed that at the beginning of the season (25th May) all spectral regions had a large fraction of wavebands significantly differentiating grassland types (>65% throughout). Compared to the 2004 reflectance data, the discriminating power of wavebands was lower towards the end of the season (last two dates). Use of continuum removal for the 2005 season (Figure 4.4d) gave quite differing results with the third date (23rd June) usually sharing most significant wavebands in all four spectral regions. At this date, at least ~40% of wavebands allowed significant discrimination between the three grassland types. Using continuum removal seemed to reduce the usability of early and late season dates considerably, and it much reduced the number of significant wavebands from the VIS, NIR and SWIR2 regions.

Comparing all four data sets (2004/05 reflectance, 2004/05 continuum removed reflectance), we observed that for continuum removed reflectance the number of significantly discriminating wavebands was generally lower than when using reflectance spectra. Also, the differences between the two years were much higher when using the continuum removed reflectance. In particular, significantly discriminating wavebands were much fewer for 2005 than for 2004.

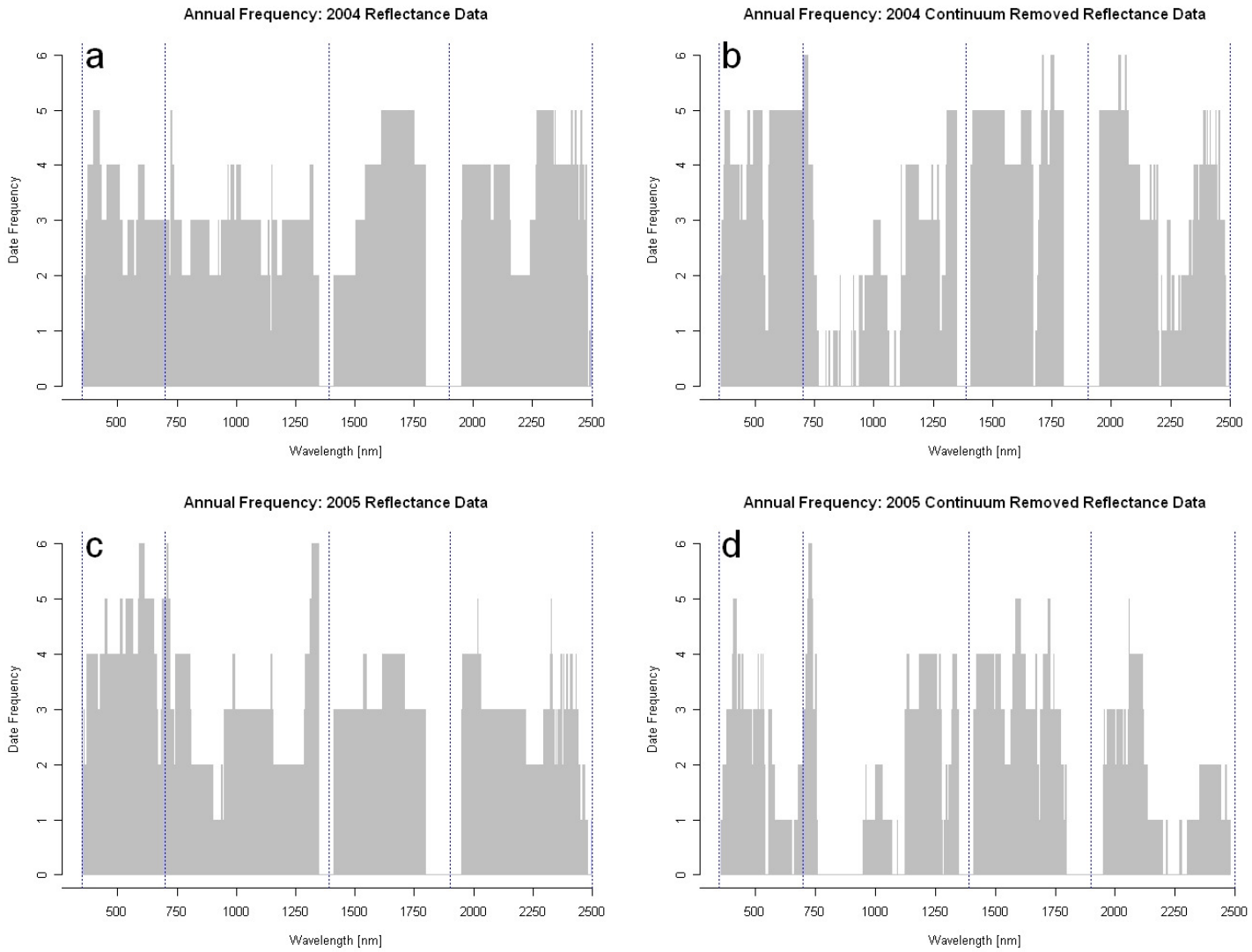

Figure 4.3 Frequency of dates the individual wavebands significantly differentiate between the grassland types throughout the seasons of 2004 (six dates) and 2005 (six dates). Vertical dotted lines indicate the boundaries of the VIS, NIR, SWIR1 and SWIR2 spectral regions.

4.2.3 Optimal wavebands, seasonal and year-to-year classification accuracies

While the previous section listed the number of significantly discriminating wavebands irrespective of their mutual correlation, we were also interested to evaluate the power to classify the three grassland types using spectral information throughout the season. The wavebands selected by the CART models with best power to classify the three grassland types are listed in Table 4.1. Analyses of the 2004 reflectance spectra showed that mostly wavebands from the visible and the near-infrared regions were chosen. Wavebands from the red absorption region were selected for five sampling dates, except July 28th where the red-edge region (~715 nm) was more powerful for classifying the grasslands (705-725 nm). Use of continuum removal showed that wavebands around the green reflectance peak at 550 nm were steadily used throughout the season. In general, use of continuum removal increased the number of optimal wavebands selected in the near-infrared but reduced the number from the shortwave-infrared region. Similar results were observed for the analyses of the 2005 season. When reflectance spectra were analysed, wavebands from the blue and red absorption region, the red-edge region and the near-infrared shoulder were most often selected to classify the three grassland types spectrally throughout the whole season. Use of continuum removal showed that wavebands were selected primarily around the green reflectance peak, the red-edge region and at the near-infrared shoulder. The number of wavebands selected from the shortwave-infrared region was very low for both the reflectance and the continuum removed reflectance spectra.

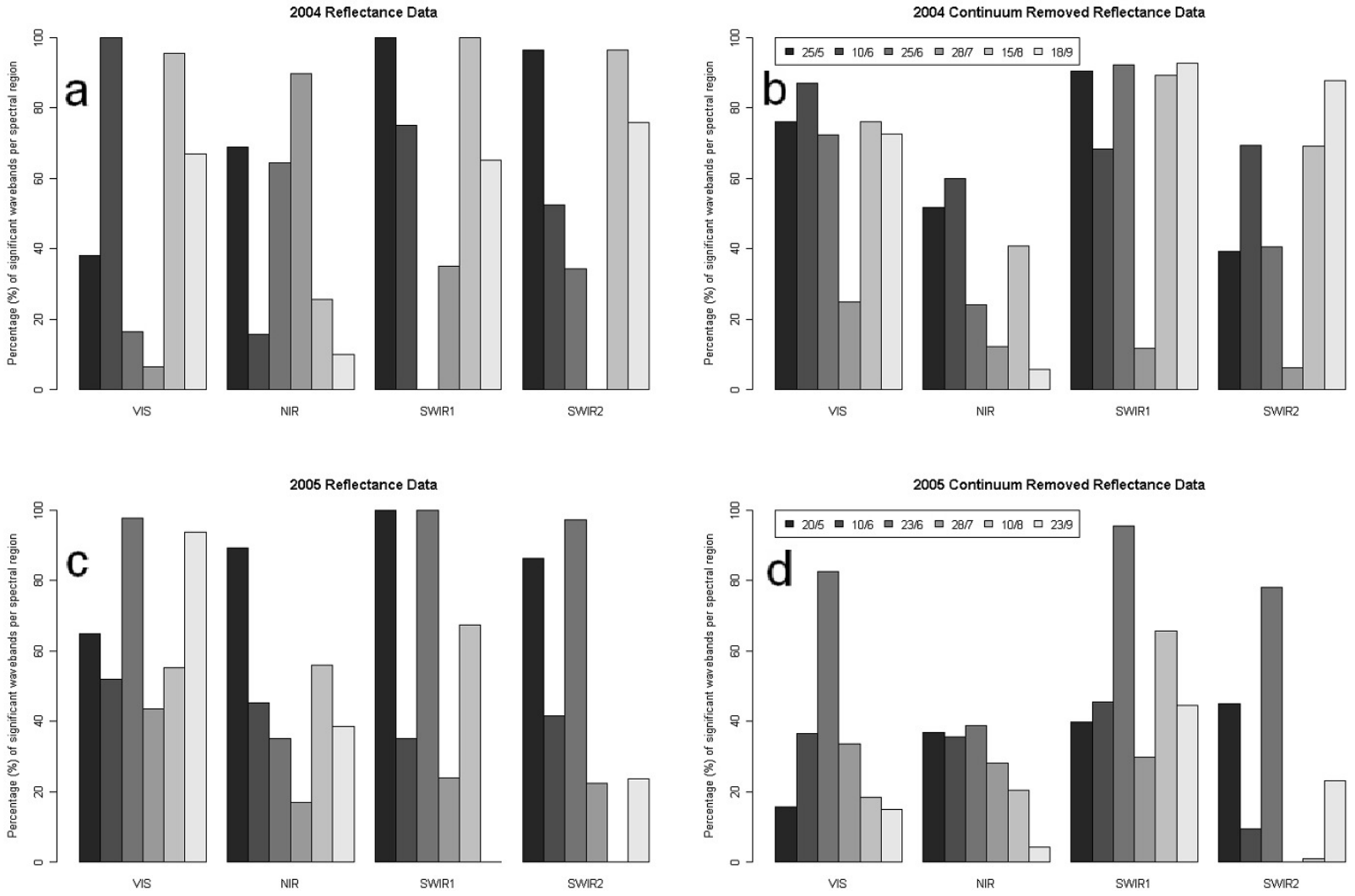

Figure 4.4 Fraction of wavebands per spectral region that significantly differentiate the three grassland types for both reflectance and continuum removed reflectance per sampling date of the years 2004 and 2005.

Table 4.1 Individual wavebands selected by classification tree analyses that discriminate the three grassland types spectrally during the growing seasons of 2004 and 2005.

Year	Date	Reflectance Spectra (nm)	Continuum Removed Reflectance Spectra (nm)
2004	25-May	474,670,871,1345,1690	534,557,851,1141,1269
	10-June	658,690,902,1579,1617	482,528,560,1140,1307,1660
	25-June	388,523,671,675,1017,2279	387,503,1709
	28-July	705,716,724,725,740,764,1262, 1282,1283,1328,1335	379,547,705,815,831,933,934, 1264,1301,1719
	15-August	350,351,409,671,1336,1660, 1775,2056	537,542,544,747,938,1123, 1261,1306
	18-September	350,672,1438,1962	499,1599
2005	20-May	386,833,1291,2213	387,1249
	10-June	403,641,696,753,921,1053, 1346,1541	514,530,547,557,706,1145, 1152,1192
	23-June	388,392,659,666,1143,2412	372,385,394,627,761
	28-July	440,593,594,753,766,1232,2421	393,515,544,545,758,822
	10-August	509,693,946,1331	544,720,980,1295,1704
	23-September	350,393,397,447,454,565,709, 1092,1966	377,547,779,1288,1347,1713, 1716,1727

The CART models generated from this analysis revealed considerable differences with respect to classification error rates between data sets and throughout the two seasons, varying between 11.5% and 34.8% (Figure 4.5). First, continuum removed reflectance spectra always performed better in classifying grasslands than did the reflectance spectra. A second important result was that data from 2004 produced less accurate classifications than did data from 2005. Both findings are in contrast with the found number of wavebands that had discriminating power (Figure 4.4). For 2005 only at the beginning and at the end of the growing season, both spectral data sets performed similarly. Finally, we observed that the middle of the growing season gave least accurate classification results. Irrespective of year and data transformation used, the beginning and partly the end of the growing season produced best models. Yet and interestingly, the continuum removed spectra performed much more consistently throughout the whole growing season, especially until end of June.

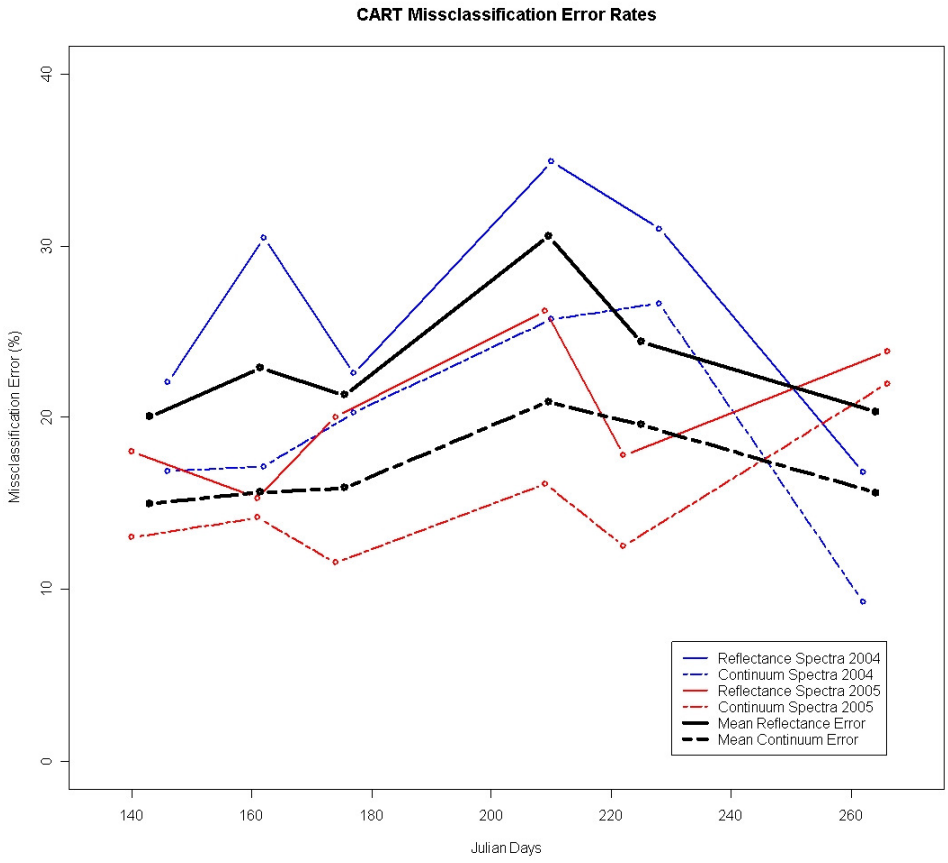

Figure 4.5 Misclassification error rates of the CART models for each individual sampling date of the growing seasons of 2004 (blue) and 2005 (red) for reflectance (solid line) and continuum removed reflectance (broken line) spectra. The mean of the two years of both spectral data sets is given in black.

4.3 Discussion and conclusions

Our analyses have revealed considerable changes in the spectral reflectance of grassland types during the course of a growing season and between consecutive years. Despite these changes, we have identified wavebands where the reflectance between the grassland types was significantly different during the season for both years. These wavebands make physical sense given what has been discussed in literature regarding spectral properties of vegetation (Elvidge 1990; Knipling 1970) and the specific biophysical characteristics of the grassland habitats as described by Eggenberg et al. (2001). For example, reflectance around 715 nm for 2004 and 700 nm for 2005 was significantly different for five and six sampling dates in 2004 and 2005, respectively. These wavebands are at the red-edge part of the spectrum where the maximum change in the slope of the vegetation reflectance spectra occurs (Filella and Peñuelas 1994; Thenkabail et al. 2000). Plant stress is best detected in the red-edge region (Elvidge and Chen 1995; Thenkabail et al. 2004) and additional information

about chlorophyll and nitrogen status of plants can be extracted (Carter 1994; Clevers and Jongschaap 2001; Elvidge and Chen 1995). Our results confirm those of several authors who have found the red-edge region to be very important for discriminating amongst various vegetation types at a single time step (Daughtry and Walthall 1998; Schmidt and Skidmore 2001; Smith and Blackshaw 2003; Thenkabail et al. 2004; Thenkabail et al. 2002) or throughout the whole growing season (Laba et al. 2005; Peña-Barragan et al. 2006).

Other important spectral domains that originated from our analyses were the 985 nm and the 1610–1750 nm regions. The size and the absorption strength of the 985 nm region have been found to be strongly related to biomass, vegetation moisture and growth stage (Peñuelas et al. 1994; Thenkabail et al. 2000). Reflectance in the 1610 – 1750 nm SWIR region is largely controlled by plant water content (Asner 1998; Thenkabail et al. 2004). Since the grassland types sampled are spread along a dry to mesic gradient having different availabilities of nutrients and water, it seems to make physical and biochemical sense that these waveband regions were important for discriminating amongst the grassland types steadily throughout both seasons.

Apart from the above discussed clear patterns, the analyses of seasonal and annual discriminating power by spectral regions did also reveal clear differences (Figure 4.4) and a considerable year-to-year variability in the number of selected wavebands. Possible reasons may be the differing weather conditions between the years that may have affected the development and phenology of vegetation (Jensen 2000), the timing of management activities, and finally the spectral reflectance properties of the grassland habitats.

In general, we judge the results from the classification trees as a proof of robust performance. More than 48% of the wavebands selected from our models were within 15 nm of optimal wavebands identified for the discrimination of vegetation and agricultural crops by earlier studies (Thenkabail et al. 2004; Thenkabail et al. 2000; Thenkabail et al. 2002). Thus, the remaining ~50% of selected bands were likely selected to cope with varying phenological aspects. Furthermore, the number of wavebands selected from the SWIR1 was higher compared to the SWIR2 (a bit less in 2005), which confirms the findings of Thenkabail and co-workers (2004) on the importance of SWIR1 over SWIR2 for discriminating different vegetation types.

For both years, the optimal times for the discrimination of the grassland types occur at the beginning of the growing season. At the beginning of the season vegetation is developing at different rates which yields different percentage of canopy closures and subsequently differences in spectral reflectance (Jensen 2000). The overall low separability in the middle of the growing season can be attributed either to the similar reflectance properties of the grassland types once they have reached complete canopy closure (Jensen 2000) or to cutting

management practices applied (Eggenberg et al. 2001), which removes vegetation biomass and minimizes reflectance differences.

The effect of the continuum removal transformation was contradictory at first sight when comparing the number of significantly discriminating wavebands with the results from the CART analyses. The transformation reduced the frequency of significant wavebands in large parts of the NIR region confirming findings of previous studies (Schmidt and Skidmore 2003). Nevertheless, the frequency of significantly different wavebands in the 1150 – 1250 nm water absorption region (Kumar et al. 2001) of the NIR increased, since continuum removal transformation enhanced the location and depth of this absorption feature (Clark and Roush 1984) and subsequently the differences between the grassland types. In the visible part, the effect was not steady, with increased number of discriminating wavebands in 2004 and reduced numbers in 2005. Schmidt and Skidmore (2003) found the same effect as we did for 2004. Nevertheless, this might not be consistent since our results for 2005 were different.

Thus, while continuum removal reduced the overall number of significantly discriminating wavebands, it actually enhanced the classification accuracy consistently throughout each season for both years investigated. This is surprising at first and requires further discussion. The most likely reason for this is that since continuum removal normalises reflectance peaks, differences in absolute reflectance are removed. Most of the removed differences however, come from adjacent spectral bands that are often highly correlated (Broge and Leblanc 2001; Thenkabail et al. 2004; Thenkabail et al. 2002) and thus fail to provide any additional information. Continuum removal enhances absorption features. Thus fewer significantly discriminating wavebands can obviously produce higher classification accuracies if located at key spectral regions. This reasoning may also hold for the comparison of the two years, where 2004 had higher numbers (Figure 4.3) and proportions (Figure 4.4) of significantly discriminating wavebands than had 2005 for both the reflectance and the continuum removed reflectance spectra. Yet again, in 2005 the misclassification error rates were clearly lower for both spectral data sets.

In summary of the above, we conclude that even though the number and the frequency of significantly different wavebands give an overview of the most important wavebands for seasonal discrimination of grasslands, only a statistical classification can answer the question of how well grasslands (or vegetation in general) can be discriminated spectrally. A second major conclusion from our analyses is that continuum removal does not only assist in the retrieval of canopy biochemical properties, but also serves as a valuable and consistent improvement of spectral discrimination of vegetation throughout seasons and years. Additionally, the use of continuum removed reflectance spectra guaranteed almost steadily low misclassification errors throughout the season meaning that is was less affected by phenological changes. Finally, the misclassification error was highest in the middle of the

growing season, which may be specific to grasslands that are partly cut at that time. In order to avoid such effects, we propose to use either early summer data and/or continuum removed reflectance spectra.

5. Spaceborne Hyperspectral Remote Sensing in Support of Estimating Aboveground Biomass Patterns in Grassland Habitats at the Landscape Scale

5.1 Introduction

Earth's grasslands contribute highly to the diversity and cultural history of agricultural landscapes. Their importance as one of the major sources of food for livestock and for biodiversity conservation purposes is also well recognised (Duelli and Obrist 2003). In Europe, natural and semi-natural grassland habitats cover a large part of the total area (Tueller 1998) playing an important economical and ecological role. Productivity of these grasslands has a strong effect on both species competition and human management schemes, since highly productive grasslands are more prone to be converted to, or remain as agricultural areas. Development of robust and timely biomass estimates is of critical importance for monitoring and designing effective management practices that optimise sustainability of these ecosystems and their goods and services over time.

Traditional methods for mapping grassland biomass involve direct measurements which are time consuming, expensive and require extensive field work. Furthermore, reliable estimates are restricted to local scales only, whereas ecologists and managers require estimates at the landscape scale. One of the major sources of information for the study of landscapes and for estimating biomass over large areas is remote sensing (Kumar et al. 2001; Wulder et al. 2004). Attempts to estimate biomass using broadband sensors with spatial resolutions of 30m to 1km have resulted in a wide range of accuracies and precision (Dengsheng 2006; Geerken et al. 2005; Kogan et al. 2004; Todd et al. 1998; Wylie et al. 2002). In most of these studies, quantity and spatial distribution of grassland biomass was estimated through the use of broadband vegetation indices (VI's). However, averaging of spectral information over broad-band widths can result in loss of critical information (Blackburn 1998a).

Recently, hyperspectral sensors (Van der Meer et al. 2001) that acquire images in a large number of narrow spectral channels (over 40) have been developed. Studies using hyperspectral data to estimate biomass have been carried out under controlled laboratory conditions (Mutanga and Skidmore 2004a; Mutanga and Skidmore 2004c) or in the field for yield estimation of agricultural crops like wheat and corn (Hansen and Schjoerring 2003; Osborne et al. 2002; Xavier et al. 2006; Zarco-Tejada et al. 2005). A limited number of studies exist that have investigated the relationship between hyperspectral remote sensing and biomass production of mixed grassland ecosystems (Beeri et al. 2007; Cho et al. 2007; Mirik

et al. 2005; Rahman and Gamon 2004; Tarr et al. 2005) and only few (Boschetti et al. 2007; Filella et al. 2004; Geerken et al. 2005), that have extended such analyses over the growing season.

Furthermore, statistical relationships between biomass and spectral information are often established between field spectrometer measurements and biomass (Filella et al. 2004; Künnemeyer et al. 2001; Mutanga and Skidmore 2004a; Osborne et al. 2002; Thenkabail et al. 2000), field spectrometer measurements resampled to match band definition of existing hyperspectral or broadband sensors and biomass (Hansen and Schjoerring 2003; Xavier et al. 2006) or between spectral reflectance extracted directly from hyperspectral sensors and concurrent field biomass sampling (Kooistra et al. 2006; Mirik et al. 2005; Zarco-Tejada et al. 2005). Only very few studies have attempted to up-scale field developed statistical models to the sensor level (Anderson et al. 2004; Zha et al. 2003) and none to our knowledge has attempted to up-scale statistical models calibrated using observations collected over the span of the growing season.

A common characteristic for many of the above mentioned studies is that they do not attempt to answer specific ecological questions using the remote sensing derived products. The relationship between productivity and species richness has been of long-standing interest to ecologists, because understanding the mechanisms driving this relationship can help us comprehend the determinants of biodiversity (Waide et al. 1999). Many ecological studies have shown that biomass is a surrogate for productivity (Bischoff et al. 2005; Mittelbach et al. 2001) especially in herb dominated communities like grasslands (Scurlock et al. 2002). Attempts to correlate species richness with NDVI (Gould 2000; Oindo and Skidmore 2002; Oindo et al. 2003) and pure hyperspectral reflectance (Carter et al. 2005) have been reported in literature but to our knowledge no study exists that examines the relationship between species richness and biomass estimates derived from hyperspectral remote sensing data.

The main objective of our study was to develop a method using field spectrometer data for estimating above ground biomass in grassland habitats along a dry-mesic gradient. The method should be independent of specific habitats or phenological period. We further aimed at investigating to what degree the calibrated biomass estimation could be scaled to hyperspectral data recorded from the Hyperion sensor. By this, we wanted to evaluate the potential to scale models calibrated from plot based estimates to larger landscapes as seen from spaceborne sensors. Finally, as a secondary objective, we aimed at using the estimated biomass distribution maps produced from the Hyperion scene to explore the relationship between species richness and biomass that is a central theme in ecological diversity studies.

5.2 Results and discussion

Descriptive statistics of the biomass measurements are reported in Table 5.1 and Figure 5.1. Highest variability of biomass was observed at the first (10th June) and second (23rd June) sampling dates. Sampled grasslands were along a dry-mesic gradient having different availability of water and nutrients that eventually lead to different rates of growth and biomass accumulation. Lower biomass variability observed later in the season could be partly attributed to the management practices applied to these fields.

Table 5.1 Summary statistics for original and log-transformed measured biomass at 50 grassland fields over 4 time steps during the 2005 growing season.

	Biomass					
	n	**Mean**	**stdev**	**Min**	**Max**	**Range**
Original measurements (kg/m^2)	50	0.7756	0.5704	0.1785	3.3180	3.1395
Log-transformed measurements log(kg/m^2)	50	-0.4523	0.6186	-1.7230	1.1990	2.9220

The best five models from the different VI categories for predicting biomass are presented in Table 5.2. Overall, models developed with existing VI's gave low adj. R^2 values. Higher values were obtained by VI's related to canopy water content (NDWI, adj. $R^2 = 0.33$). This can be explained by the strong relationship between canopy water content and biomass (Anderson et al. 2004; Mutanga et al. 2003). Asner (1998) has shown that an increase in biomass leads to an increase in canopy water content.

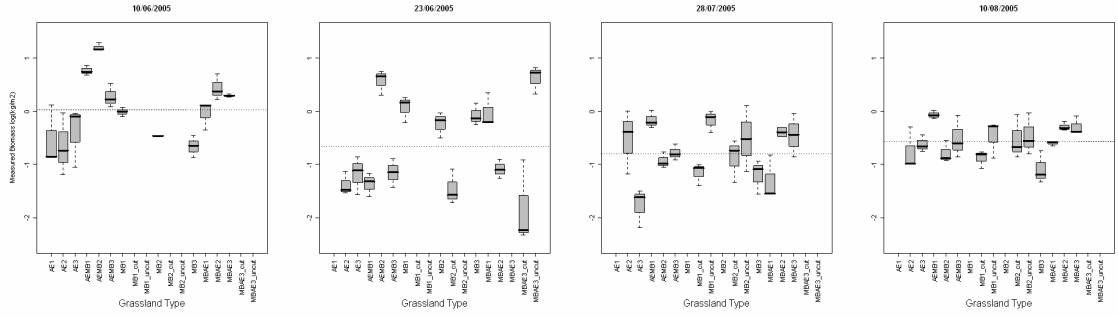

Figure 5.1 Mean biomass (log(kg/m^2)) measurements of individual sampled fields during the growing season. Dashed horizontal lines represent the mean biomass measured per sampling date.

Models using VI's that minimise the soil background influences in the spectral signal like TSAVI (Baret et al. 1989) did not improve the results (adj.R^2 = 0.28). The grasslands sampled for this study are rich in herbs and have high canopy cover during the season, thus

minimal soil reflectance. Models using the traditional NDVI and a modified version of it that is more suitable for low and high LAI values (RDVI) (Haboudane et al. 2004) gave similar adj.R^2 (0.29,0.28). Poor results (adj.R2 = 0.28) were also obtained using the Carter Index 2 (CI_2) that has been found to indicate plant stress (Carter 1994).

Table 5.2 Adjusted coefficient of determination (adj.R^2) and cross-validated biomass prediction error (CV-RMSE) of the best models calibrated with biomass (log(kg/m^2)) and spectral information (VI's, nb_$NDVI_{type}$ indices, MLR) collected at 50 grassland fields over the whole growing season using an ASD field spectroradiometer with bands resampled to simulate those of the Hyperion band widths.

Model	**Adj.R2 of models calibrated from ASD field spectral measurements**	**CV-RMSE of predicted biomass from ASD field spectral measurements**
NDWI	0.33	0.51
TSAVI	0.29	0.53
RDVI	0.29	0.52
NDVI	0.28	0.53
CI_2	0.28	0.52
nb_$NDVI_{type}$ b1326,b1710	0.65	0.36
nb_$NDVI_{type}$ b1084,b1205	0.56	0.39
nb_$NDVI_{type}$ b1074,b2264	0.52	0.41
nb_$NDVI_{type}$ b722,b1669	0.51	0.42
MLR-1 band b1710	0.52	0.42
MLR-1 band b1699	0.51	0.43
MLR-2 bands b478,b1780	0.77	0.31
MLR-2 bands b468,b1780	0.77	0.31
MLR-3 bands b518,b1699,b1710	0.82	0.27
MLR-3 bands b1185,b1205,b1235	0.82	0.29
MLR-4 bands b518,b1205,b1235,b1710	0.86	0.22
MLR-4 bands b518,b1215,b1225,b1720	0.86	0.24

All possible two band combinations were used to create nb_$NDVI_{type}$ indices. Adj.R^2 between biomass and each nb_$NDVI_{type}$ index were determined and are graphically presented in Figure 5.2. Values for adj.R^2 ranged from 0.007 to 0.74 reflecting a wide variation in the strength of the relationship between nb_$NDVI_{type}$ indices and biomass. Compared to existing VI's that primarily use the red and NIR regions, our analysis identified regions from the NIR and the shortwave infrared (SWIR) that resulted in much higher adj.R^2 values namely: 720 nm, 1200 nm, 1700 nm and 2280 nm. The best $NDVI_{type}$ index model for each one of the

above four regions is presented in Table 5.2. The 720 nm is the red-edge part of the spectrum where the maximum change in the slope of the vegetation reflectance spectra occurs (Filella and Peñuelas 1994; Thenkabail et al. 2000).

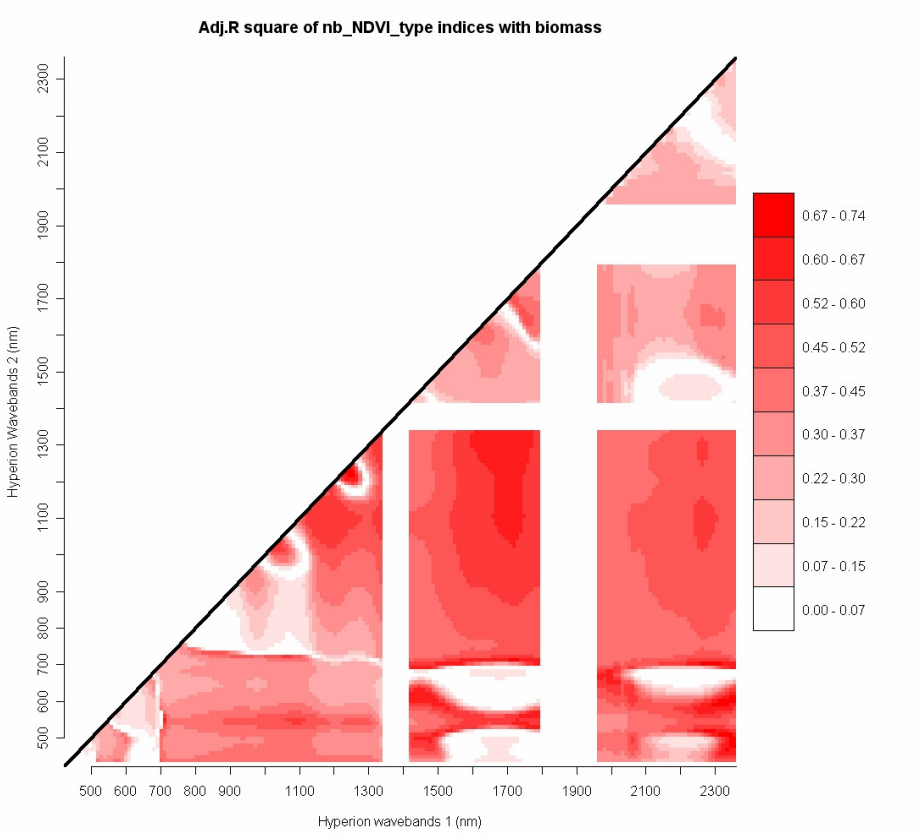

Figure 5.2 Result of the narrow band NDVI type vegetation index analyses (nb_NDVI_{type}). The graph shows the adjusted coefficient of determination (adj.R2) from the regression of biomass against nb_NDVI_{type} indices calculated from any band pairs among the simulated Hyperion bands. Light red areas indicate higher adj.R2. White gaps represent water absorption regions that were removed from the analysis.

Vegetation stress is best detected in the red-edge region (Elvidge and Chen 1995; Thenkabail et al. 2004) and additional information about chlorophyll and nitrogen status of plants can be extracted (Carter 1994; Clevers and Jongschaap 2001; Elvidge and Chen 1995). The other regions (1200 nm, 1700 nm and 2280 nm) are strongly associated to plant leaf water content that is correlated to canopy biomass and LAI (Hunt 1991) and to cellulose, starch, lignin and nitrogen concentrations (Kumar et al. 2001). In particular, Asner (1998) has shown that the water absorption feature around 1200 nm (Curran 1989) exhibits an obvious deepening as LAI and subsequently biomass are increasing. Our results confirm findings of earlier studies (Cook et al. 1989; Gong et al. 2003; Hunt 1991) that correlate the ratio between NIR and

SWIR to productivity and LAI and that of Geerken (Geerken et al. 2005) that has shown that strongest correlations between biomass of annual grasses and narrow-band indices were found between NIR-NIR and NIR-SWIR constructed narrow-band ratios.

Results of the best two MLR models for each number of predictors (1-4 bands) that were identified from the exhaustive branch-and-bound selection algorithm are reported in Table 5.2. Adj.R^2 ranged from 0.52 for one-band models to 0.86 for four-band models. Although the selection of spectral bands was solely based on statistical optimisation, these bands were located at key spectral regions with respect to physical processes of plants and vegetation biomass. The 478, 518 nm bands from the visible region are highly correlated with chlorophyll content of vegetation (Curran 1989; Kumar et al. 2001), the 1205 nm from the NIR and the 1710 nm from the SWIR are related to plant moisture and leaf mass (Asner 1998; Hunt 1991; Thenkabail et al. 2004) and the 2235 nm to biochemical canopy properties like cellulose, starch and lignin (Elvidge 1990). Even though different MLR models used slightly different bands, these were neighbouring and highly correlated to the ones mentioned above and thus provided the same type of information. In general, MLR can be considered a successful approach to optimize the retrieval of physical properties from spectral information.

The overall cross-validated biomass prediction errors (CV-RMSE) of the best VI's, nb_$NDVI_{type}$ indices and MLR models are presented in Figure 5.3 and Table 5.2. Models that used existing VI's predicted comparably poor with CV-RMSE from ~0.55 to ~0.52 log(kg/m^2) of biomass. Development of new nb_$NDVI_{type}$ indices greatly improved the predictive power of the models by reducing the CV-RMSE to 0.36 log(kg/m^2). These predictions were superior to one-band MLR models that had a CV-RMSE of 0.42 log(kg/m^2). Inclusion of additional bands in the MLR models further increased their predictive power by reducing the CV-RMSE to 0.31, 0.27 and 0.24 log(kg/m^2) for two, three, and four band MLR models respectively.

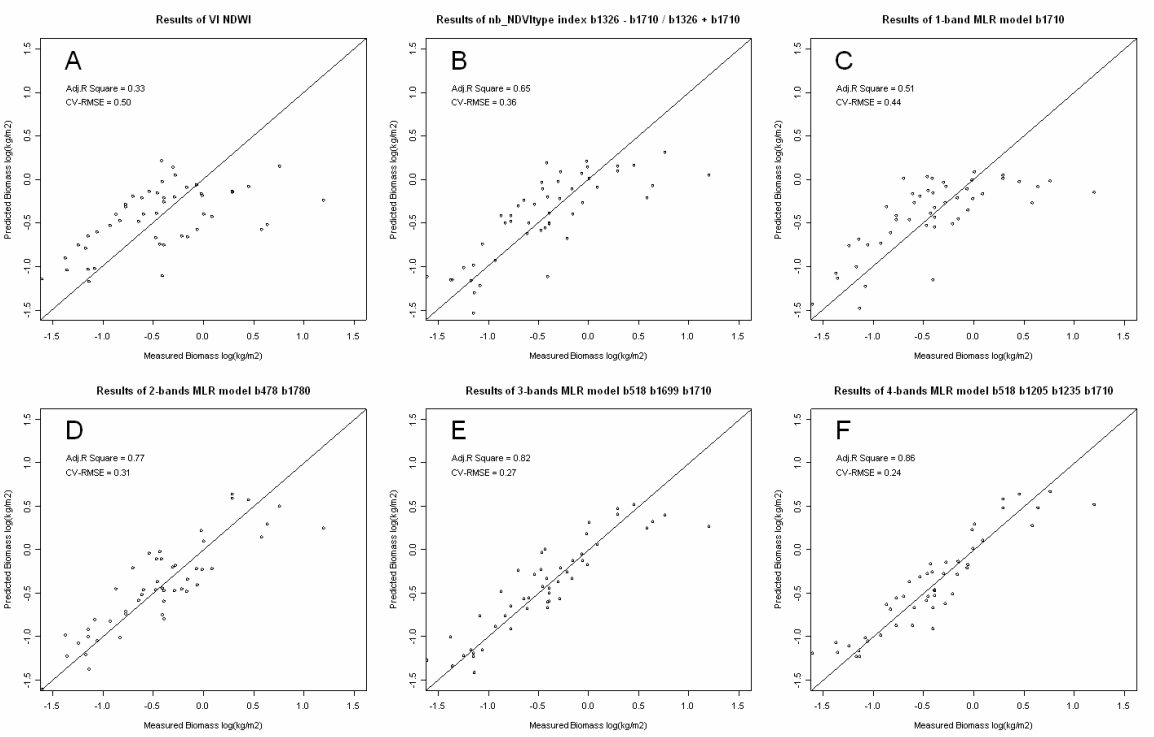

Figure 5.3 Best measured vs. predicted biomass estimates from regression models of A) existing VI's, B) nb_NDVI$_{type}$, and C-F) one to four spectral bands MLR, optimized with a 4-fold cross-validation using samples from all four sampling dates. Biomass values are in logarithmic scale.

The above models were also used in the 4-fold "Date" CV analyses (Table 5.3). A clear pattern was observed. Models calibrated with biomass samples collected on the first two sampling dates of the season (Date 1 = 10th June, Date 2 = 23rd June) predicted biomass with lower RMSE. Moreover, models calibrated using samples from only one of these dates gave poorer predictions and specifically so when the second date was removed. For example, the best nb_NDVI$_{type}$ index model for estimating biomass when calibrated with samples from Date 1 and 2 yielded RMSE of 0.30 and 0.34 log(kg/m2). RMSE increased to 0.46 and 0.50 when samples from only one of these dates were used. The reason for this pattern likely originates from the high variability of biomass samples collected on Date 1 and Date 2 (Figure 5.1). At the beginning of the season vegetation is developing at different rates which yields differences in biomass accumulation, percentage of canopy closures and subsequently differences in spectral reflectance (Jensen 2000). Spectral and biomass sampling on these dates captured differences between the grassland types along a dry-mesic gradient. Thus, models calibrated with data from these dates could account for a much broader range of variability of biomass with relation to spectral reflectance. On the contrary models calibrated primarily from late dates in the season (Date 3 = 28th July, Date 4 = 10th August) were not

able to extrapolate to the large range of biomass observed early in the season and thus created higher date cross-validated errors. In particular, RMSE of biomass prediction increased to 0.46 and 0.43 log(kg/m2). Overall, it sees very promising to use multiple dates for calibrating models in order to capture a large range of variability and to increase model stability.

Table 5.3 Biomass (log(kg/m^2)) prediction errors of best models built with three approaches. Models were calibrated on three dates and validated on the fourth. C-2,3,4/V-1 means that regression models were calibrated on Dates 2,3,4 and validated on Date 1. Recording dates were, Date-1: 10th June, Date-2: 23rd June, Date-3: 28th July and Date-4: 10th August.

	RMSE					
	Exist. VI's	**nb_ $NDVI_{type}$**	**1-band MLR**	**2-band MLR**	**3-band MLR**	**4-band MLR**
Calibration-Validation dates	NDWI	nb_$NDVI_{type}$ b1326,b1710	MLR-b1710	MLR-b478, b1780	MLR-b1185, b1205,b1235	MLR- b518, b1205, b1235,b1710
C-2,3,4/V-1	0.61	0.46	0.57	0.4	0.35	0.31
C-1,3,4/V-2	0.62	0.43	0.49	0.35	0.28	0.38
C-1,2,4/V-3	0.47	**0.30**	**0.36**	**0.21**	**0.18**	**0.15**
C-1,2,3/V-4	**0.45**	0.34	0.45	0.27	0.25	0.24
Resubstitution-RMSE	0.49	0.39	0.42	0.28	0.25	0.21

On the date of the Hyperion data acquisition differences between model predictors (VI's, nb_$NDVI_{type}$ indices, absolute reflectance) calculated using ASD field spectral measurements and spectral measurements from the Hyperion sensor for nine sampled grassland fields are reported in Table 5.4. The smallest difference between field-sensor calculated model predictors was observed for the b1084nm-b1205 nm nb_$NDVI_{type}$ index. Overall, differences were lower between field-sensor calculated VI's and nb_$NDVI_{type}$ indices than between field-sensor measured reflectance. This was due to the fact that vegetation indices can minimise external effects such as atmosphere, sun and viewing angle and normalise effects like canopy background variation and soil variations (Jackson and Heuete 1991). Differences in absolute reflectance recorded on the field and recorded by the sensor were higher in the NIR and SWIR compared to the visible (VIS) region of the spectrum. These could be attributed to poor calibration of the SWIR spectrometer of the Hyperion sensor and to difficulties in the atmospheric correction of the data. Lack of knowledge on the exact state of the atmosphere at the date of the acquisition and in particular for parameters like

water vapour content, has been found to have a more pronounced effect on the near and shortwave infrared parts of the spectrum (Liang 2004).

Table 5.4 RMSE between spectral reflectance, VI's and nb_NDVI$_{type}$ indices calculated using spectral measurements collected in the field with an ASD and spectral measurements from the Hyperion sensor for nine grassland fields sampled at the date of the Hyperion data acquisition. RMSE between field and sensor estimated VI's and nb_NDVI$_{type}$ indices are expressed as the percentage (%) of their possible value range. Possible value range for VI's and nb_NDVI$_{type}$ indices is 0 - 1 and for spectral reflectance 0 – 100. Since CI_2 that is a ratio index and not a normalised difference index the RMSE between field and sensor estimates is expressed as a percentage of the observed value range of CI_2 calculated using ASD field spectral measurements.

Model Predictors	**RMSE between Field measured and Hyperion derived model predictors (reflectance and indices)**
NDWI	5 %
TSAVI	10 %
RDVI	9 %
NDVI	8 %
CI_2	11 %
nb_NDVI$_{type}$ b1326,b1710	7 %
nb_NDVI$_{type}$ b1084,b1205	3 %
nb_NDVI$_{type}$ b1074,b2264	8 %
nb_NDVI$_{type}$ b722,b1669	8 %
MLR-1 band b1710	4.9 %
MLR-1 band b1699	5 %
MLR-2 bands b478,b1780	1.4 %/ 4.1 %
MLR-2 bands b468,b1780	2.1 % / 4.1 %
MLR-3 bands b518,b1699,b1710	1.1 %/ 5 % / 4.9 %
MLR-3 bands b1185,b1205,b1235	9.6 % / 11.8 % / 11.5 %
MLR-4 bands b518,b1205,b1235,b1710	1.1 % / 11.8 % / 11.8 % / 4.9 %
MLR-4 bands b518,b1215,b1225,b1720	1.1 % / 11.6 % / 11.3 % / 5.3 %

Using the spectral recordings of the Hyperion sensor and the statistical models developed with seasonal spectral and biomass field measurements, biomass of nine grassland fields was predicted on the date of the Hyperion data acquisition. RMSE between predicted and actual biomass measured on these nine grassland fields are presented in Table 5.5. The smallest prediction RMSE was observed for the b1084nm-b1205nm nb_NDVI$_{type}$ index model with 0.25 log(kg/m^2) of biomass. Overall, except for MLR models using two or more spectral bands all other models produced comparable low biomass prediction RMSE. The

main reason for these small RMSE was that statistical models on the field were calibrated with measurements of biomass and spectral reflectance collected and transformed in such a way that matched the spectral and spatial resolution of the Hyperion sensor.

Table 5.5 Biomass ($log(kg/m^2)$) prediction errors (RMSE) for nine grassland fields at the date of the Hyperion data acquisition (August 10, 2005). Hyperion sensor spectral measurements were used to predict biomass according to the field calibrated regression models.

Model	**RMSE of biomass predicted from Hyperion sensor spectral measurements**
NDWI	0.28
TSAVI	0.33
RDVI	0.41
NDVI	0.32
CI_2	0.29
nb_NDVI_{type} b1326,b1710	0.70
nb_NDVI_{type} b1084,b1205	0.25
nb_NDVI_{type} b1074,b2264	0.35
nb_NDVI_{type} b722,b1669	0.40
MLR-1 band b1710	0.43
MLR-1 band b1699	0.44
MLR-2 bands b478,b1780	2.72
MLR-2 bands b468,b1780	3.92
MLR-3 bands b518,b1699,b1710	1.71
MLR-3 bands b1185,b1205,b1235	3.10
MLR-4 bands b518,b1205,b1235,b1710	1.94
MLR-4 bands b518,b1215,b1225,b1720	2.79

Furthermore, the sensor predicted biomass per field was the aggregated estimation of all "pure" pixels within the grassland field. The smoothing effect of this aggregation reduced the variance of estimated biomass. Thus the value approached that of our field measurement, being the mean of several biomass measurements on the grassland field, as well. As mentioned above, MLR models using two or more spectral bands predicted biomass with high RMSE ranging from 1.71 to 3.92 $log(kg/m^2)$ of biomass. This was due to differences in absolute reflectance mainly in the NIR and the SWIR spectral regions between field and Hyperion sensor recordings that had a subsequent effect on the biomass predictions.

Even though using a ratio composed only of NIR bands could cause a conflict with the high NIR reflectance of soils in arid or semi-arid areas, Geerken et al. (2005) states that this would not be a problem in areas that have already been identified as covered from vegetation,

like our grassland fields. Furthermore, Datt et al. (2003) reported that VI's calculated using Hyperion bands from the NIR region had minimal absolute value differences from those calculated using an ASD on the ground. Therefore, we chose the model calibrated using the b1084nm-b1205nm nb_NDVI$_{type}$ index, which also had the smaller biomass prediction error using Hyperion spectral measurements (Table 5.5) to up-scale biomass estimations to the Hyperion scene. The resulting map of biomass distribution of grassland habitats within our study area is presented in Figure 5.4 and shows distinct differences in biomass patterns across the landscape.

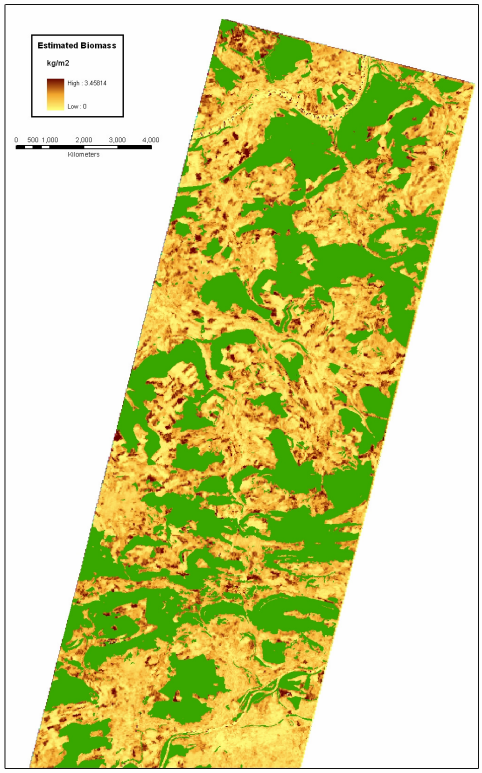

Figure 5.4 Biomass prediction map (Kg/m2) created using Hyperion spectral bands values, using a nb_NDVI$_{type}$ index regression model constructed with bands at b1084 nm and b1205 nm. Forest areas are masked with green colour.

For the 106 mapped grasslands, the relationship between species richness and estimated biomass calculated from the b1084nm-b1205nm nb_NDVI$_{type}$ index model is presented in Figure 5.5. This relationship appears to be unimodal with species richness peaking at intermediate levels of biomass. Our results agree with a number of ecological studies that have related plant biomass as a measure of productivity with plant diversity (Mittelbach et al. 2001) and have identified a hump-shaped (unimodal) relationship. The explanation for that relationship is that at low levels of productivity or high disturbance fewer species can survive, hence richness is lower. Alternatively at high levels of productivity or low disturbance,

comparably few species can monopolize the available resources and outcompete other species. It is only at intermediate levels of productivity or moderate disturbance that species richness is peaking (Palmer and Hussain 1997).

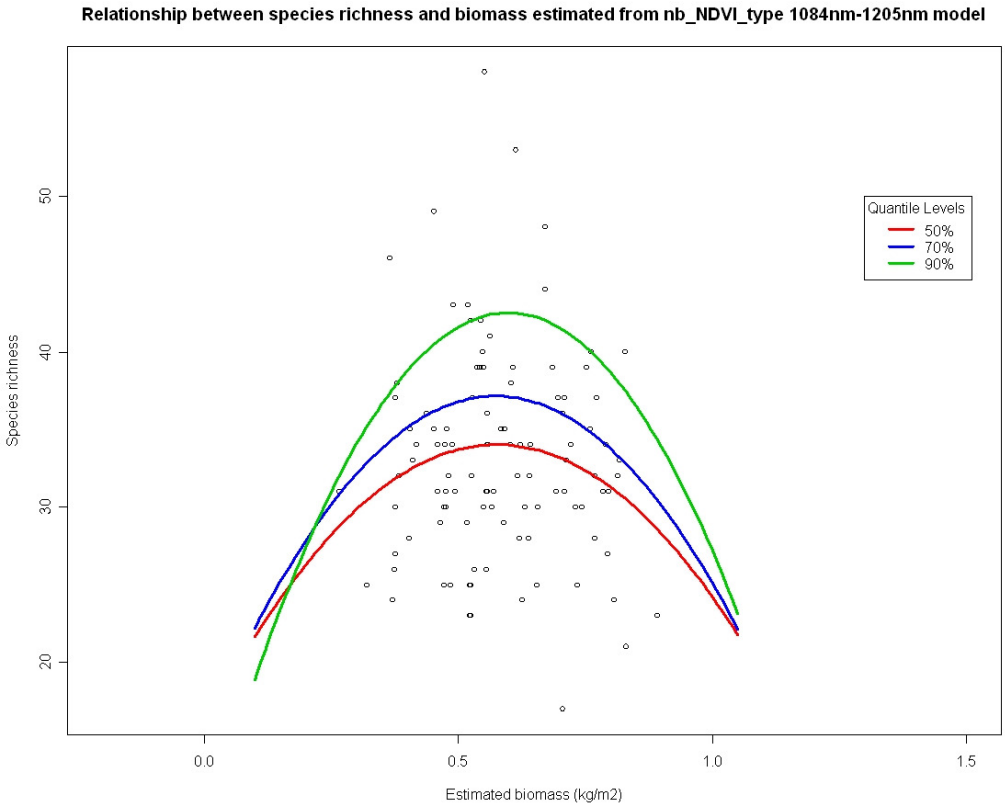

Figure 5.5 Quantile regression models of type: Richness = b0 + b1*Biomass + b2*Biomass2 between species richness and estimated biomass for 106 grassland fields. The mean (50% quantile) represents a simple quadratic regression model, while the higher quantiles represent a model fit through the top 30 (70% quantile) and the top 10 (90% quantile) percent of the data range.

Our results show that higher species richness is mainly observed at intermediate levels of biomass. However, this relationship is not statistically significant since there are a number of low species richness values at intermediate biomass levels as well. The main reason for this is possibly related to the time during the growing season when the Hyperion scene was acquired. In particular, many of the highly productive grasslands (and thus the ones with low species richness) were already cut and were at the stage of accumulating new biomass. Therefore, the estimated biomass from the Hyperion scene did not reliably represent the productivity of these grassland habitats. We believe that these grasslands would have been towards the highly productive end of the unimodal curve if the scene was acquired earlier and in particular at the peak of the growing season.

5.3 Conclusions

Results presented in this paper demonstrated the potential of hyperspectral remote sensing for estimating biomass of grassland habitats throughout a whole growing season. Our analyses actually highlighted the importance of acquiring multitemporal spectral and biomass measurements especially at the beginning of the growing season in order to capture a larger range of biomass and seasonal variability observed and therefore to be able to create reliable and phenology-independent models. An additional conclusion of this study is that appropriate spectral and spatial scaling of field observations can assist towards successful up-scaling of field developed statistical models to satellite recorded remote sensing data. Even though MLR models using spectral bands gave better estimates and predictions on the field level, they could not be scaled easily to the sensor level. Therefore, for up-scaling field developed models and for better estimation of grassland biomass we propose to use narrow-band $NDVI_{type}$ vegetation indices constructed with bands in spectral regions related to canopy water content. Finally, our research has exhibited the potential and the need to link the high accuracy hyperspectral remote sensing products (e.g. biomass) with nature conservation topics like biodiversity monitoring.

6. Coupling Imaging Spectroscopy and Ecosystem Process Modelling − The Importance of Spatially Distributed Foliar Biochemical Concentration Estimates for Modelling NPP of Grassland Habitats

6.1 Introduction

During the last century, human activities have increasingly affected the climate of the Earth (IPCC 2007). Improving our capability to predict the response of ecosystems to these environmental and climate changes relies on our ability to model the terrestrial carbon cycle at regional to global scales and in particular of processes like net primary production (NPP). NPP is critical for understanding the role of biosphere in regulating atmospheric CO_2 concentrations (Turner et al. 2004b), thus accurate estimates, along with information on its spatial and seasonal variability are required (Curran 1994). At local scales NPP can be estimated through in-situ sampling with flux-towers, but over regional and global scales and under different climate scenarios the only feasible way is to use ecosystem simulation models that synthesize environmental data into single coherent analysis of terrestrial carbon fluxes (White et al. 2000). Ecosystem process models simplify reality by simulating important biological processes that drive NPP (Aber 1997; Nemani et al. 1993; Running 1994). Such models require data to parameterise them, drive them and if possible validate them (Curran 1994). Over regional and global scales, remote sensing provides the only feasible source of such information (Wulder et al. 2004).

A number of studies exist where key remotely-sensed structural and physiological parameters of vegetation directly linked to underlying ecological processes were coupled with ecosystem process models. Parameters were (a) LAI (Hazarika et al. 2005; Lucas and Curran 1999; Running et al. 1989) that is linked to the minimum light levels within the canopy that will activate stomata opening and regulate canopy precipitation and the interception and absorption of incoming radiation, (b) aboveground biomass (Green et al. 1996; Kimball et al. 2000) that is used to initialise carbon pools, simulate local carbon budgets and estimate autotrophic respiration (c) APAR (Field et al. 1995) that can be a limiting factor for the rate at which a plant can assimilate CO_2 from the atmosphere for the production of carbohydrates and (d) land use classifications (He et al. 1998; Ollinger et al. 1998) since vegetation cover types differ significantly in morphological and ecophysiological characteristics that drive certain ecological processes.

However, another very important parameter that controls terrestrial biogeochemical processes is foliar canopy chemistry (Curran 1994; Wessman 1994a). Canopy concentrations of chlorophyll, nitrogen and lignin drive key processes since chlorophyll is directly related to

the rate of photosynthetic production (Curran 2001), nitrogen to the availability of nutrients and to carbon allocation (Schimel 1995) and lignin to the rate of nutrient and carbon cycling via their influence on decomposition rates (White et al. 2000). Specifically, the foliar Carbon/Nitrogen ratio (C:N) drives processes such as decomposition and mineralization and thus strongly influences soil organic matter concentrations and turnover rates. Consequently, foliar C:N is a core variable of a number of ecosystem process models. White et. al (2000) showed that foliar C:N was one of the most sensitive input parameters to the ecosystem process model Biome-BGC (Thornton 1998), exerting significant control on NPP estimates for all biomes. Yet, C:N values used as input to ecosystem models are almost exclusively derived from mean values of global point measurements derived from the literature. Given the importance of foliar C:N for terrestrial carbon cycling, there is a need for spatially explicit data to be coupled with ecosystem process models for better understanding biogeochemical processes.

Hyperspectral sensors (Van der Meer et al. 2001) make use of the unique spectral characteristics of vegetation (Curran 1989; Elvidge 1990) and thus offer the potential to estimate foliar biochemistry (Ustin et al. 2004b). Studies using hyperspectral remote sensing to estimate leaf and canopy biochemical concentrations have been carried out in different ways: under controlled laboratory conditions (Curran 1989; Curran et al. 2001; Kokaly and Clark 1999; Mutanga et al. 2003; Phillips et al. 2006), in the field using a spectroradiometer (Ferwerda et al. 2005; Hansen and Schjoerring 2003; Strachan et al. 2002; Thulin et al. 2004) and using data collected from airborne and spaceborne hyperspectral sensors (Beeri et al. 2007; Boegh et al. 2002; Huang et al. 2004; Mutanga and Skidmore 2004b; Townsend et al. 2003). Most of the above studies, however focus on developing new statistical methodologies to accomplish higher accuracies in predicting foliar biochemical concentration and few have attempted to relate remote sensing derived foliar biochemistry with productivity. In particular, Smith et. al (2002) used foliar N concentration predictions from the AVIRIS sensor as a direct scalar of NPP of forests. Only limited studies exist that have used these spatially explicit foliar concentrations information as input to ecosystem process models for forest NPP estimations (Lucas and Curran 1999; Martin and Aber 1997; Ollinger and Smith 2005) and none to our knowledge that have extended their research on grassland ecosystems.

This study evaluates the effects of using spatial estimates of foliar C:N derived from hyperspectral remote sensing for simulating NPP of grasslands by means of the ecosystem process model Biome-BGC. The main objectives of this study are (a) to calibrate statistical spatial models for the prediction of foliar C:N for grassland habitats at the regional scale using airborne HyMap hyperspectral data, (b) to use the foliar C:N predictions as input to the ecosystem process model Biome-BGC and to derive annual NPP estimates, (c) compare these results to simulated NPP estimates when using a C:N value from “global” or “regional” field

measurements, and (d) to investigate the sensitivity of the NPP estimates to errors of predicted foliar C:N, induced during the statistical modelling process.

6.2 Results

Descriptive statistics of grassland foliar N and C concentration from samples collected at the 27 plots are reported in Table 6.1. High variability is observed for the N samples reflecting the differences in nutrient availability and species composition among the grassland types where the samples were collected from. Furthermore, low variability of the canopy C concentrations was observed.

Table 6.1 Summary statistics of measured foliar biochemical concentrations at 27 grassland plots at the study area.

		% Dry Weight				
	n	**Mean**	**Stdev**	**Min**	**Max**	**Range**
Foliar N concentration	27	2.271	0.6931	0.997	3.187	2.19
Foliar C concentration	27	44.05	0.7352	41.89	45.27	3.377

Results from the PLS regression modelling using HyMap (a) reflectance spectra and (b) continuum-removed reflectance spectra with grassland foliar N samples are summarised in Table 6.2. These results indicated that PLS regression models developed from HyMap continuum-removed reflectance were consistently better than the PLS models developed from absolute reflectance spectra.

Table 6.2 Performance of PLS regression models for predicting foliar N concentration for grassland habitats

	Reflectance Spectra		**Continuum-removed Reflectance Spectra**	
No. of PLS factors	**N % variance explained**	**PLS Model N CV-RMSE (% Dry Weight)**	**N % variance explained**	**PLS Model N CV-RMSE (% Dry Weight)**
1	14.05	0.7421	33.62	0.6637
2	21.81	0.6837	48.87	0.5664
3	58.82	0.5429	67.01	0.4677
4	73.41	0.5530	79.59	0.4181
5	82.56	0.6418	83.63	0.4172
6	85.94	0.6251	86.74	0.4283

Using continuum-removed spectra, PLS models performed better both in terms of explained variation in the N data, and in terms of prediction accuracy, regardless of the number of

factors used. The optimal PLS model for predicting foliar N concentration was the one using four factors (Figure 6.1). This model accounted for 79.59% of the observed variation in the N data while it produced a cross-validated N prediction error (CV-RMSE) of 0.4181 N % Dry Weight.

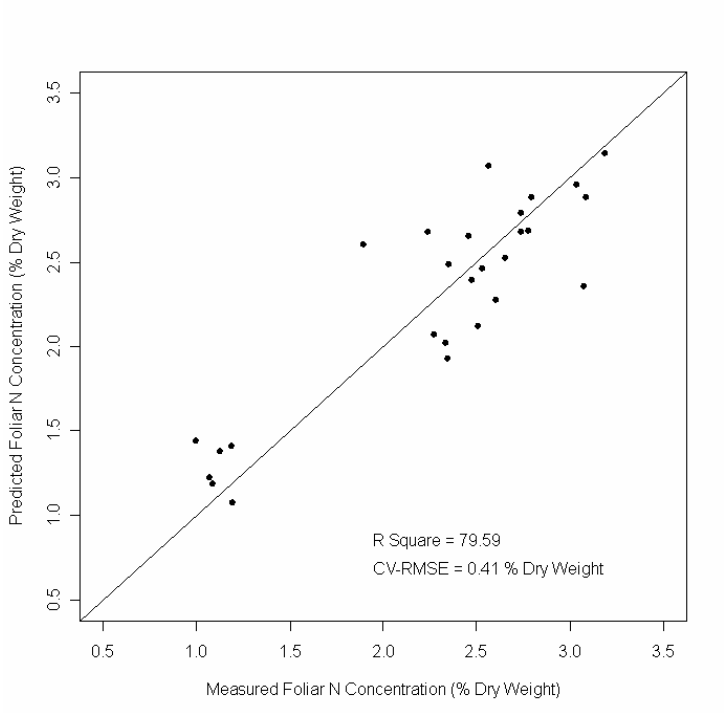

Figure 6.1 Measured vs. predicted foliar N concentration of grassland habitats using four-factor partial least squares regression based on HyMap continuum-removed reflectance.

Even though inclusion of additional factors in the models increased the percentage of explained variation in the N data to 83.63% and 86.74% for the five- and six-factor models respectively, it had a different effect on their N prediction accuracy. In fact, only a marginal decrease of the CV-RMSE was observed for the five-factor model (0.4172 N % Dry Weight), while the CV-RMSE for the six-factor model actually increased (0.4280 N % Dry Weight). Therefore, the four-factor continuum-removed reflectance PLS model was selected to predict grassland foliar N concentrations across the whole extent of our study area (Figure 6.2).

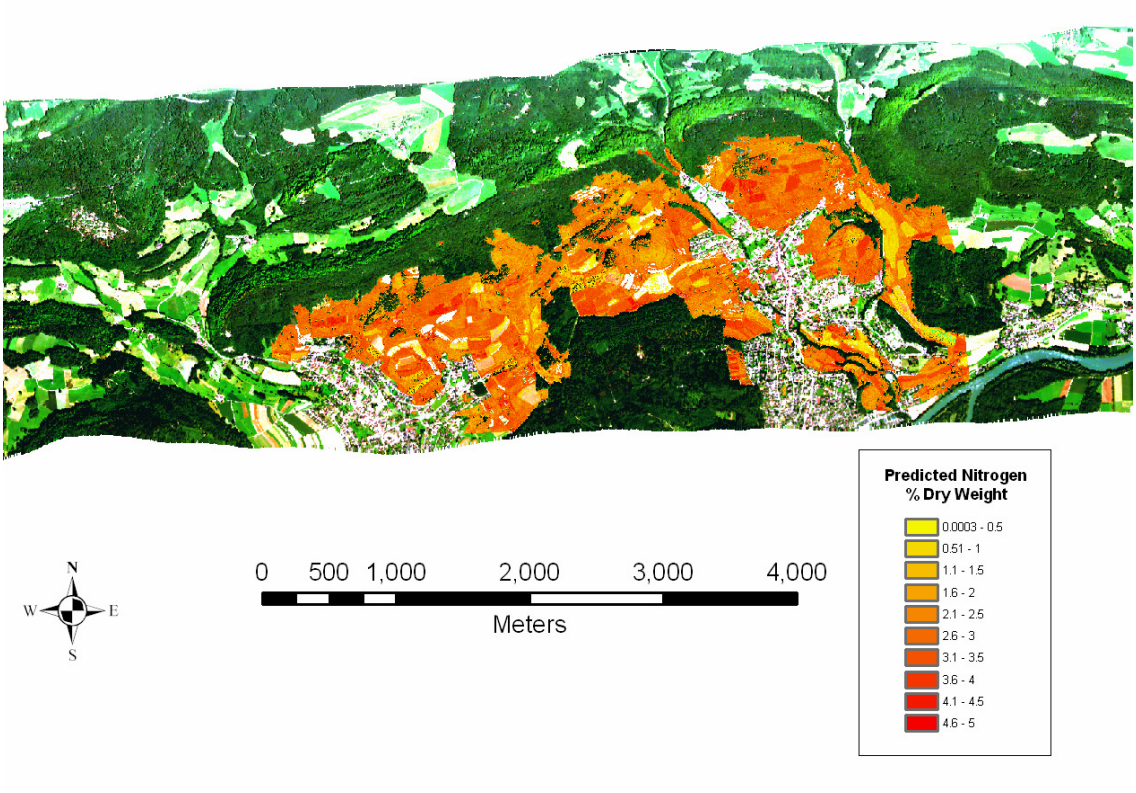

Figure 6.2 HyMap predicted foliar nitrogen concentration (% Dry Weight) for the grassland habitats of the study area. The four-factor PLS regression model with the continuum removed reflectance was used.

Using a constant carbon concentration (i.e., C_{CNT} = 44.05) and the predicted foliar N concentration of the four-factor PLS model, C:N ratio for every 5 x 5 m pixel was calculated. Distribution of the C:N values across the study area are presented in Figure 6.3. Overall, C:N values were lower than the Regional C:N (i.e., $C:N_{REG}$ = 22.24). In particular, the mean C:N value was 18.2 while the first and third quartile were 14.65 and 20.49 respectively. For the *HyMap C:N* + ε scenario, C:N values were calculated by adding the possible N prediction error of the PLS model on the initial model predictions. C:N values for the study area were very similar to the ones of the *HyMap C:N* scenario, with a mean value of 18.69 while the first and third quartile were 13.94 and 21.67, respectively.

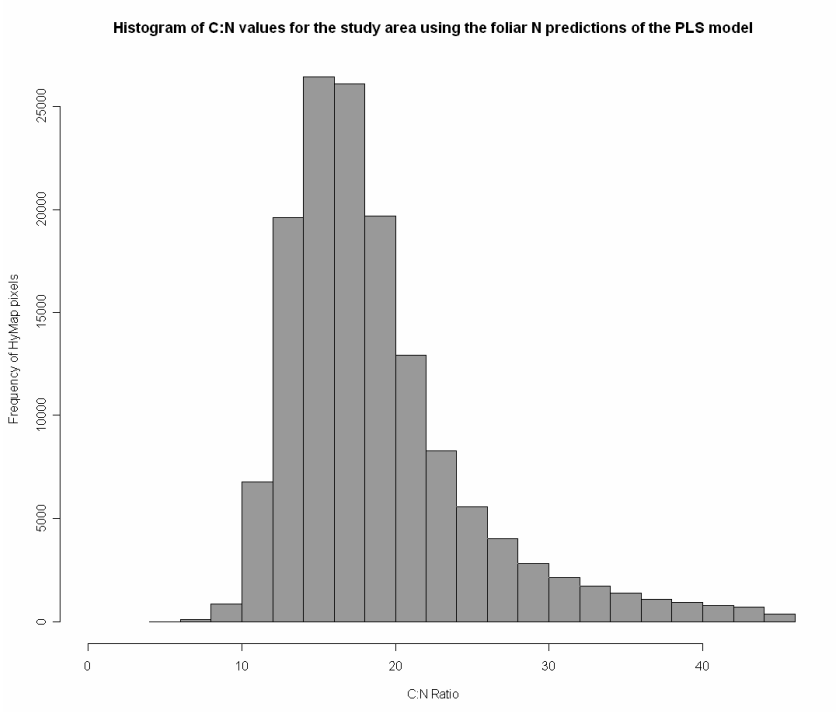

Figure 6.3 Distribution of C:N ratio values for the study area. C:N ratio was calculated using a constant carbon concentration (C_{CNT} = 44.05) and the nitrogen concentration predictions of the HyMap four-factor PLS regression model.

Even though Biome-BGC NPP estimates covered the period 1931-2001, comparison of the C:N scenarios is done using the results of 2001. Only this year was chosen since (a) it was closest to the time of the HyMap image acquisition and (b) overall NPP estimates were representative for this 71-year period (results shown later). Effects of the different C:N scenarios on the mean NPP estimates for the study area are summarized in Figure 6.4. Results demonstrated increasing NPP values, with lowest mean estimates produced by the *Global C:N* scenario (597 gC/m2/year) and highest by the *HyMap C:N* + ε scenario (660 gC/m2/year). The *Regional C:N* and *HyMap C:N* scenarios produced mean NPP of 622 and 658 gC/m2/year, respectively. Statistical analyses of these results revealed significant differences between NPP estimates of the different C:N scenarios. In particular, apart from NPP estimates between the *HyMap C:N* and *HyMap C:N*+ ε, all other scenarios produced estimates that were significantly different from each other (Figure 6.4).

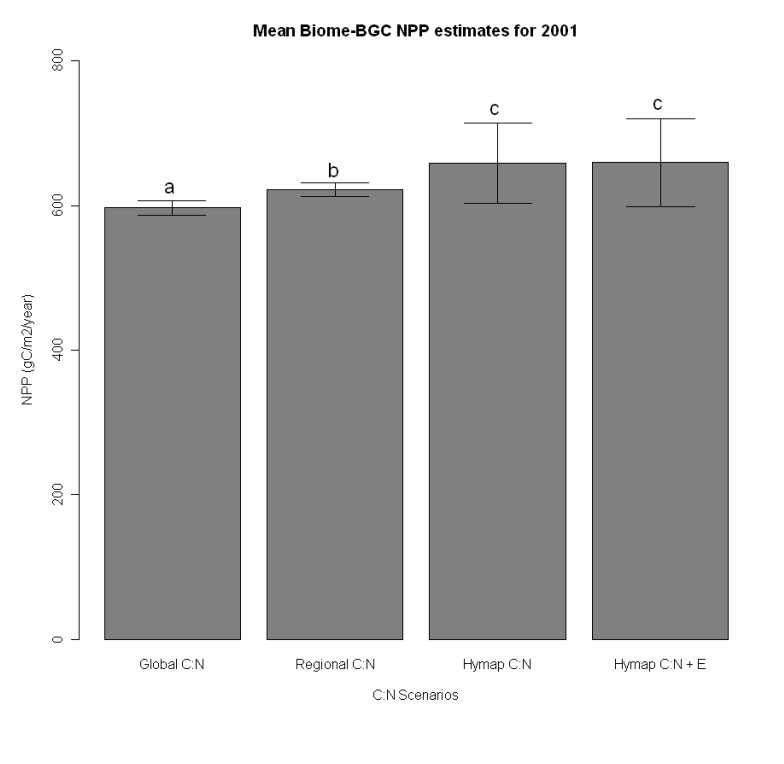

Figure 6.4 Mean (± std. dev.) Biome-BGC NPP estimates for the whole study area using the different C:N scenarios. NPP estimates are for the year 2001 and different letters represent a significant difference between mean NPP estimates of the four C:N scenarios calculated from paired t-tests at p = 0.05.

For the different C:N scenarios, distribution of the 5 x 5 m NPP estimates for 2001 are presented in Figure 6.5. The use of the four scenarios had a considerable effect on the range of NPP values across the study area. In particular, the range of NPP values for the *Global C:N* and *Regional C:N* scenarios was limited from 576 and 602 gC/m2/year to 648 and 672 gC/m2/year respectively. On the contrary, use of the *HyMap C:N* and the *HyMap C:N* + ε scenarios as input to the Biome-BGC model produced a much wider extent of NPP estimates that ranged from 456 to 787 gC/m2/year. Additionally, results showed that for the *Global C:N* and *Regional C:N* scenarios, very large areas had either similar or marginally different NPP values. On the contrary, NPP values for the other two scenarios demonstrated fine scale variation along the whole extent of the study area (Figure 6.6).

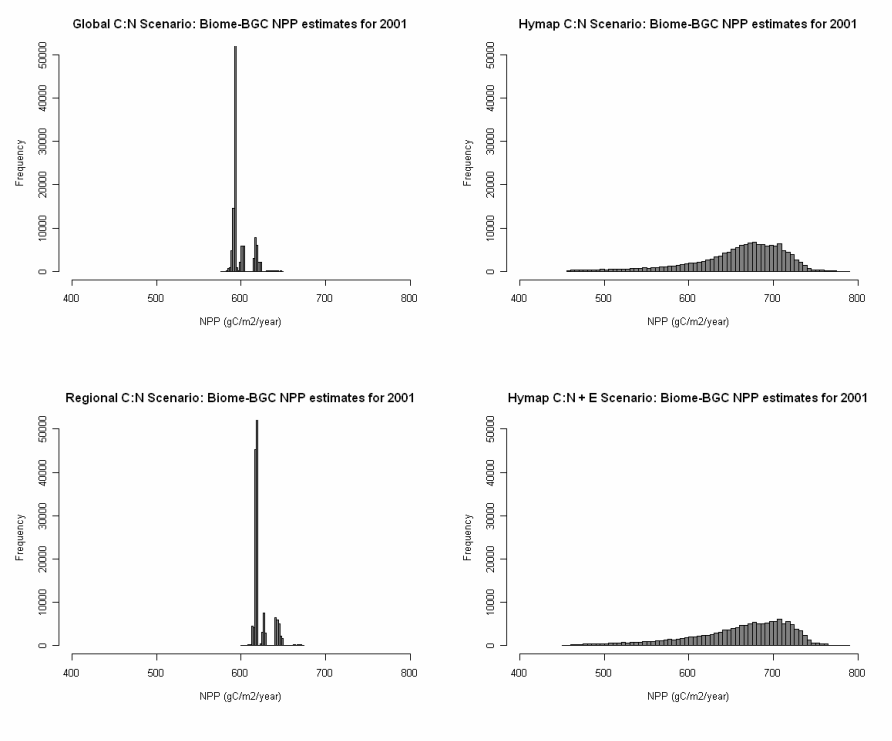

Figure 6.5 Distribution of Biome-BGC simulated NPP estimates of the year 2001 for the study area using the different C:N scenarios.

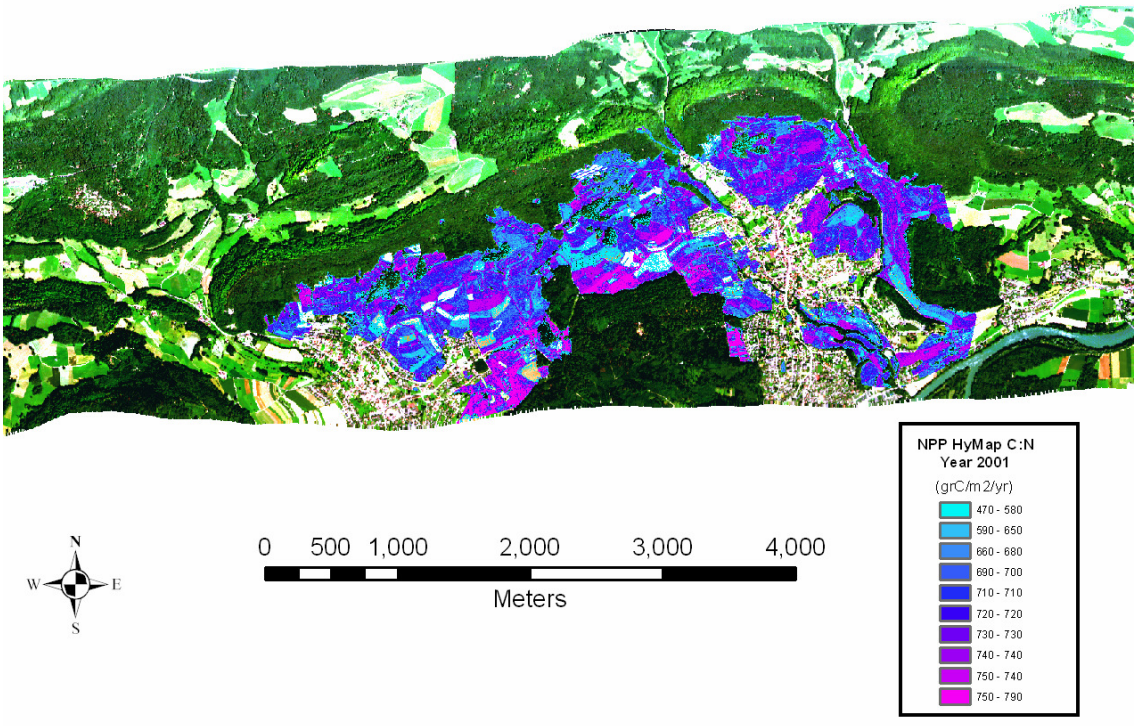

Figure 6.6 Net primary productivity (gC/m2/year) of grasslands estimated for the study area with the Biome-BGC ecosystem process model using the HyMap derived spatially explicit estimates of C:N ratio.

The distribution of NPP differences between every 5 x 5 m pixel for the *HyMap C:N* and the *Global C:N* scenarios are summarized in Figure 6.7. Results shown here are specifically chosen between these two scenarios since (a) the *Global C:N* scenario is the most likely to be used by researchers when regional C:N data is unavailable and (b) no significant differences existed between NPP estimates of the *HyMap C:N* and *HyMap C:N* + ε scenarios. Results indicated that more than 85% of the total study area had higher NPP estimates when the *HyMap C:N* scenario was used as input to the Biome-BGC model. In particular, NPP differences for 68% of the study area were more than 50 gC/m2/year higher in the *HyMap C:N* scenario. Even though certain areas existed where NPP estimates were lower using the *HyMap C:N* scenario, the mean increase of NPP over the whole study area was 63 gC/m2/year.

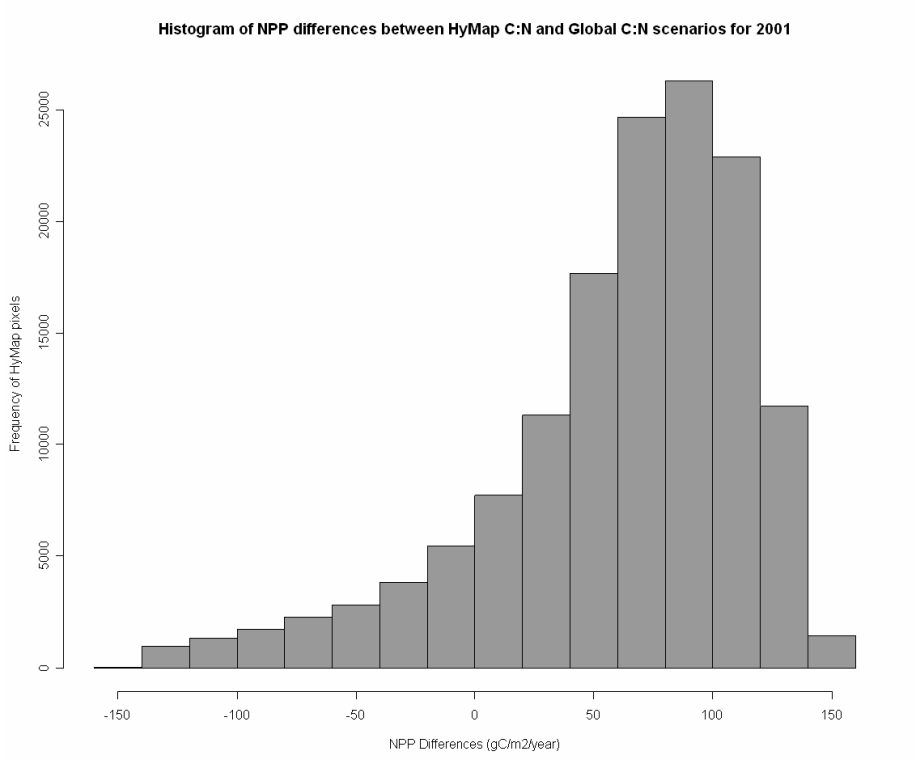

Figure 6.7 Distribution of NPP differences between Hymap C:N and Global C:N scenarios for the study area. NPP estimates are for the year 2001.

Our study included the simulation of NPP over the study area for the whole period of 1931 – 2001. Mean historical NPP differences between the *HyMap C:N* and the *Global C:N* scenarios are presented in Figure 6.8. Results showed that the use of the *HyMap C:N* scenario produced consistently higher mean NPP estimates for the whole 71-year period. Smallest

mean NPP difference between the two scenarios was observed for the year 1947 with 31 gC/m2/year, whereas the maximum difference was for the year 1977 with a mean of 83 gC/m2/year. Overall, the use of the *HyMap C:N* scenario as input to Biome-BGC increased the NPP estimates of the study area by a mean of 61 gC/m2/year over the full 71 year period.

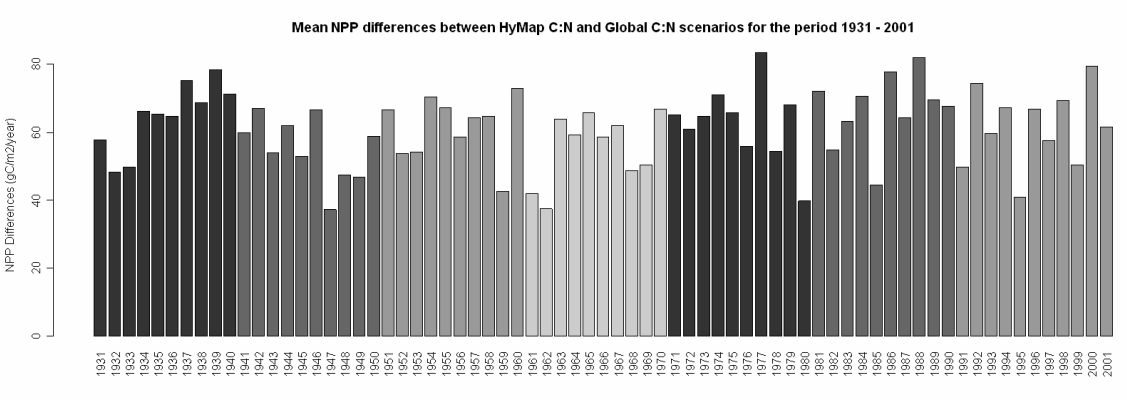

Figure 6.8 Mean NPP differences between Hymap C:N and Global C:N scenarios for the period 1931-2001. For clarity, differences in grey shading represent 10-year blocks, except for the last block (1991-2001) that has 11 years.

6.3 Discussion and conclusions

The main purpose of this was study was to evaluate the importance of using spatial estimates of grassland foliar C:N derived from hyperspectral remote sensing, in the ecosystem process model Biome-BGC and investigate their effect on the estimation of NPP. In order to derive spatial estimates of foliar C:N, partial least squares regression based on HyMap hyperspectral airborne imagery was used. Our analyses have indicated that PLS regression models produced high accuracies of predicted foliar biochemical concentrations confirming results of previous studies (Hansen and Schjoerring 2003; Ollinger and Smith 2005; Smith et al. 2002). In addition, PLS regression based on continuum-removed reflectance spectra produced higher accuracies compared to absolute reflectance spectra. These results are consistent with those of Huang et. al (2004). Our findings can be attributed to the fact that continuum-removal transformation enhances the depth of spectral absorption features, thus improving the estimation of foliar biochemical concentrations (Kokaly and Clark 1999; Mutanga et al. 2003). Furthermore, results of this study demonstrated the importance of carefully selecting the optimal number of factors when building a PLS regression model, especially when the sample size is small (n=27). Inclusion of many factors could potentially lead to overfitting of the model on the training dataset (Table 6.2, six-factor model) and thus

reduce its ability to generalise and predict accurately on an independent dataset (Cho et al. 2007; Crawley 2005).

A very important finding of this study was that significant differences between NPP estimates occurred when spatial predictions of foliar C:N were used as input to an ecosystem process model, contrary to using single C:N values representing individual biome or regions. Interestingly, NPP estimates using spatial predictions of foliar C:N where higher when compared to the two other scenarios (Figure 6.7). The main reason for these differences was the ability of hyperspectral remote sensing to detect subtle differences in spectral absorption features thus allowing detailed mapping of grassland foliage concentrations (Curran 1989; Kumar et al. 2001). Fine scale predictions for the study area indicated an overall lower mean C:N value compared to values reported in the literature (White et al. 2000). These differences were possibly due to highly productive grasslands and some agricultural areas (that had potentially received nitrogen fertilisation treatment) within our study area. Additionally, the presence of these highly productive grasslands within the selected study area, were the possible reason for the significant differences between NPP estimates of the *HyMap C:N* and the *Regional C:N* scenarios. Since grassland samples were collected mainly from natural and semi-natural habitats the $C:N_{REG}$ value used for the *Regional C:N* scenario was not representative of the highly productive grasslands, which had high foliar N concentrations, thus lower C:N values (Figure 6.3). Foliar N is directly linked to the process of photosynthesis (Turner et. al. 2004), while foliar C:N within the Biome-BGC model determines factors like the nitrogen required to construct leaves (LAI), the amount of nitrogen available for photosynthetic processes and the leaf respiration rates (Thornton 1998; White et al. 2000). Therefore, use of the overall lower spatial estimates of foliar C:N derived from hyperspectral remote sensing resulted in higher mean NPP estimates for the study area.

Another finding of this study was that inclusion of the PLS model prediction error did not significantly change the NPP estimates of the Biome-BGC model (Figure 6.4). This result can be explained by the high accuracy of the PLS model predictions, that produced a cross-validated error of 0.4181 (N % Dry Weight) or 18.4 % of the measured mean N concentration of the grassland samples. Nevertheless, further analysis on the sensitivity of the Biome-BGC model to foliage C:N would be required before a specific model accuracy threshold can be established. This is especially important since Biome-BGC sensitivity to foliage C:N has shown to depend on the biome and the particular plant species under investigation (Tatarinov and Cienciala 2006; White et al. 2000).

As expected, the ability of hyperspectral remote sensing to map fine-scale variation in foliar C:N concentrations had a subsequent effect on the range of NPP estimates across the study area (Figure 6.5). The limited variability of NPP using the *Global C:N* and the *Regional C:N* scenarios can be attributed to differences in soil profile parameters which changed

marginally within the small extent of the study area. Contrary, the wide range of NPP estimates for the *HyMap C:N* and *HyMap C:N* + ε scenarios was driven by the detailed C:N spatial estimates used as input to the Biome-BGC model. These detailed NPP maps have a substantial ecological meaning since they can assist towards a better understanding of small scale interactions of biogeochemical cycles thus improving the up-scaling of regional observations to the landscape scale (Curran 1994; Lucas and Curran 1999).

Finally, for the period 1931-2001, results from this study showed that yearly NPP estimates using the *HyMap C:N* scenario were always significantly higher compared to those where the *Global C:N* scenario was used (Figure 6.8). However, mean NPP differences between the two scenarios showed considerable fluctuations over the years. These fluctuations can be attributed to the changing meteorological conditions. In fact, parameters like temperature, precipitation, radiation and humidity have the most important control on vegetation processes (Thornton et al. 2002). Flux estimates in Biome-BGC depend strongly on daily weather conditions, while the overall model behaviour over time is driven by the climate history of a region (Running and Hunt 1993). Thus, even though the use of spatial C:N estimates as input to the Biome-BGC model was the main driver for the significantly higher estimates of NPP, meteorological characteristics of each year may enhance or reduce these differences.

It should be noted that results from this study were limited by the spatial extent and availability of hyperspectral data. Multiple datasets covering different regions would provide a more complete understanding of the effects of grassland NPP estimations from coupling foliar biochemical concentrations derived from imaging spectroscopy with ecosystem process models. Future research should be directed towards the use of foliar canopy concentrations derived from e.g., the spaceborne hyperspectral Hyperion sensor (Smith et al. 2003; Townsend et al. 2003) into ecosystem process models. The main advantages of the Hyperion sensor over airborne hyperspectral sensors are the continuous seasonal coverage and the possibility to acquire information over diverse regions of the globe. Attention should also be paid to broad-band sensors, since recent research by Phillips et. al (2006) showed the potential of ASTER in estimating canopy C:N ratio of rangelands at the landscape scale.

In summary, results presented in this study demonstrated the importance of using spatial estimates of foliar biochemical concentration as input to ecosystem process models. NPP estimates using C:N data derived from hyperspectral remote sensing differed significantly from results obtained when using C:N values reported in the literature or values from regional mean measurements. Results from this research may be used as an intermediate step in resolving the critical scaling issue related to the task of validating products from coarse-resolution sensors like MODIS to ground measurements. In addition, results from this research showed that PLS regression models based on continuum-removed spectra from the

HyMap sensor provided a better alternative to absolute reflectance values for estimation of foliar N concentrations of grasslands habitats. Overall, given the importance of parameters like C:N ratio in terrestrial carbon cycling and the ability of hyperspectral remote sensing in providing such high accuracy products, we stress the importance and the need to couple these two synergistic technologies in order to initialise, validate and adjust better ecological process models.

7. Conclusions and Outlook

7.1 Conclusions and main findings

The main objectives of this dissertation were to explore the potential of hyperspectral remote sensing for biodiversity conservation of species-rich grasslands and for deriving vegetation properties relevant to ecosystem productivity. The first part of this dissertation investigated the spectral separability of grassland habitats during the growing season for two consecutive years using spectral data collected with a field spectroradiometer (chapter 4). In the second part of the dissertation, statistical models were calibrated to predict above-ground biomass of grasslands using data collected in the field during the whole growing season. Additionally, the feasibility of up-scaling these models to data collected from the Hyperion sensor was evaluated (chapter 5). In the third part of this dissertation, novel statistical models and airborne hyperspectral data were combined to predict grassland foliar biochemistry at the regional scale. This information was then used to initialise and drive the Biome-BGC ecosystem process model for NPP estimation at the regional scale (chapter 6).

Coming back to the research questions posed at the beginning of this dissertation, we conclude that species-rich grassland habitats could be discriminated successfully by using hyperspectral remote sensing. Acquisition of seasonal spectral measurements coupled with the ability of hyperspectral sensors to record multiple narrow spectral bands, made it possible to identify in detail the specific parts of the spectrum that contributed best to the separability of the grasslands types during two growing seasons. More importantly, our method demonstrated that the beginning of the growing season was the best period for discriminating grassland habitats from hyperspectral remote sensing measurements. A second conclusion of our research was that continuum removal transformation should not only be used for deriving leaf or canopy biochemical properties but has also great potential for vegetation discrimination since it was found to be less affected by seasonal phenology changes throughout the whole growing season.

These findings are important for ecological purposes and in particular for biodiversity conservation of grassland habitats. By using hyperspectral data collected from airborne or spaceborne sensors, different habitats types can be mapped and eventually discriminated using the spectral separability information derived from our research. The grassland types examined here cover a gradient of mesic-dry habitats that differ considerably with regards to biodiversity and productivity. Seasonal mapping over certain time periods may provide a useful monitoring scheme of productivity and thus biodiversity trends. Since more productive grasslands have the highest probability to be converted to agricultural land, such areas where

potential loss of biodiversity is highest may need to be targeted specifically for appropriate management.

Results from the study of grassland biomass estimation from hyperspectral remote sensing demonstrated that the construction of robust statistical models is feasible, provided that multiple samples during the growing season were collected. Seasonal sampling, especially early in the growing season, was shown to be very important in order to cover the normally occurring variability, due to variations in phenology stage, spatial patterns and management. Highest accuracies of biomass retrieval at the field level were achieved with the 4-band multiple linear regression models, using a novel subset variable selection algorithm. Additionally, results from this study indicated that exploiting the multiple spectral bands of hyperspectral data by constructing narrow band NDVI type indices, provided to be a better alternative to existing hyperspectral or broadband indices for biomass retrieval. Overall, spectral regions related to canopy water content were identified to be more suitable for building statistical models for the retrieval of biomass across the whole growing season. Our study also indicated that even though the 4-band multiple linear regression models gave the best predictions in the field, up-scaling the data to Hyperion was best done when narrow band NDVI type indices were used. Finally, this study showed that it was not possible to establish a significant relationship between plant species richness and above-ground biomass estimates, since these originated from samples taken late in the growing season after management practises like cutting and/or mowing were already applied, and thus were not representative surrogates of grassland productivity.

The ability to retrieve accurate estimates of above-ground biomass independent of a specific grassland habitat and phelological period from hyperspectral remote sensing has a number of useful applications. Reliable spatial estimates of biomass can be used by managers and decision makers, in order to monitor the effects of applied management schemes and to modify them if necessary. Furthermore, knowledge of above-ground grassland biomass provides crucial information for estimation of available below-ground soil carbon stocks and therefore total NPP (Gill et al. 2002). In addition, several ecosystem process models simulate natural processes on a daily time step with above and below ground biomass accumulation being two of the most significant parameters that are simulated. Accurate and timely biomass estimates retrieved from hyperspectral remote sensing may therefore be used to validate and periodically reset the values estimated from the ecosystem process model. Finally, accurate estimates of vegetation biomass may be used in combination with ecosystem process models in order to initialise carbon pools, simulate local carbon budgets and more important, estimate autotrophic respiration (Turner et al. 2004b).

The objective of the third part of this dissertation was to parameterise and drive the ecological process model Biome-BGC using grassland foliar biochemical information

predicted from HyMap airborne data and field sampling. Results from our study revealed that accurate predictions of foliar biochemical information could be achieved successfully, provided that continuum-removal transformation was applied to the reflectance spectra prior to calibrating the statistical models. Furthermore, we conclude that it was possible to run the Biome-BGC model in a spatially distributed mode, by using the spatially explicit C:N predictions, thus deriving detailed NPP estimates of the study area. The most important findings, however, were that NPP of the study area using spatial predictions of C:N was significantly higher than NPP estimated using C:N values widely applied in literature or even from using regionally measured mean C:N values. These findings suggest that it is possible that carbon sequestration dynamics of certain ecosystems − in our case of managed grassland habitats − might be underestimated regionally. Finally, it was shown that statistical modelling errors originating from the development of regional canopy C:N models, are not expected to affect the sensitivity of Biome-BGC for NPP estimations assuming that high prediction accuracies in C:N values are achieved. Nevertheless, further research is required before specific prediction accuracy thresholds can be established.

Results from our research may be used as an intermediate step between NPP measurements from flux towers and NPP estimates from coarse-resolution sensors like MODIS. Even though the spatial coverage of the study site is relatively small, we found significant differences between land-cover averaged and spatially-distributed C:N values for NPP modelling along a whole growing season. By establishing a network of data acquired over diverse biomes around the globe, NPP estimates from the coupling of hyperspectral remote sensing and ecosystem process modelling may serve as an improvement for modelling global NPP estimates from MODIS or other spatial data sources. Furthermore, detailed information and spatial monitoring of NPP patterns may enhance our knowledge about local scale interactions between biosphere and atmosphere. In fact, this would assist to investigate the sensitivity of ecosystems to future climate change conditions and facilitate socio-economic impact modelling.

In this dissertation, retrieval of biophysical and biochemical parameters of grassland habitats was based on empirical modelling approaches. Even though thorough conceptual consideration of model parameters (with regards to physical properties of vegetation and the parameter under investigation) was performed, developed models and their accuracies could potentially be limited to the place where our data were collected (Verstraete et al. 1996). The grassland types examined here were the most representative types of low elevation sites of the Swiss Plateau. Therefore, our results may be extended to large areas of low elevation managed grasslands that have similar management and species compositions characteristics. An additional sampling would however be required for higher elevation alpine grasslands, which have different morphological, structural and biochemical characteristics and are

equally important for biodiversity conservation. Furthermore, and especially for the first part of this dissertation, considerations of climate parameters like temperature and precipitation would assist towards a better understanding of the effects of yearly climate variation upon the phenology of grassland species compositions, thus increasing the potential to extend results to other habitat types. Use of physical, deterministic models that are based on diverse representations of light interactions with vegetation at the leaf and canopy scale represent an alternative to deal with the uncertainties of empirical modelling techniques. Radiative transfer models range in complexity, from simple plate leaf models to complex 3-D canopy models (Ustin et al. 2004a). However the factors used to explain the radiative transfer are very often limited, while increased complexity of the models limits the retrieval of vegetation parameters due to the ill-posed nature of the RT models inversion (Combal et al. 2003). Currently, retrieval of vegetation biochemical parameters through the inversion of RT models is limited to chlorophyll concentration and not to other parameters of interest like nitrogen or lignin (Vohland and Jarmer 2008). Furthermore, understanding the species competition dynamics, plant community interactions and more importantly how to represent these interactions in a radiative transfer manner in order to link biodiversity with physical models still remains a great challenge not only for remote sensing scientists but also for ecologists.

7.2 Future Challenges

Availability of timely and reliable information on the status of natural ecosystems is of major importance for ecological, political and economical purposes. Existing literature and findings of this dissertation showed that retrieval of parameters like LAI, APAR, biomass and foliar nitrogen concentration have significantly improved our understanding and our ability to map NPP at regional to global scales. Nevertheless, future research needs to focus on the retrieval and use of other parameters as well. Derivation of a foliage clumping index in addition to LAI assists in better characterisation of the canopy and in particular the separation between sunlit and shaded leaves. For better estimation of NPP Chen et al. (2003) propose that a combination of LAI and clumping index parameters should be preferred over traditional methods. These methods estimate NPP by using APAR without, however considering how APAR is shared between sunlit and shaded leaved. Attempts to create regional and global maps of a foliage clumping index using multi-angular POLDER data currently exist (Chen et al. 2005b; Leblanc et al. 2005), while research using data from high spatial resolution spaceborne (CHRIS) or airborne spectroradiometers with high radiometric and angular precisions (APEX) (Nieke et al. 2004) should be intensified. Foliar lignin concentration is another crucial parameter affecting the global carbon cycle. Foliar lignin is related to litter decomposition rates, thus to the releases of CO_2 by heterogenic respiration of decomposing

organic matter (Wessman 1994b) and to the fraction of soil carbon accumulation after decomposition. Even though estimation of lignin at the canopy scale has received some attention from the hyperspectral remote sensing community (Martin and Aber 1997; Serrano et al. 2002) efforts to decouple the biochemical from the canopy structural signal should receive more attention. Accurate spatial estimates of foliar N and lignin could be used to parameterise and drive ecosystem process models thus improving productivity estimates of terrestrial ecosystems.

Overall, a long term goal should be the routine assimilation of remotely-sensed land surface parameters into Earth System models at near real-time. Assimilation of remote sensing data from various sensors and ground-based observations into dynamic land surface models is expected to improve our understanding on the state and dynamics of terrestrial ecosystems (Clark et al. 2001; European Space Agency 2006). Development of long term time series of remote sensing data, improvement of current models and the joint use of space and in-situ measurements at the appropriate scales are some of the aspects where increased focus must be put. Current initiatives include the Terrestrial Observation and Prediction System (TOPS) that is a system designed to integrate data from satellite, aircraft and ground sensors with climate data and application models to produce operational forecasts of ecological conditions (Nemani et al. 2005). TOPS has been operating at spatial scales ranging from vineyard blocks and predicting weekly irrigation requirements to global scales producing regular monthly assessments of global vegetation net primary production. Overall, forecasting and nowcasting ecosystem response to human induced disturbances requires further initiatives in this direction, so that scientists and decision-makers can develop optimal management schemes for sustainable management of the Earth's resources.

References

Aber, J.D., Driscoll, C., Federer, C.A., Lathrop, R., Lovett, G., Melillo, J.M., Stendler, P., & Vogelman, J. (1993). A strategy for the regional analysis of the effects of physical and chemical climate change on biogeochemical cycles in northeastern (US) forests. *Ecological Modelling, 67*, 37-47

Aber, J.D., S. V. Ollinger, and C. T. Driscoll, . (1997). Modeling nitrogen saturation in forest ecosystems in response to land use and atmospheric deposition. *Ecological Modelling, 101*, 61-78

Achard, F., Eva, H.D., Stibig, H.-J., Mayaux, P., Gallego, J., Richards, T., & Malingreau, J.-P. (2002). Determination of Deforestation Rates of the World's Humid Tropical Forests *Science, 297*, 999 - 1002

Ahl, D.E., Gower, S.T., Burrows, S.N., Shabanov, N.V., Myneni, R.B., & Knyazikhin, Y. (2006). Monitoring spring canopy phenology of a deciduous broadleaf forest using MODIS. *Remote Sensing of Environment, 104*

Alrababah, M.A., Alhamad, M.A., Suwaileh, A., & Al-Gharaibeh, M. (2007). Biodiversity of semi-arid Mediterranean grasslands: Impact of grazing and afforestation. *Applied Vegetation Science, 10*, 257-264

Anderson, M.C., Neale, C.M.U., Li, F., Norman, J.M., Kustas, W.P., Jayanthi, H., & Chavez, J. (2004). Upscaling ground observations of vegetation water content,canopy height, and leaf area index during SMEX02 using aircraft and Landsat imagery. *Remote Sensing of Environment, 92*, 447-464

Andréfouët, S., Muller-Karger, F.E., Hochberg, E.J., Hu, C., & Carder, K.L. (2001). Change detection in shallow coral reef environments using Landsat 7 ETM+ data. *Remote Sensing of Environment, 78*, 150-162

Aplin, P. (2005). Remote sensing: ecology. *Progress in Physical Geography, 29*, 104-113

Araújo, M.B., & Rahbek, C. (2006). How Does Climate Change Affect Biodiversity? *Science, 313*, 1396 - 1397

ASD (2000). *FieldSpec Pro User's Guide*. Boulder, CO:Analytical Spectral Devices, Inc

Asner, G.P. (1998). Biophysical and Biochemical Sources of Variability in Canopy Reflectance. *Remote Sensing of Environment, 64*, 234-253

Asner, G.P., Wessman, C.A., Bateson, A.C., & Privette, J.L. (2000). Impact of Tissue, Canopy, and Landscape Factors on the Hyperspectral Reflectance Variability of Arid Ecosystems. *Remote Sensing of Environment, 74*, 69-84

Bacour, C., Baret, F., Beal, D., Weiss, M., & Pavageau, K. (2006). Neural network estimation of LAI, fAPAR, fCover and LAIxC(ab), from top of canopy MERIS reflectance data: principles and validation. *Remote Sensing of Environment, 105*, 313-325

Bajcsy, P., & Groves, P. (2004). Methodology for Hyperspectral Band Selection. *Photogrammetric Engineering and Remote Sensing Journal, 70*, 793-802

Baret, F., & Guyot, G. (1991). Potentials and Limits of Vegetation Indices for LAI and APAR Assessment. *Remote Sensing of Environment, 35*, 161-173

Baret, F., Guyot, G., & Major, D. (1989). TSAVI: A vegetation index which minimizes soil brightness effects on LAI or APAR estimation. In, *12th Canadian Symposium on Remote Sensing and IGARSS 1990* Vancouver, Canada, July 10-14.

Baret, F., Vanderbilt, V.C., Steven, M.D., & Jacquemoud, S. (1994). Use of Spectral Analogy to Evaluate Canopy Reflectance Sensitivity to Leaf Optical Properties. *Remote Sensing of Environment, 48*, 253-260

Barry, P. (2001). EO-1 / Hyperion Science Data User's Guide, Level 1_B. In. Redondo Beach, CA: TRW Space Defense & Information Systems

Bartalev, S.A., Belward, A.S., Erchov, D.V., & Isaev, A.S. (2003). A new SPOT4-VEGETATION derived land cover map of Northern Eurasia. *International Journal of Remote Sensing, 24*, 1977-1982

Batistella, M., Robeson, S., & Moran, E.F. (2003). Settlement design, forest fragmentation, and landscape change in Rondonia, Amazonia. *Photogrammetric Engineering and Remote Sensing, 69*, 805-812

Beeri, O., Phillips, R., Hendrickson, J., Frank, A.B., & Kronberg, S. (2007). Estimating forage quantity and quality using aerial hyperspectral imagery for northern mixed-grass prairie. *Remote Sensing of Environment, 110*, 216-225

Bischoff, A., Auge, H., & Mahn, E. (2005). Seasonal changes in the relationship between plant species richness and community biomass in early succession. *Basic and Applied Ecology, 6*, 385-394

Bittencourt, H.R., & Clarke, R.T. (2004). Feature Selection by Using Classification and Regression Trees (CART). In, *The International Archives of the Photogrammetry, Remote Sensing and Spatial Information Sciences,*. Istanbul

Blackburn, G.A. (1998a). Quantifying chlorophylls and carotenoids at leaf and canopy scales:An evaluation of some hyperspectral approaches. *Remote Sensing of Environment, 66*, 273-285

Blackburn, G.A. (1998b). Spectral indices for estimating photosynthetic pigment concentrations: A test using senescent tree leaves. *International Journal of Remote Sensing, 19*, 657-675

Boegh, E., Soegaard, H., Broge, N., Hasager, C.B., Jensen, N.O., Schelde, K., & Thomsen, A. (2002). Airborne multispectral data for quantifying leaf area index, nitrogen concentration, and photosynthetic efficiency in agriculture. *Remote Sensing of Environment, 81*, 179-193

Boschetti, M., Bocchi, S., & Brivio, P.A. (2007). Assessment of pasture production in the Italian Alps using spectrometric and remote sensing information. *Agriculture, Ecosystems and Environment, 118*, 267-272

Breiman, L., Friedman, J.H., Olshen, R.A., & Stone, C.J. (1984). *Classification and Regression Trees*. Wadsworth, Belmont-CA

Broge, N.H., & Leblanc, E. (2001). Comparing prediction power and stability of broadband and hyperspectral vegetation indices for estimation of green leaf area index and canopy chlorophyll density. *Remote Sensing of Environment, 76*, 156-172

Brown, M.E., & Funk, C.C. (2008). Food security under climate change. *Science, 319*, 580 - 581

Buckland, S.M., Thompson, K., Hodgson, J.G., & Grime, J.P. (2001). Grassland invasions: effects of manipulations of climate and management. *Journal of Applied Ecology, 38*, 301–309

Cane, M.A., Eshel, G., & Buckland, R.W. (1994). Forecasting Zimbabwean maize yield using eastern equatorial Pacific sea surface temperature. *Nature, 370*, 204 - 205

Cao, M., & Woodward, I. (1998). Net primary and ecosystem production and carbon stocks of terrestrial ecosystems and their response to climate change. *Global Change Biology, 4*, 185-198

Carlson, K.M., Asner, G.P., Hughes, R.F., Ostertag, R., & Martin, R.E. (2007). Hyperspectral Remote Sensing of Canopy Biodiversity in Hawaiian Lowland Rainforests. *Ecosystems, 10*, 536-549

Carpenter, S. (1996). Microcosm experiments have limited relevance for community and ecosystem ecology. *Ecology, 77*, 677-680

Carter, G.A. (1994). Ratios of leaf reflectances in narrow wavebands as indicators of plant stress. *International Journal of Remote Sensing, 15*, 697-703

Carter, G.A., Knapp, A.K., Anderson, J.E., Hoch, G.A., & Smith, M.D. (2005). Indicators of plant species richness in AVIRIS spectra of a mesic grassland. *Remote Sensing of Environment, 98*, 304-316

Chen, D., Huang, J., & Jackson, T.J. (2005a). Vegetation water content estimation for corn and soybeans using spectral indices derived from MODIS near- and short-wave infrared bands. *Remote Sensing of Environment, 98*, 225-236

Chen, J.M., Liu, J., Leblanc, S.G., Lacaze, R., & Roujean, J.L. (2003). Multi-angular optical remote sensing for assessing vegetation structure and carbon absorption. *Remote Sensing of Environment, 84*, 516-525

Chen, J.M., Menges, C.H., & Leblanc, S.G. (2005b). Global mapping of foliage clumping index using multi-angular satellite data. *Remote Sensing of Environment, 97*, 447-457

Cho, M.A., Skidmore, A., Corsi, F., van Wieren, S.E., & Sobhan, I. (2007). Estimation of green grass/herb biomass from airborne hyperspectral imagery using spectral indices and partial least squares regression. *International Journal of Applied Earth Observation and Geoinformation, 9*, 414-424

Chuvieco, E., Riaño, D., Aguado, I., & Cocero, D. (2002). Estimation of fuel moisture content from multitemporal analysis of Landsat Thematic Mapper reflectance data: applications in fire danger assessment. *International Journal of Remote Sensing, 23*, 2145-2162

Cihlar, J., Beaubien, J., Xiao, Q., Chen, J., & 23:, L.Z. (1997). Land cover of the BOREAS region from AVHRR and Landsat data. *Canadian Journal of Remote Sensing of Environment, 23*, 163-175

Clark, J.S., Carpenter, S.R., Barber, M., Collins, S., Dobson, A., Foley, J.A., Lodge, D.M., Pascual, M., Pielke, R., Jr., Pizer, W., Pringle, C., Reid, W.V., Rose, K.A., Sala, O., Schlesinger, W.H., Wall, D.H., & Wear, D. (2001). Ecological forecasts: An emerging imperative. *Science, 293*, 657-660

Clark, M.L., Roberts, D.A., & Clark, D.B. (2005). Hyperspectral discrimination of tropical rain forest tree species at leaf to crown scales. *Remote Sensing of Environment, 96*, 375-398

Clark, R.N. (1999). Chapter 1:Spectroscopy of Rocks and Minerals, and Principles of Spectroscopy, in Manual of Remote Sensing. In A.N. Rencz (Ed.), *Manual of Remote Sensing, Volume 3, Remote Sensing for the Earth Sciences* (pp. 3- 58). New York: John Wiley and Sons

Clark, R.N., & Roush, T.L. (1984). Reflectance Spectroscopy: Quantitative Analysis Techniques for Remote Sensing Applications. *Journal of Geophysical Research, 89*, 6329-6340

Clausen, J. (1999). Branch and bound algorithms - principles and examples. In, *Branch and bound algorithms - principles and examples* (p. 30). Copenhagen: University of Copenhagen

Clevers, J.G.P.W. (1991). Application of the WDVI in estimating LAI at the generative stage of barley. *ISPRS Journal of Photogrammetry and Remote Sensing, 46*, 37-47

Clevers, J.P.G.W., & Jongschaap, R.E.E. (2001). Imaging spectrometry for agriculture. In F. Van der Meer & S.M. De Jong (Eds.), *Imaging Spectrometry.Basic principles and prospective applications* (pp. 157-199). Dordrecht: Kluwer Academic Press

Cochrane, M.A. (2001). Using vegetation reflectance variability for species level classification of hyperspectral data. *International Journal of Remote Sensing, 21*, 2075-2087

Cocks, T., Jenssen, R., Stewart, A., Wilson, I., & Shields, T. (1998). The HyMapTM airborne hyperspectral sensor: the system, calibration and performance. In, *Proceedings of the 1st EARSeL Workshop on Imaging Spectroscopy* (pp. 37-42). Zurich

Cohen, W.B., & Goward, S.N. (2004). Landsat's role in ecological applications of remote sensing. *BioScience, 54*, 535-545

Cohen, W.B., Maiersperger, T.K., Turner, D.P., Ritts, W.D., Pflugmacher, D., Kennedy, R.E., Kirschbaum, A., Running, S.W., Costa, M., & Gower, S.T. (2006). MODIS land cover and LAI collection 4 product quality across nine sites in the western hemisphere. *IEEE Transactions on Geoscience and Remote Sensing, 44*, 1843-1857

Cohen, W.B., Spies, T.A., Alig, R.J., Oetter, D.R., Maiersperger, T.K., & Fiorella, M. (2002). Characterizing 23 years (1972–1995) of stand replacement disturbance in western Oregon forests with Landsat imagery. *Ecosystems, 5*, 122–137

Colwell, R.N. (Ed.) (1983). *Manual of Remote Sensing. 2nd Edition*. Falls Church. Virginia: American Society of Photogrammetry

Combal, B., Baret, F., Weiss, M., Trubuil, A., Mace, D., Pragnere, A., Myneni, R., Knyazikhin, Y., & Wang, L. (2003). Retrieval of canopy biophysical variables from bidirectional reflectance - Using prior information to solve the ill-posed inverse problem. *Remote Sensing of Environment, 84*, 1-15

Cook, E.A., Iverson, L.R., & Graham, R.L. (1989). Estimating forest productivity with Thematic Mapper and biogeographical data. *Remote Sensing of Environment, 28*, 131-141

Coppin, P.R., & Bauer, M.E. (1994). Processing of Multitemporal Landsat TM Imagery to Optimize Extraction of Forest Cover Change Features. *IEEE Transactions on Geoscience and Remote Sensing, 32*, 918-927

Cramer, W., Kicklighter, D.W., Bondeau, A., Moore III, B., Churkina, G., Nemry, B., Ruimy, A., & Schloss, A.L. (1999). Comparing global models of terrestrial net primary productivity (NPP): overview and key results. *Global Change Biology, 5*, 1-15

Crawley, M. (2005). *Statistical Computing: An Introduction to Data Analysis using S-Plus*: John Wiley & Sons, Inc

Curran, P.J. (1989). Remote-Sensing of Foliar Chemistry. *Remote Sensing of Environment, 30*, 271-278

Curran, P.J. (1994). Attempts to drive ecosystem simulation models at local to regional scales. In G.M. Foody & P.J. Curran (Eds.), *Environmental Remote Sensing from Regional to Global Scales* (pp. 149-166). Chichester: Wiley and Sons

Curran, P.J. (2001). Imaging spectrometry for ecological applications. *International Journal of Applied Earth Observation and Geoinformation, 3*, 305-312

Curran, P.J., Dungan, J.L., & Peterson, D.L. (2001). Estimating the foliar biochemical concentration of leaves with reflectance spectrometry: Testing the Kokaly and Clark methodologies. *Remote Sensing of Environment, 76*, 349-359

Datt, B., McVicar, T.R., Van Niel, T.G., Jupp, D.L.B., & Pearlman, J.S. (2003). Preprocessing EO-1 Hyperion Hyperspectral Data to Support the Application of Agricultural Indexes. *IEEE Transactions on Geoscience and Remote Sensing, 41*, 1246-1259

Daughtry, C.S.T., & Walthall, C.L. (1998). Spectral Discrimination of Cannabis sativa L. Leaves and Canopies. *Remote Sensing of Environment, 64*, 192-201

Daughtry, C.S.T., Walthall, C.L., Kim, M.S., Brown de Colstoun, E., & McMurtrey, J.E. (2000). Estimating corn leaf chlorophyll concentration from leaf and canopy reflectance. *Remote Sensing of Environment, 74*, 229-239

Dawson, T.P., Curran, P.J., North, P.R.J., & Plummer, S.E. (1999). The Propagation of Foliar Biochemical Absorption Features in Forest Canopy Reflectance: A Theoretical Analysis. *Remote Sensing of Environment, 67*, 147-159

De Jong, S.M., Pebesma, E.J., & Lacaze, B. (2003). Above-ground biomass assessment of Mediterranean forests using airborne imaging spectrometry: the DAIS Peyne experiment. *International Journal of Remote Sensing, 24*, 1505-1520

De Jong, S.M., Pebesma, E.J., & Van der Meer, F.D. (2005). Spatial Variability, Mapping Methods, Image Analysis and Pixels. In S.M. De Jong & F.D. Van der Meer (Eds.), *Remote Sensing Image Analysis: Including the Spatial Domain* (pp. 17-35). Dordrecht: Kluwer Academic Press

De Lange, R., Van Til, M., & Dury, S. (2004). The use of hyperspectral data in coastal zone vegetation monitoring. In, *3rd EARSEL Workshop on Imaging Spectroscopy* (pp. 143-153). Herrsching

Deering, D.W., Rouse, J.W., Haas, R.H., & Schell, J.A. (1975). Measuring "Forage Production" of Grazing Units From Landsat MSS Data. In, *Proceedings of the 10th International Symposium on Remote Sensing of Environment II* (pp. 1169-1178)

Defries, R., & Bounoua, L. (2004). Consequences of land use change for ecosystem services:A future unlike the past. *GeoJournal, 61*, 345-351

DeFries, R., Hansen, M., & Townshend, J. (1994). Global discrimination of land cover types from metrics derived from AVHRR pathfinder data. *Remote Sensing of Environment, 54*, 209-222

DeFries, R.S., Field, C.B., Fung, I., Collatz, G.J., & Bounoua, L. (1999). Combining satellite data and biogeochemical models to estimate global effects of humaninduced land cover change on carbon emissions and primary productivity. *Global Biogeochemical Cycles, 13*, 803-815

Delarze, R., Gonseth, Y., & Galland, P. (1999). *Lebensräume der Schweiz.Ökologie-Gefährdung-Kennarten.*: Ott Verlag,Thun

Deng, F., Chen, J.M., Plummer, S., Chen, M.Z., & Pisek, J. (2006). Algorithm for global leaf area index retrieval using satellite imagery. *IEEE Transactions on Geoscience and Remote Sensing Symposium, IGARSS, 44*, 2219–2229

Dengsheng, L. (2006). The potential and challenge of remote sensing-based biomass estimation. *International Journal of Remote Sensing, 27*, 1297-1328

Diaconis, P., & Efron, B. (1983). Computer-intensive methods on statistics. *Scientific American, 248*, 96-108

DIVERSITAS (2002). DIVERSITAS Science Plan. In, *DIVERSITAS reports*. Paris

Dorigo, W.A., Zurita-Milla, R., de Wit, A.J.W., Brazile, J., Singh, R., & Schaepman, M.E. (2007). A review on reflective remote sensing and data assimilation techniques for enhanced agroecosystem modeling. *International Journal of Applied Earth Observation and Geoinformation, 9*, 165-193

Duelli, P., & Obrist, M.K. (2003). Regional biodiversity in an agricultural landscape: the contribution of seminatural habitat islands. *Basic and Applied Ecology, 4*, 129-138

Eckert, S., & Kneubühler, M. (2004). Application of HYPERION data to agricultural land classification and vegetation properties estimation in Switzerland. In, *ISPRS Conference 2004, Istanbul.*

Eggenberg, S., Dalang, T., Dipner, M., & Mayer, C. (2001). Cartography and evaluation of dry grasslands sites of national importance:Technical report. In, *Environmental Series No. 325* (p. 252). Berne: Swiss Agency for the Environment Forests and Landscape (SAEFL)

Elvidge, C.D. (1990). Visible and near infrared reflectance characteristics of dry plant materials. *International Journal Of Remote Sensing, 11*, 1775-1795

Elvidge, C.D., & Chen, Z. (1995). Comparison of broad-band and narrow-band red and near-infrared vegetation indices. *Remote Sensing of Environment, 54*, 38-48

Eswaran, H., Van den Berg, E., & Reich, P. (1993). Organic carbon in soils of the world. *Soil Science Society of America Journal, 57*, 192–194

European Space Agency (2006). The Changing earth : new scientific challenges for ESA's Living Planet Programme. In (p. 83). Noordwijk, The Netherlands: ESA Publications

Fang, H., & Liang, S. (2005). A hybrid inversion method for mapping leaf area index from MODIS data: experiments and application to broadleaf and needleleaf canopies. *Remote Sensing of Environment, 94*, 405-424

Fassnacht, K.S., Gower, S.T., MacKenzie, M.D., Nordheim, E.V., & Lillesand, T.M. (1997). Estimating the leaf area index of north central Wisconsin forests using the Landsat Thematic Mapper. *Remote Sensing of Environment, 61*, 229–245

Feddema, J.J., Oleson, K.W., Bonan, G.B., Mearns, L.O., Buja, L.E., Meehl, G.A., & Washington, W.M. (2005). The importance of land-cover change in simulating future climates. *Science, 310*, 1674 - 1678

Ferwerda, J.G., Skidmore, A.K., & Mutanga, O. (2005). Nitrogen detection with hyperspectral normalized ratio indices across multiple plant species. *International Journal of Remote Sensing, 26*, 4083-4095

Field, C.B., Randerson, J.T., & Malmström, C.M. (1995). Global net primary production: Combining ecology and remote sensing. *Remote Sensing of Environment, 51*, 74-88

Filella, I., & Peñuelas, J. (1994). The red edge position and shape as indicators of plant chlorophyll content, biomass and hydric status. *International Journal of Remote Sensing, 15*, 1459-1470

Filella, I., Peñuelas, J., Llorens, L., & Estiarte, M. (2004). Reflectance assessment of seasonal and annual changes in biomass and CO2 uptake of a Mediterranean shrubland submitted to experimental warming and drought. *Remote Sensing of Environment, 90*, 308-318

Fischer, M., & Wipf, S. (2002). Effect of low-intensity grazing on the species-rich vegetation of traditionally mown subalpine meadows *Biological Conservation, 104*, 1-11

Foley, J.A. (1994). Net primary productivity in the terrestrial biosphere: the application of a global model. *Journal of Geophysical Research-Atmospheres, 99*, 20773-20783

Foley, J.A., DeFries, R., Asner, G.P., Barford, C., Bonan, G., Carpenter, S.R., Chapin, F.S., Coe, M.T., Daily, G.C., Gibbs, H.K., Helkowski, J.H., Holloway, T., Howard, E.A., Kucharik, C.J., Monfreda, C., Patz, J.A., Prentice, I.C., Ramankutty, N., & Snyde, P.K. (2005). Global consequences of land use. *Science, 309*, 570-574

Foody, G.M., Boyd, D.S., & Cutler, M.E.J. (2003). Predictive relations of tropical forest biomass from Landsat TM data and their transferability between regions. *Remote Sensing of Environment, 85*, 463-474

Fourty, T., Baret, F., Jacquemoud, S., Schmuck, G., & Verdebout, J. (1996). Leaf optical properties with explicit description of its biochemical composition: Direct and inverse problems. *Remote Sensing of Environment, 56*, 104-117

Galvão, L.S., Formaggio, A.R., & Tisot, D.A. (2005). Discrimination of sugarcane varieties in Southeastern Brazil with EO-1 Hyperion data. *Remote Sensing of Environment, 94*, 523-534

Gamon, J.A., Peñuelas, J., & Field, C.B. (1992). A narrow-waveband spectral index that tracks diurnal changes in photosynthetic efficiency. *Remote Sensing of Environment, 41*, 35–44

Gao, B.-C. (1996). NDWI—A normalized difference water index for remote sensing of vegetation liquid water from space. *Remote Sensing of Environment, 58*, 1996

Garcia, A. (1992). Conserving the species-rich meadows of Europe. *Agriculture, Ecosystems and Environment, 40*, 219–232

Gaston, K.J. (2000). Global patterns in biodiversity. *Nature, 405*, 220–227

Gausman, H.W. (1985). *Plant leaf optical properties in visible and near-infrared light.* . Lubbock, Texas, USA

Geerken, R., Batikha, N., Celis, D., & Depauw, E. (2005). Differentiation of rangeland vegetation and assessment of its status : field investigations and MODIS and SPOT VEGETATION data analyses. *International Journal of Remote Sensing, 26*, 4499-4526

Geladi, P., & Kowalski, B.R. (1986). Partial least-squares regression: a tutorial. *Analytica Chimica Acta, 185*, 1-17.

Gill, R.A., Kelly, R.H., Parton, W.J., Day, K.A., Jackson, R.B., Morgan, J.A., Scurlock, J.M.O., Tieszen, L.L., Castle, J.V., Ojima, D.S., & Zhang, X.S. (2002). Using simple environmental variables to estimate below-ground productivity in grasslands *Global Ecology & Biogeography, 11*, 79-86

Gitelson, A.A., Gritz, Y., & Merzlyak, M.N. (2003). Relationships between leaf chlorophyll content and spectral reflectance and algorithms for non-destructive chlorophyll assessment in higher plant leaves. *Journal of Plant Physiology, 160*, 271-282

Gitelson, A.A., & Merzlyak, M.N. (1994). Spectral reflectance changes associated with autumn senescence of aesculus hippocastanum L. and Acer plataniodes L. Leaves. Spectral features and relation to chlorophyll estimation. *Journal of Plant Physiology, 143*, 286-292

Gitelson, A.A., & Merzlyak, M.N. (1996). Signature analysis of leaf reflectance spectra: algorithm development for remote sensing of chlorophyll. *Journal of Plant Physiology, 148*, 495-500

Goetz, A.F.H., Vane, G., Solomon, J.E., & Rock, B.N. (1985). Imaging Spectrometry for Earth Remote Sensing. *Science, 228*, 1147 - 1153

Gong, P., Pu, R., Biging, G.S., & Larrieu, M.R. (2003). Estimation of forest leaf area index using vegetation indices derived from Hyperion hyperspectral data. *IEEE Transactions on Geoscience and Remote Sensing, 41*, 1355-1362

Goodenough, D.G., Dyk, A., Niemann, K.O., Pearlman, J.S., Chen, H., Han, T., Murdoch, M., & West, C. (2003). Processing Hyperion and ALI for Forest Classification. *IEEE Transactions on Geoscience and Remote Sensing, 41*, 1321-1331

Gould, W. (2000). Remote sensing of vegetation, plant species richness, and regional biodiversity hotspots. *Ecological Applications, 20*, 1861–1870

Goward, S.N., & Williams, D.L. (1997). Landsat and earth systems science: development of terrestrial monitoring. *Photogrammetric Engineering and Remote Sensing, 63*, 887–900

Gower, S.T., Kucharik, C.J., & Norman, J.M. (1999). Direct and indirect estimation of leaf area index, f[APAR] and net primary production of terrestrial ecosystems. *Remote Sensing of Environment, 70*, 29-51

Green, R.M., Lucas, N.S., Curran, P.J., & Foody, G.M. (1996). Coupling remotely sensed data to an ecosystem simulation model-an example involving a coniferous plantation in upland Wales. *Global Ecology and Biogeography Letters, 5*, 192-205

Guo, X., Price, K.P., & Stiles, J.M. (2003). Grasslands discriminant analysis using Lansat TM single and multitemporal data. *Photogrammetric Engineering and Remote Sensing, 69*, 1255-1262

Haboudane, D., Miller, J.R., Pattey, E., Zarco-Tejada, P.J., & Strachan, I. (2004). Hyperspectral vegetation indices and novel algorithms for predicting green LAI of crop canopies: Modeling and validation in the context of precision agriculture. *Remote Sensing of Environment, 90*, 337-352

Hall, D.O., Ojima, D.S., Parton, W.J., & Scurlock, J.M.O. (1995). Response of temperate and tropical grasslands to CO2 and climate change *Journal of Biogeography, 22*, 537-547

Hall, D.O., & Scurlock, J.M.O. (1991). Climate change and productivity of natural grasslands. *Annals of Botany, 67*, 49-55

Hansen, M., DeFries, R.S., Townshend, J.R.G., Sohlberg, R., Dimiceli, C., & Carroll, M. (2002). Towards an operational MODIS continuous field of percent tree cover algorithm: examples using AVHRR and MODIS data. *Remote Sensing of Environment, 83*, 303-319

Hansen, P.M., & Schjoerring, J.K. (2003). Reflectance measurement of canopy biomass and nitrogen status in wheat crops using normalized difference vegetation indices and partial least squares regression. *Remote Sensing of Environment, 86*, 542-553

Hazarika, M.K., Yasuoka, Y., Ito, A., & Dye, D. (2005). Estimation of net primary productivity by integrating remote sensing data with an ecosystem model. *Remote Sensing of Environment, 94*, 298-310

He, H.S., Mladenoff, D.J., Radeloff, V.C., & Crow, T.R. (1998). Integration of GIS data and classified satellite imagery for regional forest assessment *Ecological Applications, 8*, 1072-1083

He, Y., Guo, X., & Wilmshurst, J. (2006). Studying mixed grassland ecosystems I:suitable hyperspectral vegetation indices. *Canadian Journal of Remote Sensing, 32*, 98-107

Hill, M.J. (2004). Grazing Agriculture: Managed Pasture, Grassland, and Rangeland. In S. Ustin (Ed.), *Remote Sensing for Natural Resource Management and Environmental Monitoring* (pp. 449-530). New York: John Wiley and Sons

Hill, T., & Lewicki, P. (2006). *Statistics:methods and applications. A comprehensive reference for science, industry and data mining.* Tulsa: Statsoft Inc

Huang, Z., Turner, B.J., Dury, S.J., Wallis, I.R., & Foley, W.J. (2004). Estimating foliage nitrogen concentration from HYMAP data using continuum removal analysis. *Remote Sensing of Environment, 93*, 18-29

Huete, A.R. (1988). A Soil-Adjusted Vegetation Index (SAVI). *Remote Sensing of Environment, 25*, 53-70

Hunt, E.R. (1991). Airborne remote sensing of canopy water thickness scaled from leaf spectrometer data. *International Journal Of Remote Sensing, 12*, 643–649

Hyde, P., Nelson, R., Kimes, D., & Levine, E. (2007). Exploring LiDAR–RaDAR synergy—predicting aboveground biomass in a southwestern ponderosa pine forest using LiDAR, SAR and InSAR. *Remote Sensing of Environment, 106*, 28-38

IPCC (2007). *Climate change 2007: Mitigation. Contribution of Working group III to the Fourth Assessment Report of the Intergovernmental Panel on Climate Change*. Cambridge, United Kingdom and New York, NY, USA: Cambridge University Press

Jackson, R.D., & Heuete, A.R. (1991). Interpreting vegetation indices. *Journal of Preventive Veterinary Medicine, 11*, 185-200

Jackson, T.J., Chen, D., Cosh, M., Li, F., Anderson, M., Walthall, C., Doriaswamy, P., & Hunt, E.R. (2004). Vegetation water content mapping using Landsat data derived normalized difference water index for corn and soybeans. *Remote Sensing of Environment, 92*, 475-482

Jacquemoud, S., Baret, F., Andrieu, B., Danson, F.M., & Jaggard, K. (1995a). Extraction of vegetation biophysical parameters by inversion of the PROSPECT + SAIL models on sugar beet canopy reflectance data. Application to TM and AVIRIS sensors. *Remote Sensing of Environment, 52*, 163-172

Jacquemoud, S., Verdebout, J., Schmuck, G., Andreoli, G., & Hosgood, B. (1995b). Investigation of leaf biochemistry by statistics. *Remote Sensing of Environment, 54*, 180–188

Jago, R.A., Cutler, M.E.J., & Curran, P.J. (1999). Estimating Canopy Chlorophyll Concentration from Field and Airborne Spectra. *Remote Sensing of Environment, 68*, 217-224

Jensen, J.R. (2000). *Remote sensing of the environment: an earth resource perspective*: Prentice-Hall, Inc.

Jiang, H., Apps, M.J., Zhang, Y., Peng, C., & Woodard, P.M. (1999). Modelling the spatial pattern of net primary productivity in Chinese forests. *Ecological Modelling, 122*, 275-288

Justice, C.O., Giglio, L., Korontzi, S., Owens, J., Morisette, J.T., Roy, D., Descloitres, J., Alleaume, S., Petitcolin, F., & Kaufman, Y. (2002). The MODIS fire products. *Remote Sensing of Environment, 83*, 244-262

Kaufmann, H., Segl, K., Chabrillat, S., Müller, A., Richter, R., Schreier, G., Hofer, S., Stuffler, T., Haydn, R., Bach, H., & Benz, U. (2005). EnMAP – An Advanced Hyperspectral Mission. In B. Zagajewski & M. Sobczak (Eds.), *Proceedings of the 4th EARSel Workshop on Imaging Spectroscopy* (pp. 55-60). Warsaw

Kerr, J.T., & Ostrovsky, M. (2003). From space to species: ecological applications for remote sensing. *Trends in Ecology & Evolution, 18*, 299-305

Kimball, J.S., Keyser, A.R., Running, S.W., & Saatchi, S.S. (2000). Regional assessment of boreal forest productivity using an ecological process model and remote sensing parameter maps. *Tree Physiology, 20*, 761-775

Kimes, D., Knyazikhin, Y., Privette, J.L., Abuelgasim, A.A., & Gao, F. (2000). Inversion Methods for Physically-based Models. *Remote Sensing Reviews, 18*, 381-439

Klimek, S., Richter gen. Kemmermann, A., Hofmann, M., & Isselstein, J. (2007). Plant species richness and composition in managed grasslands: The relative importance of field management and environmental factors. *Biological Conservation, 134*, 559-570

Knipling, E.B. (1970). Physical and physiological basis for the reflectance of visible and near-infrared radiation from vegetation. *Remote Sensing of Environment, 1*, 155-159

Knorr, W., & Heimann, M. (2001). Uncertainties in global terrestrial biosphere modelling: Part II. Global constraints for a process-based vegetation model. *Global Biogeochemical Cycles, 15*, 227– 246

Koetz, B., Schaepman, M., Morsdorf, F., Bowyer, P., Itten, K., & Allgower, B. (2004). Radiative transfer modeling within a heterogeneous canopy for estimation of forest fire fuel properties. *Remote Sensing of Environment, 92*, 332-344

Koetz, B., Sun, G., Morsdorf, F., Ranson, K.J., Kneubühler, M., Itten, K., & Allgöwer, B. (2007). Fusion of imaging spectrometer and LIDAR data over combined radiative transfer models for forest canopy characterization. *Remote Sensing of Environment, 106*, 449-459

Kogan, F., Stark, R., Gitelson, A.A., Jargalsaikhan, L., Dugrajav, C., & Tsooj, S. (2004). Derivation of pasture biomass in Mongolia from AVHRR-based vegetation health indices. *International Journal of Remote Sensing, 25*, 2889–2896

Kokaly, R.F., & Clark, R.N. (1999). Spectroscopic determination of leaf biochemistry using band-depth analysis of absorption features and stepwise multiple linear regression. *Remote Sensing of Environment, 67*, 267-287

Kokaly, R.F., Despain, D.G., Clark , R.N., & Livo, K.E. (2003). Mapping vegetation in Yellowstone National Park using spectral feature analysis of AVIRIS data. *Remote Sensing of Environment, 84*, 437-456

Kooistra, L., Suarez Barranco, M.D., Van Dobben, H.F., & Schaepman, M.E. (2006). Monitoring vegetation biomass in river floodplains using imaging spectroscopy. In,

ISPRS 2006 : ISPRS mid-term symposium 2006 remote sensing : from pixels to processes. Enschede, the Netherlands

Küchler, A.W., & Zonneveld, I.S. (Eds.) (1988). *Vegetation Mapping, Handbook of Vegetation Science*. Dordrecht, The Netherlands: Kluwer Academic Publishers

Kumar, L., Schmidt, K.S., Dury, S., & Skidmore, A.K. (2001). Imaging spectrometry and vegetation science. In F. Van der Meer & S.M. De Jong (Eds.), *Imaging Spectrometry.Basic principles and prospective applications* (pp. 111-155). Dordrecht: Kluwer Academic Press

Künnemeyer, R., Schaare, P.N., & Hanna, M.M. (2001). A simple reflectometer for on-farm pasture assessment. *Computers and Electronics in Agriculture, 31*, 125-136

Kupiec, J.A., & Curran, P.J. (1995). Decoupling Effects of the Canopy and Foliar Biochemicals in Aviris Spectra. *International Journal of Remote Sensing, 16*, 1731-1739

Kurz, W., & Apps, M. (2006). Developing Canada's National Forest Carbon Monitoring, Accounting and Reporting System to Meet the Reporting Requirements of the Kyoto Protocol. *Mitigation and Adaptation Strategies for Global Change, 11*, 33-43

Laba, M., Tsai, F., Ogurcak, D., Smith, S., & Richmond, M. (2005). Field determination of optimal dates for the discrimination of invasive wetland plant species using derivative spectral analysis. *Photogrammetric Engineering and Remote Sensing, 71*, 603-611

Langley, S.K., Cheshire, H.M., & Humes, K.S. (2001). A comparison of single date and multitemporal satellite image classifications in a semi-arid grassland. *Journal of Arid Environments, 49*, 401-411

Law, B.E., & Waring, R.H. (1994). Combining Remote Sensing and Climatic Data to Estimate Net Primary Production Across Oregon. *Ecological Applications, 4*, 717-728

Lawrence, R.L., Wood, S.D., & Sheley, R.L. (2006). Mapping invasive plants using hyperspectral imagery and Breiman Cutler classifications (randomForest). *Remote Sensing of Environment, 100*, 356-362

Leblanc, S.G., Chen, J.M., White, H.P., Latifovic, R., Lacaze, R., & Roujean, J.L. (2005). Canada-wide foliage clumping index mapping from multiangular POLDER measurements *Canadian Journal of Remote Sensing, 31*, 364-376

Leckie, D.G., Jay, C., Gougeon, F.A., Sturrock, R.N., & Paradine, D. (2004). Detection and assessment of trees with Phellinus weirii (laminated root rot) using high resolution multi-spectral imagery. *International Journal of Remote Sensing, 25*, 793-818

Lefsky, M.A., Harding, D., Cohen, W.B., Parker, G., & Shugart, H.H. (1999). Surface Lidar Remote Sensing of Basal Area and Biomass in Deciduous Forests of Eastern Maryland, USA. *Remote Sensing of Environment, 67*, 83-98

Liang, S. (2004). *Quantitative Remote Sensing of Land Surfaces*. Hoboken, NJ, USA: Wiley & Sons

Lieth, H. (1975). Modeling the primary productivity of the world. In H. Lieth & R.H. Whitaker (Eds.), *Primary Productivity of the Biosphere*. New York: Springer-Verlag

Lieth, H., & Whitaker, R.H. (Eds.) (1975). *Primary productivity of the biosphere*. New York: Springer-Verlag

Liu, J., Chen, J.M., Cihlar, J., & Park, W.M. (1997). A process-based boreal ecosystem productivity simulator using remote sensing inputs. *Remote Sensing of Environment, 62*, 158-175

Loreau, M., Naeem, S., Inchausti, P., Bengtsson, J., Grime, J.P., Hector, A., Hooper, D.U., Huston, M.A., Raffaelli, D., Schmid, B., Tilman, D., & Wardle, D.A. (2001). Knowledge and Future Challenges Biodiversity and Ecosystem Functioning: Current Challenges. *Science, 294*, 804-808

Los, S.O., Collatz, G.J., Sellers, P.J., Malmstrom, C.M., Olllack, N.H., DeFries, R.S., Bounoua, L., Parris, M.T., Tucker, C.J., & Dazlich, D.A. (2000). A GLOBAL 9-YR biophysical land surface dataset from NOAA AVHRR data. *Journal of Hydrometeorology, 1*, 183-199

Loveland, T.R., Reed, B.C., Brown, J.F., Ohlen, D.O., Zhu, Z., Yang, L., & Merchant, J.W. (2000). Development of a global land cover characteristics database and IGBP DISCover from 1 km AVHRR data. *International Journal of Remote Sensing, 21*, 1303-1330

Lucas, N.S., & Curran, P.J. (1999). Forest ecosystem simulation modelling: the role of remote sensing. *Progress in Physical Geography, 23*, 391 - 423

Lucas, N.S., Curran, P.J., Plummer, S.E., & Danson, F.M. (2000). Estimating the stem carbon production of a coniferous forest using an ecosystem simulation model drivel by the remotely sensed red edge. *International Journal of Remote Sensing, 21*, 619-631

Martin, M.E., & Aber, J.D. (1997). High spectral resolution remote sensing of forest canopy lignin, nitrogen, and ecosystem processes *Ecological Applications, 7*, 431-443

Matsushita, B., & Tamura, M. (2002). Integrating remotely sensed data with an ecosystem model to estimate net primary productivity in East Asia. *Remote Sensing of Environment, 81*, 58-66

Melillo, J.M., McGuire, A.D., Kicklighter, D.W., Moore, B., Vorosmarty, C.J., & Schloss, A.L. (1993). Global climate change and terrestrial net primary production. *Nature, 363*, 234-240

Meroni, M., Colombo, R., & Panigada, C. (2004). Inversion of a radiative transfer model with hyperspectral observations for LAI mapping in poplar plantations. *Remote Sensing of Environment, 92*, 195-206

Miller, A.J. (2002). *Subset selection in regression*. Boca Raton, Florida: Chapman & Hall/CRC

Miller, J.R., Jiyou, W., Boyer, M.G., Belanger, M., & Hare, E.W. (1991). Seasonal patterns in leaf reflectance red-edge characteristics. *International Journal of Remote Sensing, 12*, 1509–1523

Mirik, M., Norland, J.E., Crabtree, R.L., & Biondini, M.E. (2005). Hyperspectral One-Meter-Resolution Remote Sensing in Yellowstone National Park, Wyoming: II. Biomass. *Rangeland Ecology & Management, 58*, 459-465

Mittelbach, G.G., Steiner, C.F., Scheiner, S.M., Gross, K.L., Reynolds, H.L., Waide, R.B., Willig, M.R., Dodson, S.I., & Gough, L. (2001). What is the observed relationship between species richness and productivity? *Ecology, 82*, 2381-2396

Moreau, S., Bosseno, R., Gu, X.F., & Baret, F. (2003). Assessing the biomass dynamics of Andean bofedal and totora high-protein wetland grasses from NOAA/AVHRR. *Remote Sensing of Environment, 85*, 516-529

Morsdorf, F., Kotz, B., Meier, E., Itten, K.I., & Allgower, B. (2006). Estimation of LAI and fractional cover from small footprint airborne laser scanning data based on gap fraction. *Remote Sensing of Environment, 104*, 50-61

Mücher, C.A. (Ed.) (2000). *PELCOM project. Development of a consistent methodology to derive land cover information on a European scale from remote sensing for environmental modelling.Final Report*

Müller, A.M., Richter, R., Habermeyer, M., Dech, S., Segl, K., Kaufmann, H., & 2 (2005). Spectroradiometric requirements for the reflective module of the airborne spectrometer ARES. *IEEE Geoscience and Remote Sensing Letters, 2*, 329-332

Mutanga, O., & Skidmore, A.K. (2004a). Hyperspectral band depth analysis for a better estimation of grass biomass (Cenchrus ciliaris) measured under controlled laboratory conditions. *International Journal of Applied Earth Observation and Geoinformation, 5*, 87-96

Mutanga, O., & Skidmore, A.K. (2004b). Integrating imaging spectroscopy and neural networks to map grass quality in the Kruger National Park. *Remote Sensing of Environment, 90*, 104-115

Mutanga, O., & Skidmore, A.K. (2004c). Narrow band vegetation indices overcome the saturation problem in biomass estimation. *International Journal of Remote Sensing, 25*, 3999-4014

Mutanga, O., Skidmore, A.K., & Van Wieren, S. (2003). Discriminating tropical grass (Cenchrus ciliaris) canopies grown under different nitrogen treatments using spectroradiometry. *ISPRS Journal of Photogrammetry and Remote Sensing, 57*, 263-272

Myneni, R.B., Hoffman, S., Knyazikhin, Y., Privette, J.L., Glassy, J., Tian, Y., Wang, Y., Song, X., Zhang, Y., Smith, G.R., Lotsch, A., Friedl, M., Morisette, J.T., Votava, P., Nemani, R.R., & Running, S.W. (2002). Global products of vegetation leaf area and fraction absorbed PAR from year one of MODIS data. *Remote Sensing of Environment, 83*, 214-231

Nagendra, H. (2001). Using remote sensing to assess biodiversity. *International Journal of Remote Sensing, 22*, 2377-2400

Nagler, P.L., Inoue, Y., Glenn, E.P., Russ, A.L., & Daughtry, C.S.T. (2003). Cellulose absorption index (CAI) to quantify mixed soil–plant litter scenes. *Remote Sensing of Environment, 87*, 310-325

National Research Council (1999). *Global Environmental Change: Research Pathways for the Next Decade*. Washington, D.C.: National Academy Press

Nemani, R., & Running, S.W. (1996). Implementation of a hierarchical global vegetation classification in ecosystem function models. *Journal of Vegetation Science, 7*, 337-346

Nemani, R., Running, S.W., Band, L.E., & Peterson, D.L. (1993). Regional hydroecological simulation system: An illustration of the integration of ecosystem models in a GIS. In M.F. Goodchild, B.O. Parks & L.T. Steyaert (Eds.), *Environmental Modeling with GIS* (p. 488). New York: Oxford University Press

Nemani, R., Votava, P., Michaelis, A., White, M., Melton, F., Milesi, C., Pierce, L., Golden, K., Hashimoto, H., Ichii, K., Johnson, L., Jolly, M., Myneni, R., Tague, C., Coughlan, J., & Running, S. (2005). Terrestrial Observation and Prediction System (TOPS): Developing ecological nowcasts and forescasts by integrating surface, satellite and climate data with simulation models. In, . http://ecocast.arc.nasa.gov/content/view/106/134/

Nieke, J., Itten, K.I., Kaiser, J.W., Schläpfer, D., Brazile, J., Debruyn, W., Meuleman, K., Kempeneers, P., Neukom, A., Feusi, H., Adolph, P., Moser, R., Schilliger, T., Van Quickelberghe, M., Alder, J., Mollet, D., De Vos, L., Kohler, P., Meng, M., Piesbergen, J., Strobl, P., Schaepman, M.E., Gavira, J., Ulbrich, G., & Meynart, R. (2004). APEX: Current Status of the Airborne Dispersive Pushbroom Imaging Spectrometer. In, *SPIE's 49th Annual Meeting*. 2-6 Aug 2004, Denver, USA

Oindo, B.O., & Skidmore, A.K. (2002). Interannual variability of NDVI and species richness in Kenya. *International Journal of Remote Sensing, 23*, 285-298

Oindo, B.O., Skidmore, A.K., & De Salvo, P. (2003). Mapping habitat and biological diversity in the Maasai Mara ecosystem. *International Journal of Remote Sensing, 24*, 1053-1069

Ollinger, S.V., J.D., A., & Federer, A. (1998). Estimating regional forest productivity and water yield using an ecosystem model linked to a GIS. *Landscape Ecology, 13*, 323-334

Ollinger, S.V., & Smith, M.-L. (2005). Net Primary Production and Canopy Nitrogen in a Temperate Forest

Landscape: An Analysis Using Imaging spectroscopy, Modeling and Field Data. *Ecosystems, 8*, 760-778

Oppelt, N., & Mauser, W. (2004). Hyperspectral monitoring of physiological parameters of wheat during a vegetation period using AVIS data. *International Journal of Remote Sensing, 25*, 145-159

Osborne, S.L., Schepers, J.S., Francis, D.D., & Schlemmer, M.R. (2002). Use of Spectral Radiance to Estimate In-Season Biomass and Grain Yield in Nitrogen- and Water Stressed Corn. *Crop Science, 42*, 165-171

Owensby, C.E. (1997). The impacts of global climate change on grassland ecosystems. In J.G. Buchanan-Smith, L.D. Bailey & P. McCaughey (Eds.), *XVIII International Grassland Congress, Canadian Forage and Grassland Society* (pp. III:189-192). Toronto

Palmer, M.W., & Hussain, M. (1997). The unimodal (species richness-biomass) relationship in microcommunities Emerging from Soil Seed Banks. *Proceedings of the Oklahoma Academy of Science, 77*, 17-26

Pärtel, M., Mändla, R., & Zobel, M. (1999). Landscape history of a calcareous (alvar) grassland in Hanila, western Estonia during the last three hundred years. *Landscape Ecology, 14*, 187-196

Parton, W.J., Scurlock, J.M.O., Ojima, D.S., Schimel, D.S., & Hall, D.O. (1995). Impact of climate change on grassland production and soil carbon worldwide. *Global Change Biology, 1*, 13-22

PCI Geomatics (2006). OrthoEngine, User's Guide Version 10.0.

Pearlman, J.S., Barry, P.S., Segal, C.C., Shepanski, J., Beiso, D., & Carman, S.L. (2003). Hyperion, a Space-Based Imaging Spectrometer. *IEEE Transactions on Geoscience and Remote Sensing, 41*, 1160-1173

Peña-Barragan, J., Lopez-Granados, F., Jurado-Expoosito, M., & Garcia-Torres, L. (2006). Spectral discrimination of Ridolfia segetum and sunflower as affected by phenological stage. *Weed Research, 46*, 10-21

Pengra, B.W., Johnston, C.A., & Loveland, T.R. (2007). Mapping an invasive plant, Phragmites australis, in coastal wetlands using the EO-1 Hyperion hyperspectral sensor. *Remote Sensing of Environment, 108*, 74-81

Peñuelas, J., Gamon, J.A., Fredeen, A.L., Merino, J., & Field, C.B. (1994). Reflectance indices associated with physiological changes in nitrogen- and water-limited sunflower leaves. *Remote Sensing of Environment, 48*, 135-146

Peñuelas, J., Piñol, J., Ogaya, R., & Filella, I. (1997). Estimation of plant water concentration by the reflectance Water Index (R900/R970). *International Journal of Remote Sensing, 18*, 2869-2875

Phillips, R.L., Beeri, O., & Liebig, M. (2006). Landscape estimation of canopy C:N ratios under variable drought stress in Northern Great Plains rangelands. *Journal of Geophysical Research, 111*, G02015

Piao, S., Fang, J., Zhou, L., Ciais, P., & Zhu, B. (2006). Variations in satellite-derived phenology in China's temperate vegetation. *Global Change Biology, 12*, 672-685

Piekarczyk, J. (2005). Spectral discrimination of arable from fallow fields as landscape components. *Polish Journal of Ecology, 53*, 299-311

Plummer, S.E. (2000). Perspectives on combining ecological process models and remotely sensed data. *Ecological Modelling, 129*, 169-186

Potter, C.S., Raltderson, J.T., Field, C.B., Matson, P.A., Vitousek, P.M., Mooney, H.A., & Klooster, S.A. (1993). Terrestrial ecosystem production: a process model based on global satellite and surface data. *Global Biogeochemical Cycles, 7*, 811-841

Price, K., Crooks, T., & Martinko, E. (2001). Grasslands across time and scale: A remote sensing perspective. *Photogrammetric Engineering and Remote Sensing, 67*, 414-420

Price, K.P., Guo, X., & Stiles, J.M. (2002). Optimal Landsat TM band combinations and vegetation indices for discrimination of six grassland types in eastern Kansas. *International Journal of Remote Sensing, 23*, 5031-5042

R Development Core Team (2004). R: A language and environment for statistical computing

Rahman, A.F., & Gamon, J.A. (2004). Detecting biophysical properties of a semi-arid grassland and distinguishing burned from unburned areas with hyperspectral reflectance. *Journal of Arid Environments, 58*, 597-610

Ranson, K.J., Sun, G., Weishanpel, J.F., & Knox, R.G. (1997). Forest biomass from combined ecosystem and radar backscatter modelling. *Remote Sensing of Environment, 59*, 118–133

Rauste, Y. (2005). Multi-temporal JERS SAR data in boreal forest biomass mapping. *Remote Sensing of Environment, 97*, 263-275

Reich, P., Walters, M., & Ellsworth, D. (1997). From tropics to tundra: Global convergence in plant functioning. *Proceedings of the National Academy of Sciences, 94*, 13730–13734

Reich, P.B., Knops, J., Tilman, D., Craine, J., Ellsworth, D., Tjoelker, M., Lee, T., Wedin, D., Naeem, S., Bahauddin, D., Hendrey, G., Jose, S., Wrage, K., Goth, J., & Bengston, W. (2001). Plant diversity enhances ecosystem responses to elevated CO2 and nitrogen deposition. *Nature, 410*, 809-810

Riaño, D., Chuvieco, E., Ustin, S., Zomer, R., Dennison, P., Roberts, D., & Salas, J. (2002). Assessment of vegetation regeneration after fire through multitemporal analysis of

AVIRIS images in the Santa Monica Mountains. *Remote Sensing of Environment, 79*, 60-71

Riaño, D., Meier, E., Allgöwer, B., Chuvieco, E., & Ustin, S.L. (2003). Modeling airborne laser scanning data for the spatial generation of critical forest parameters in fire behavior modeling. *Remote Sensing of Environment, 86*, 177-186

Riaño, D., Vaughan, P., Chuvieco, E., Zarco-Tejada, P.J., & Ustin, S.L. (2005). Estimation of fuel moisture content by inversion of radiative transfer models to simulate equivalent water thickness and dry matter content: analysis at leaf and canopy level. *IEEE Transactions on Geoscience and Remote Sensing, 43*, 819-826

Richter, R. (2003). *Atmospheric / Topographic Correction for Airborne Imagery. ATCOR-4 User Guide, Version 3.0,*: DLR-IB564-02/03, DLR, pp.66.

Richter, R., & Schlaepfer, D. (2002). Geo-atmospheric processing of airborne imaging spectrometry data. Part 2: atmospheric/topographic correction. *International Journal of Remote Sensing, 23*, 2631-2649

Riedo, M., Gyalistras, D., Fischlin, A., & Fuhrer, J. (1999). Using an ecosystem model linked to GCM-derived local weather scenarios to analyse effects of climate change and elevated CO2 on dry matter production and partitioning, and water use in temperate managed grasslands. *Global Change Biology, 5*, 213-223

Ripley, B. (2005). tree: Classification and regression trees. *R package version 1.0-19.*

Roberts, D.A., Dennison, P.E., Peterson, S., Sweeney, S., & Rechel, J. (2006). Evaluation of AVIRIS and MODIS measures of live fuel moisture and fuel condition in a shrubland ecosystem in southern California. *Journal of Geophysical Research, 111*

Rogan, J., Miller, J., Stow, D., Franklin, J., Levien, L., & Fischer, C. (2003). Land-cover change monitoring with classification trees using Landsat TM and ancillary data. *Photogrammetric Engineering and Remote Sensing, 69*, 793-804

Rondeaux, G., Steven, M., & Baret, F. (1996). Optimization of soil-adjusted vegetation indices. *Remote Sensing of Environment, 55*, 95-107

Rougean, J.-L., & Breon, F.M. (1995). Estimating PAR absorbed by vegetation from bidirectional reflectance measurements. *Remote Sensing of Environment, 51*, 375–384

Roujean, J.-L., & Breon, F.-M. (1995). Estimating PAR absorbed by vegetation from bidirectional reflectance measurements. *Remote Sensing of Environment, 51*, 375-384

Rouse, J.W., Haas, R.H., Schell, J.A., Deering, D.W., & Harlan, J.C. (1974). Monitoring the vernal advancements and retrogradation of natural vegetation. In, *NASA/GSFC, FInal Report* (pp. 1-137). Greenbelt, MD

Ruimy, A., Saugier, B., & Dedieu, G. (1994). Methodology for the estimation of terrestrial net primary production from remotely sensed data. *Journal of Geophysical Research, 99*, 5263–5283

Running, S.W. (1994). Testing Forest-BGC ecosystem process simulations across a climatic gradient in Oregon. *Ecological Applications, 4*, 238–247

Running, S.W., Baldocchi, D.D., Turner, D.P., Gower, S.T., Bakwin, P.S., & Hibbard, K.A. (1999). A Global Terrestrial Monitoring Network Integrating Tower Fluxes, Flask Sampling, Ecosystem Modeling and EOS Satellite Data. *Remote Sensing of Environment, 70*, 108-127

Running, S.W., & Coughlan, J.C. (1988). A general model of forest ecosystem process for regional applications. 1. Hydrologic balance, canopy gas exchange and primary production processes. *Ecological Modelling, 42*, 125-154

Running, S.W., & Hunt, J., E. R. (1993). Generalization of a forest ecosystem process model for other biomes, BIOME-BGC, and an application for global scale models. In J.R. Ehleringer & C. Field (Eds.), *Scaling Physiological Processes Leaf to Globe* (p. 141−158). San Diego, CA: Academic Press

Running, S.W., Nemani, R., Peterson, D.L., Band, L.E., & Potts, D.F. (1989). Mapping regional forest evapotranspiration and photosynthesis by coupling satellite data with ecosystem simulation. *Ecology, 70*, 1090-1101

Running, S.W., & Nemani, R.R. (1988). Relating seasonal patterns of AVHRR vegetation index to simulated photosynthesis and transpiration of forests in different climates. *Remote Sensing of Environment, 24*, 347– 367

Schaaf, C.B., Gao, F., Strahler, A.H., Lucht, W., Li, X., Tsang, T., Strugnell, N.C., Zhang, N.C., Jin, Y., Muller, J.-P., Lewis, P., Barnsley, M., Hobson, P., Disney, M., Roberts, G., Dunderdale, M., Doll, C., d' Entremon, R.P., Hug, B., Liang, S., Privette, J.L., & Roy, D. (2002). First operational BRDF, albedo nadir reflectance products from MODIS. *Remote Sensing of Environment, 83*, 135-148

Schaepman, M., Koetz, B., Schaepman-Strub, G., Zimmermann, N.E., & Itten, K. (2004). Quantitative retrieval of biogeophysical characteristics using imaging spectroscopy – a mountain forest case study. *Community Ecology, 5*, 93-104

Schimel, D. (1995). Terrestrial biogeochemical cycles: Global estimates with remote sensing *Remote Sensing of Environment, 51*, 49-56

Schläpfer, D., & Richter, R. (2002). Geo-atmospheric processing of airborne imaging spectrometry data. Part 1: parametric orthorectification. *International Journal of Remote Sensing, 23*, 2609-2630

Schlerf, M., & Atzberger, C. (2006). Inversion of a forest reflectance model to estimate structural canopy variables from hyperspectral remote sensing data *Remote Sensing of Environment, 100*, 281-294

Schlerf, M., Atzberger, C., & Hill, J. (2005). Remote sensing of forest biophysical variables using HyMap imaging spectrometer data. *Remote Sensing of Environment, 95*, 177-194

Schmidt, K.S., & Skidmore, A.K. (2001). Exploring spectral discrimination of grass species in African rangelands. *International Journal of Remote Sensing, 22*, 3421-3434

Schmidt, K.S., & Skidmore, A.K. (2003). Spectral discrimination of vegetation types in a coastal wetland. *Remote Sensing of Environment, 85*, 92-108

Schmidt, K.S., Skidmore, A.K., Kloosterman, E.H., van Oosten, H., Kumar, L., & Janssen, J.A.M. (2004). Mapping coastal vegetation using an expert system and hyperspectral imagery. *Photogrammetric Engineering and Remote Sensing, 70*, 703-715

Schulze, E.D., De Vries, W., & Hauhs, M. (1989). Critical loads for nitrogen deposition in forest ecosystems. *Water Air and Soil Pollution, 48*, 451-456

Schwarz, M., & Zimmermann, N.E. (2005). A new GLM-based method for mapping tree cover continuous fields using regional MODIS reflectance data. *Remote Sensing of Environment, 95*, 428-443

Scurlock, J.M.O., & Hall, D.O. (1998). The global carbon sink: A grassland perspective. *Global Change Biology, 4*, 229– 233

Scurlock, J.M.O., Johnson, K., & Olson, R.J. (2002). Estimating net primary productivity from grassland biomass dynamics measurements. *Global Change Biology, 8*, 736-753

Seabloom, E.W., Dobson, A.P., & Stoms, D.M. (2002). Extinction rates under nonrandom patterns of habitat loss. *Proceedings of the National Academy of Sciences, 99*, 11229-11234

Sellers, P., Hall, F., Margolis, H., Kelly, B., Baldocchi, D., Denhartog, G., Cihlar, J., Ryan, M.G., Goodison, B., Crill, P., Ranson, K.J., Lettenmaier, D., & Wickland, D.E. (1995). The Boreal Ecosystem-Atmosphere Study (BOREAS): An overview and early results from the 1994 field year. *Bulletin of the American Meteorological Society, 76*, 1549-1577

Sellers, P.J., Dickinson, R.E., Randall, D.A., Betts, A.K., Hall, F.G., Berry, J.A., Collatz, G.J., Denning, A.S., Mooney, H.A., Nobre, C.A., Sato, N., Field, C.B., & Henderson-Sellers, A. (1997). Modeling the exchanges of energy, water, and carbon between continents and the atmospher. *Science, 275*, 502-509

Serrano, L., Peñuelas, J., & Ustin, S.L. (2002). Remote sensing of nitrogen and lignin in Mediterranean vegetation from AVIRIS data: Decomposing biochemical from structural signals. *Remote Sensing of Environment, 81*, 355-364

Serrano, L., Ustin, S.L., Roberts, D.A., Gamon, J.A., & Peñuelas, J. (2000). Deriving water content of chaparral vegetation from AVIRIS data. *Remote Sensing of Environment, 74*, 570-581

Shimabukuro, Y.E., Aragao, L.E.O.C., Espirito-Santo, F.D.B., & Williams, M. (2005). Combining Landsat ETM+ and terrain data for scaling up leaf area index (LAI) in

eastern Amazon: an intercomparison with MODIS product. *Geoscience and Remote Sensing Symposium, IGARSS, 3*, 2050 - 2053

Sims, D.A., & Gamon, J.A. (2002). Relationships between leaf pigment content and spectral reflectance across a wide range of species, leaf structures and developmental stages. *Remote Sensing of Environment, 81*, 337–354

Smith, A.M., & Blackshaw, R.E. (2003). Weed-crop discrimination using remote sensing: A detached leaf experiment *Weed Technology, 17*, 811-820

Smith, M.-L., Martin, M.E., Plourde, L., & Ollinger, S.V. (2003). Analysis of Hyperspectral Data for Estimation of Temperate Forest Canopy Nitrogen Concentration: Comparison Between an Airborne (AVIRIS) and a Spaceborne (Hyperion) Sensor. *IEEE Transactions on Geoscience and Remote Sensing, 41*, 1332-1337

Smith, M.-L., Ollinger, S.V., Martin, M.E., Aber, J.D., Hallett, R.A., & Goodale, C.L. (2002). Direct estimation of aboveground forest productivity through hyperspectral remote sensing of canopy nitrogen. *Ecological Applications, 12*, 1286-1302

Stenseke, M. (2006). Biodiversity and the local context: linking seminatural grasslands and their future use to social aspects. *Environmental Science & Policy, 9*, 350-359

Strachan, I.B., Pattey, E., & Boisvert, J.B. (2002). Impact of nitrogen and environmental conditions on corn as detected by hyperspectral reflectance. *Remote Sensing of Environment, 80*, 213-224

Swisstopo (2007). http://www.swisstopo.ch (last visited: December 2007).

Symeonakis, E., & Drake, N. (2004). Monitoring desertification and land degradation over sub-Saharan Africa. *International Journal of Remote Sensing, 25*, 573–592

Tarr, A.B., Moore, K.J., & Dixon, P.M. (2005). Spectral reflectance as a covariate for estimating pasture productivity and composition. *Crop Science, 45*, 996-1003

Tasser, E., & Tappeiner, U. (2002). Impact of land use changes on mountain vegetation *Applied Vegetation Science, 5*, 173-184

Tatarinov, F.A., & Cienciala, E. (2006). Application of BIOME-BGC model to managed forests 1. Sensitivity analysis. *Forest Ecology and Management, 237*, 267–279

Thenkabail, P.S., Enclona, E.A., Ashton, M.S., & Van der Meer, B. (2004). Accuracy assessments of hyperspectral waveband performance for vegetation analysis applications. *Remote Sensing of Environment, 91*, 354-376

Thenkabail, P.S., Smith, R.B., & De Pauw, E. (2000). Hyperspectral Vegetation Indices and Their Relationships with Agricultural Crop Characteristics. *Remote Sensing of Environment, 71*, 158-182

Thenkabail, P.S., Smith, R.B., & De Pauw, E. (2002). Evaluation of narrowband and broadband vegetation indices for determining optimal hyperspectral wavebands for

agricultural crop characterization. *Photogrammetric Engineering and Remote Sensing, 68*, 607-621

Theodose, T.A., & Bowman, W.D. (1997). Nutrient availability, plant abundance, and species diversity in two alpine tundra communities *Ecology, 78*, 1861-1872

Thomson, M.C., Doblas-Reyes, F.J., Mason, S.J., Hagedorn, R., Connor, S.J., Phindela, T., Morse, A.P., & Palmer, T.N. (2006). Malaria early warnings based on seasonal climate forecasts from multi-model ensembles. *Nature, 439*, 576-579

Thornton, P.E. (1998). Regional ecosystem simulation: combining surfaceand satellite-based observations to study linkages between terrestrial energy and mass budgets. Ph.D. thesis. In, *University of Montana*. Missoula, MT

Thornton, P.E., Law, B.E., Gholz, H.L., Clark, K.L., Falge, E., Ellsworth, D.S., Goldstein, A.H., Monson, R.K., Hollinger, D., Falk, M., Chen, J., & Sparks, J.P. (2002). Modeling and measuring the effects of disturbance history and climate on carbon and water budgets in evergreen needleleaf forests *Agricultural and Forest Meteorology, 113*, 185–222

Thornton, P.E., & Running, S.W. (1999). An improved algorithm for estimating incident daily solar radiation from measurements of temperature, humidity,and precipitation. *Agricultural and Forest Meteorology, 93*, 211–228

Thulin, S., Hill, M.J., & Held, A. (2004). Spectral sensitivity to carbon and nitrogen content in diverse temperate pastures of Australia. In, *IGARSS 2004.IEEE International Geoscience and Remote Sensing Symposium*. 20-24 September, 2004, Anchorage, Alaska

Todd, S.W., Hoffer, R.M., & Milchunas, G.G. (1998). Biomass estimation on grazed and ungrazed rangelands using spectral indices. *International Journal of Remote Sensing, 19*, 427-438

Townsend, P.A., Foster, J.R., Chastain, R.A.J., & Currie, W.S. (2003). Application of Imaging Spectroscopy to Mapping Canopy Nitrogen in the Forests of the Central Appalachian Mountains Using Hyperion and AVIRIS. *IEEE Transactions on Geoscience and Remote Sensing, 41*, 1347-1353

Treuhaft, R.N., Law, B.E., & Asner, G.P. (2004). Forest attributes from radar interferometric structure and its fusion with optical remote sensing. *BioScience, 54*, 561-571

Trimble (2005). GPS Pathfinder Office Software, Trimble.

Tueller, P.T. (1998). *Vegetation science applications for rangeland analysis and management*. Dordrecht: Kluwer Academic Publishing

Turner, D.P., Guzy, M., Lefsky, M.A., Ritts, W.D., Van Tuyl, S., & Law, B.E. (2004a). Monitoring Forest Carbon Sequestration with Remote Sensing and Carbon Cycle Modeling. *Environmental Management, 33*, 457-466

Turner, D.P., Ollinger, S.V., & Kimball, J.S. (2004b). Integrating Remote Sensing and Ecosystem Process Models for Landscape- to Regional Scale Analysis of the Carbon Cycle. *BioScience, 54*, 573-584

Turner, D.P., Ritts, W.D., Cohen, W.B., Gower, S.T., Running, S.W., Zhao, M., Costa, M.H., Kirschbaum, A.A., Ham, J.M., Saleska, S.R., & Ahl, D.E. (2006). Evaluation of MODIS NPP and GPP products across multiple biomes. *Remote Sensing of Environment, 102*, 282-292

Turner, D.P., Ritts, W.D., Cohen, W.B., Gower, S.T., Zhao, M., Running, S.W., Wofsye, S.C., Urbanskie, S., Dunne, A.L., & Mungere, J.W. (2003a). Scaling Gross Primary Production (GPP) over boreal and deciduous forest landscapes in support of MODIS GPP product validation. *Remote Sensing of Environment, 88*, 256-270

Turner, W., Spector, S., Gardiner, N., Fladeland, M., Sterling, E., & Steininger, M. (2003b). Remote sensing for biodiversity science and conservation. *Trends in Ecology & Evolution, 18*, 306-314

UNCED (1992). Convention on biological diversity—a global biodiversity strategy. In, *United Nations Conference on Environment and Development (Earth Summit)*. Rio de Janeiro: Brazil

Underwood, E., Ustin, S., & DiPietro, D. (2003). Mapping nonnative plants using hyperspectral imagery. *Remote Sensing of Environment, 86*, 150-161

UNEP (2007). *Global Environment Outlook (GEO-4)*. Nairobi, Kenya: United Nations Environment Programme

Ustin, S.L., Jacquemoud, S., Zarco-Tejada, P.J., & Asner, G.P. (2004a). Remote Sensing of the Environment: State of the Science and New Directions. In S. Ustin (Ed.), *Remote Sensing for Natural Resource Management and Environmental Monitoring* (pp. 679-729). New York: John Wiley and Sons

Ustin, S.L., Roberts, D.A., Gamon, J.A., Asner, G.P., & Green, R.O. (2004b). Using Imaging Spectroscopy to Study Ecosystem Processes and Properties. *BioScience, 54*, 523-534

Ustin, S.L., Roberts, D.A., Pinzón, J., Jacquemoud, S., Gardner, M., Scheer, G., Castañeda, C.M., & Palacios-Orueta, A. (1998). Estimating canopy water content of chaparral shrubs using optical methods. *Remote Sensing of Environment, 65*, 280-291

Van de Meer, F., Schmidt, K.S., Bakker, W., & Bijker, W. (2002). New environmental remote sensing systems. In A.K. Skidmore (Ed.), *Environmental Modelling with GIS and Remote Sensing* (pp. 26-51). New York: Taylor & Francis

Van der Meer, F., De Jong, S.M., & Bakker, W. (2001). Analytical techniques in spectrometry. In F. Van der Meer & S.M. De Jong (Eds.), *Imaging Spectrometry.Basic principles and prospective applications* (pp. 17-61). Dordrecht: Kluwer Academic Press

Van Tuyl, S., Law, B.E., Turner, D.P., & Gitelman, A.I. (2005). Variability in net primary production and carbon storage in biomass across Oregon forests - an assessment integrating data from forest inventories, intensive sites, and remote sensing. *Forest Ecology and Management, 209*, 273-291

Verstraete, M.M., Pinty, B., & Myneni, R.B. (1996). Potential and Limitations of Information Extraction on the Terrestrial Biosphere from Satellite Remote Sensing *Remote Sensing of Environment, 58*, 201-214

Vitousek, P.M., Aber, J.D., Howarth, R.W., Likens, G.E., Matson, P.A., Schindler, D.W., Schlesinger, W.H., & Tilman, D.G. (1997). Human alteration of the global nitrogen cycle: Sources and consequences. *Ecological Applications, 7*, 737-750

Vogelmann, J.E., Howard, S.M., Yang, L., Larson, C.R., Wylie, B.K., & Van Driel, N. (2001). Completion of the 1990's National Land Cover Data Set for the conterminous United States from Landsat Thematic Mapper data and ancillary data sources. *Photogrammetric Engineering and Remote Sensing, 67*, 650–662

Vogelmann, J.E., Rock, B.N., & Moss, D.M. (1993). Red edge spectral measurements from sugar maple leaves. *International Journal of Remote Sensing, 14*, 1563-1575

Vohland, M., & Jarmer, T. (2008). Estimating structural and biochemical parameters for grassland from spectroradiometer data by radiative transfer modelling (PROSPECT plus SAIL) *International Journal of Remote Sensing, 29*, 191-209

Waide, R.B., Willig, M.R., Steiner, C.F., Mittelbach, G.G., Gough, L., Dodson, S.I., Juday, G.P., & Parmenter.R. (1999). The relationship between primary productivity and species richness. *Annual Review of Ecology and Systematics, 30*, 257-300

Watkinson, A.R., & Ormerod, S.J. (2001). Grasslands, grazing and biodiversity: editors' introduction. *Journal of Applied Ecology, 38*, 233–237

Wessman, C.A. (1994a). Estimating canopy biochemistry through imaging spectrometry. In J. Hill & J. Mégier (Eds.), *Imaging Spectrometry - a Tool for Environmental Observations* (pp. 57-70). Dordrecht: Kluwer Academic Publishers

Wessman, C.A. (1994b). Remote sensing and the estimation of ecosystem parameters and functions. In J. Hill & J. Mégier (Eds.), *Imaging Spectrometry - a Tool for Environmental Observations* (pp. 39-56). Dordrecht: Kluwer Academic Publishers

White, J.D., Running, S.W., Nemani, R., Keane, R.E., & K.C., R. (1997a). Measurements and remote sensing of LAI in Rocky Mountain montane ecosystems. *Canadian Journal of Forest Research, 27*, 1714-1727

White, M.A., & Nemani, R.R. (2006). Real-time monitoring and short-term forecasting of land surface phenology. *Remote Sensing of Environment, 104*, 43-49

White, M.A., Thornton, P.E., & Running, S.W. (1997b). A continental phenology model for monitoring vegetation responses to interannual climatic variability. *Global Biogeochemical Cycles, 11*, 217-234

White, M.A., Thornton, P.E., Running, S.W., & Nemani, R.R. (2000). Parameterization and sensitivity analysis of the BIOME–BGC terrestrial ecosystem model: Net primary production controls. *Earth Interactions, 4*, 1-85

Wood, A.W., Maurer, E.P., Edwin, P., Kumar, A., & Lettenmaier, D.P. (2001). Long-range experimental hydrologic forecasting for the eastern United States. *Journal of Geophysical Research (Atmospheres), 107*, pp. ACL 6-1, CiteID 4429, DOI 4410.1029/2001JD000659

Wulder, M.A., Hall, R.J., N.C., C., & S.E., F. (2004). High Spatial Resolution Remotely Sensed Data for Ecosystem Characterization. *BioScience, 54*, 511-521

Wylie, B.K., Meyer, D.J., Tieszen, L.L., & Mannel, S. (2002). Satellite mapping of surface biophysical parameters at the biome scale over the North American grasslands A case study. *Remote Sensing of Environment, 79*, 266-278

Xavier, A.C., Rudorff, B.F.T., Moreira, M.A., Alvarenga, B.S., de Freitas, J.G., & Salomon, M.V. (2006). Hyperspectral field reflectance measurements to estimate wheat grain yield and plant height. *Scientia Agricola, 63*, 130-138

Yoder, B.J., & Pettigrew-Crosby, R.E. (1995). Predicting nitrogen and chlorophyll content and concentrations from reflectance spectra (400-2500 nm) at leaf and canopy scales. *Remote Sensing of Environment, 53*, 199-211

Zagolski, F., Pinel, V., Romier, J., Alcayde, D., Fontanri, J., Gastellu-Etchegorry, J.P., Giordano, G., Marty, G., Mougin, E., & Joffre, R. (1996). Forest canopy chemistry with high spectral resolution remote sensing. *International Journal of Remote Sensing, 17*, 1107-1128

Zarco-Tejada, P.J., Miller, J.R., Harron, J., Hu, B., Noland, T.L., Goel, N., Mohammed, G.H., & Sampson, P. (2004). Needle chlorophyll content estimation through model inversion using hyperspectral data from boreal conifer forest canopies. *Remote Sensing of Environment, 89*, 189-199

Zarco-Tejada, P.J., Miller, J.R., Noland, T.L., Mohammed, G.H., & Sampson, P.H. (2001). Scaling-up and model inversion methods with narrowband optical indices for chlorophyll content estimation in closed forest canopies with hyperspectral data. *IEEE Transactions on Geoscience and Remote Sensing, 39*

Zarco-Tejada, P.J., Rueda, C.A., & Ustin, S.L. (2003). Water content estimation in vegetation with MODIS reflectance data and model inversion methods. *Remote Sensing of Environment, 85*, 109-124

Zarco-Tejada, P.J., Ustin, S.L., & Whiting, M.L. (2005). Temporal and spatial relationships between within-field yield variability in cotton and high-spatial hyperspectral remote sensing imagery. *Agronomy Journal, 97*, 641-653

Zebiak, S.E. (2003). Research potential for improvements in climate prediction. *Bulletin of the American Meteorological Society, 84*, 1692–1696

Zha, Y., Gao, J., Ni, S., Liu, Y., Jiang, J., & Wei, Y. (2003). A spectral reflectance-based approach to quantification of grassland cover from Landsat TM imagery. *Remote Sensing of Environment, 87*

Zhan, X., Sohlberg, R.A., Townshend, J.R.G., DiMiceli, C., Carroll, M.L., Eastman, J.C., Hansen, M.C., & DeFries, R.S. (2002). Detection of land cover changes using MODIS 250 m data. *Remote Sensing of Environment, 83*, 336-350

Acknowledgements

I would like to extend my warmest acknowledgements to all the people who helped and supported me during the time of this PhD.

First of all I would like to extend my deepest gratitude to my first supervisor Dr. Niklaus Zimmermann who offered me the possibility to do this PhD and supported me continuously throughout all these years. His scientific guidance, his generous way of unconstrained research activities and his great enthusiasm created the optimal working environment. He has not only helped me to develop as a young scientist, but also helped me to become a better person with his unique character.

I deeply acknowledge Prof. Dr. Klaus Itten for accepting to supervise this thesis but also for helping me with his valuable experience and advice. I would also like to thank Dr. Mathias Kneubühler, my second supervisor, for his much-valued feedback on my papers that improved this work, his help with my field spectroradiometer sampling but also for his cheerful character and his supporting words.

I would like to acknowledge the Swiss Federal Research Institute WSL and the Swiss Agency for the Environment, Forest and Landscape (SAEFL) for funding this research. Additional funding came from the 6th framework program of the EU (contract numbers GOCE-CT-2003-505376 and GOCE-CT-2007-036866).

I am further grateful to my officemate Katharina Steinmann for her help, scientific support but mostly for the endless discussions especially during the difficult periods of this PhD, my ex-officemate Dr. Sophie Rickebush for helping me with almost every difficulty I had adjusting to the “Swiss-way-of-doing-things” and Dr. Silvia Huber for her help with my field work, my work at RSL and for her motivating words during the whole PhD period. Special thanks go to Dr. Felix Herzog from Agroscope-Reckenholz who was the first to offer me the possibility to work in Switzerland.

I would also like to thank “Rafa” Wueest and Dr. Jacqueline Gehrig-Fasel for making every lunch and coffee break as enjoyable as one can imagine and Dr. Lukas Mathys for translating my PhD abstract in German and for the fruitful discussions on remote sensing aspects of my research.

Special thanks goes to Dr. Dirk Schmatz for supporting me with all the cluster processing and for his willingness to answer all my Unix and Mac related questions, to the “Treeline Group” for the scientific discussions and the nice times we had together: Dr. Stefan Leyk, Dr. Gillian Rutherford and Dr. Mario Gellrich and to all the colleagues I worked and met at WSL or RSL for creating a pleasant and motivating working atmosphere.

I would also like to thank all the friends I made during my stay in Zurich and to whom I own the nice times I had outside work: Petra, U2, Guido, Melly, Heike, Mark, Jürg, Daniel

and many others. A special thanks goes to Ed, my best friend in Zurich, with whom I lived the whole Switzerland adventure right from the beginning and with whom I develop my football "watching" skills to unthinkable levels!

Finally, I am grateful to Fenia for her support, understanding and for her love, without which all these years would not have been so beautiful.

Last but not least, I am deeply grateful to my parents Ioannis and Evangelia and to my brother Akis for their long lasting help, love and support throughout my entire life but also for their courage and strength to face all the difficult situations that came when I was not close to help them.

Personal Bibliography

Peer reviewed journals

Psomas, A., Kneubühler, M., Huber, S., Itten, K., & Zimmermann, N.E. (2008). Coupling imaging spectroscopy and ecosystem process modelling - the importance of spatially distributed foliar biochemical concentration estimates for modelling NPP of grassland habitats. *Journal of Geophysical Research, Submitted*

Psomas, A., Kneubühler, M., Itten, K.I., & Zimmermann, N.E. (2008). Space-borne hyperspectral remote sensing in support of estimating aboveground biomass and species richness patterns in grassland habitats at the landscape scale. *International Journal of Remote Sensing, Submitted*

Psomas, A., Kneubühler, M., Huber, S., Itten, K.I., & Zimmermann, N.E. (2007). Continuum removal in multi-temporal spectrometer data enhances the classification accuracy of grasslands along a dry-mesic gradient. *Remote Sensing of Environment, In revision*

Huber, S., Kneubühler, M., **Psomas, A.,** Itten, K.I., & Zimmermann, N.E. (2008). Estimating foliar biochemistry from hyperspectral data in mixed forest canopy. *Forest Ecology and Management, Accepted*

Conference and workshop contributions

Psomas, A., Kneubühler, M., Huber, S., Itten, K.I., & Zimmermann, N.E. (2007). Modeling biochemical concentrations of grassland habitats from in situ and imaging spectroscopy data. In, *Proceedings of the 5th EARSEL Workshop on Imaging Spectroscopy*. Brugge, Belgium

Psomas, A., Kneubühler, M., Itten, K.I., & Zimmermann, N.E. (2007). Hyperspectral remote sensing for seasonal estimation of aboveground biomass in grassland habitats. In, *Proceedings of the 10th International Symposium on Physical Measurements and Signatures in Remote Sensing* (pp. 482-487). Davos, Switzerland

Psomas, A., Kneubuehler, M., Huber, S., Itten, K.I., & Zimmermann, N.E. (2005). Seasonal variability in spectral reflectance for discriminating grasslands along a dry-mesic gradient in Switzerland. In, *Proceedings of the 4th EARSEL Workshop on Imaging Spectroscopy* (pp. 709-722). Warsaw, Poland

Huber, S., Zimmermann, N.E., Kneubühler, M., **Psomas, A.,** & Itten, K.I. (2005). Estimating Nitrogen in Mixed Forests from HyMap Data using Band-Depth Analysis and Branch-and-Bound Algorithm. In, *Proceedings of the 9th International Symposium on Physical Measurements and Signatures in Remote Sensing* (pp. 533-535). Beijing, China